CONSTRUCTION MATERIALS CONSULTANTS, INC.

Investigation of Extensive Cracking of a Swimming Pool from Petrographic Examinations of Four Composite Cores of Pool Plaster and Shotcrete

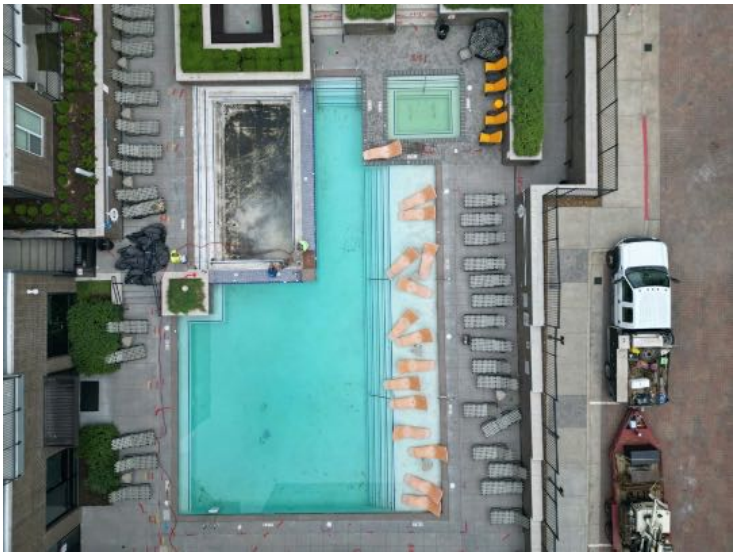

U-Center on Turner
625 S 4th Street
Columbia, MO 65203

September 12, 2023
CMC 0823176

Table of Contents

EXECUTIVE SUMMARY

Background - The present investigation centered around extensive cracking and subsequent water leaking of an in-ground exterior swimming pool in Columbia, Missouri. Reportedly constructed around 2017, the pool has developed extensive longitudinal cracks through the walls and steps to the floor. The pool was constructed with a shotcrete body and off-white cementitious plaster. Cracks are: (a) short, discontinuous at the edges of steps, (b) long, continuous on the interior walls, (c) long, continuous from the walls that have traversed though the steps to floor, (d) long, continuous on the floor, (e) X-shaped intersecting cracks at the corners of steps.

Pool Cores – In order to investigate the reasons for extensive cracking, four composite cores (Nos. 1 to 4) were provided from four different locations across the pool. Core 1 was drilled from a step from a visually crack-free surface but adjacent to short, discontinuous cracks along the edge of the step. Core 2 was drilled over a long, continuous crack on the step. Core 3 was drilled over an intersecting X-shaped cracks at the corner of steps. Core 4 was drilled over long, continuous crack on the floor. All these cores were drilled after removal of pool water, which has helped visualization of cracks at the core locations as well as at other locations. Several field photographs provided with the cores have shown the cracks in the pool as well as at the locations of four cores.

Crack Repair Attempts - Field photos and two of the four cores received (Cores 2 and 3 from over a long continuous crack, and X-shaped intersecting corner cracks on a step, respectively) show previous repair attempts on many of these cracks with an elastomeric crack sealer/filler, which, however, was ineffective in preventing water leakage through the cracks. In Cores 2 and 3, an elastomeric crack sealant was detected, which, however, did not penetrate deep enough into the cracks to create an effective seal. In both cores, sealer was present just on the exposed surface end of the cracks, though apparently well-bonded at least at the small area of examination, but with little or no penetration into the empty cracks beneath. In both cores, water can still penetrate through the empty cracks.

Pool Components in Cores – Three of the four cores (Nos. 1 to 3) came from the steps where No. 1 showed no visible crack on the exposed end (though drilled from a location adjacent to short discontinuous cracks on the edge of step) whereas Nos. 2 and 3 both show visible cracks on the plaster surface that have penetrated through the plaster into the shotcrete body. Core 4 was from the floor, which too showed visible crack transected through the plaster and entered into the shotcrete body.

Core ID	1 (Step Edge, No Crack)	2 (Step, On a crack)	3 (Step, On Corner Cracks)	4 (Floor, On a crack)
Core Length, in. (mm)	14″ (350 mm)	14″ (350 mm)	14 ″(350 mm)	11″ (270 mm)
Main Vertical Crack length and Surface Width (mm)	None	10.5″(260 mm) 1.5 mm	5.25″(130 mm) 1.5 mm	11″ (270 mm) 1.5 mm
Off-White Pool Plaster Thickness, mm	15 mm	9 mm	11 mm	8-11 mm
Gray Leveling Course, mm	2-7 mm	2 mm	3-4 mm	None
Variably Dark Gray Shotcrete Body Thicknesses of D-Dense, and CV-shotcrete with coarse voids in the top 8 in. of cores examined	60 mm D 60 mm CV 70 mm D	60 mm D 60 mm CV 70 mm D	80 mm CV 40 mm D 20 mm CV 40 mm D	130 mm D 55 mm CV

Methodologies – All four cores were examined in detail by petrographic examinations following the procedures of ASTM C 856, and scanning electron microscopy and energy-dispersive X-ray microanalysis by following the procedures of ASTM C 1723.

Pool Plaster – Pool plaster is compositionally similar ***cementitious plaster coat*** across all four cores and consist of: (a) ***off-white Portland cement***, ***minor limestone fines***, and ***2 to 3 mm nominal size well-sorted, well-distributed siliceous (quartz, quartzite) filler***. In all four cores, plaster showed ***extensive shrinkage cracking in paste fractions due to high paste volume relative to silica fillers*** where cracks are confined within the plaster and did not extend into the underlying leveling coat or shotcrete. These extensive fine, hairline shrinkage cracks in plaster paste are invisible on the exposed surface of plaster relative to the major visible cracks that have transected through plaster into the shotcrete body and formed entirely due to shrinkage of a high paste-volume cementitious plaster.

Gray Leveling Course – Three cores (Nos. 1 to 3) from the steps but not the fourth one (No. 4) from the floor showed the presence of a thin medium gray (compared to darker gray shotcrete body) leveling course applied on the shotcrete body prior to the placement of pool plaster, which is determined to be a calcium aluminate cement, minor limestone fine, and very fine crushed silica sand based course as opposed to white Portland cement and limestone fine at the top plaster or gray Portland cement and minor fly ash based binder used in the underlying main shotcrete body. This thin leveling course is well bonded to the shotcrete body beneath, as well as to the pool plaster above.

Main Shotcrete Body – Shotcrete is compositionally similar in terms of ingredients across all four cores consisting of: (a) ¼ in. (6.25 mm) nominal maximum size ***crushed limestone and argillaceous dolomitic limestone aggregate***, (b) noticeably finer nominal 2-3 mm size ***crushed siliceous (quartz, quartzite) sand aggregates***, and (c) variably dense and medium to darker gray paste of ***major amount of Portland cement and minor amount of fly ash*** having water-cementitious materials ratios estimated to be 0.40 to 0.42 in the denser and darker gray areas to 0.42 to 0.46 in the medium gray areas. Shotcrete is ***non-air-entrained*** but coarse entrapped air voids are seen throughout the recovered lengths of cores, which vary from 3 to 4 percent in the denser areas to as high as 8 to 10 percent in areas having many very coarse (honeycombed) visible voids. As shown in the Table in the previous page, there are zones in shotcrete that are rich in coarse (honeycombed) voids, whereas other zones noticeably denser and lack coarse visible voids which is the result of pneumatic project of wet-mix shotcrete to the pool walls. Same wet mix of shotcrete is judged to have used at the locations of all four cores, i.e., from walls through steps to the floor. Lapped cross sections of all four cores showed a more or less 'homogeneous' shotcrete body in terms of the absence of any typical color banding of alternating lighter and dark gray color tones of paste that are typically seen in a dry-mix gunite counterpart where water is added at the tips of hose during projection of dry sand-cement mix as opposed to pneumatic projection of a previously wet mixed mass of aggregates, cement, and water in shotcrete.

Initial Stages of Alkali-Carbonate Reactive Potentially Unsound Crushed Argillaceous Dolomitic Limestone Aggregate: Many argillaceous dolomitic limestone particles in aggregate showed dark reaction rims along the periphery of the aggregates and many of those particles additionally showed lighter cream-colored carbonation rims in paste immediately adjacent to those particles. These particles show characteristic texture of many known alkali-carbonate reactive rocks of Missouri[1] in having rhombic crystals of dolomite floats in finer-grained matrix of calcite,

[1] Alkali Reactivity of Carbonate Rocks in Missouri, Missouri State Highway Department, Division of Materials and Research, August 1967.

quartz, and clay. The dark reaction rims are rich in coarse-grained dolomite compared to the core, and carbonated paste rims are the result of alkali-carbonate (de-dolomitization) reaction (ACR) where dolomite rhombs in aggregate reacted with alkali hydroxide in pore solutions of shotcrete to form calcite (which has caused carbonation of adjacent paste), fibrous brucite (magnesium hydroxide, which was difficult to detect), and alkali carbonate (which can potentially participate in a second reaction with calcium hydroxide component of Portland cement hydration to form calcium carbonate and regenerate alkali hydroxide to continue de-dolomitization reaction). Mechanism of ACR by de-dolomitization reaction is well-known in the literature, e.g., Axon and Lind 1966, Gillot and Swenson 1969, Grattan-Bellew et al., 2010, Hadley 1961, Katayama 2010, Lo et al., 2022, Mather et al., 1967, Ozol 2006, Swenson and Gillot 1964, Tang et al., 1987, and Walker 1978.

Absence of Cracking from ACR - Despite finding abundant (estimated to be 60 to 70 percent of crushed limestone-dolomite aggregate) dolomitic limestone with dark reaction rims (and many with additional lighter carbonation rims in paste) and characteristic texture of many reactive alkali-carbonate rocks of Missouri in having dolomite rhombs floating in finer-grained matrix of calcite, quartz, and clay, however, none of the four cores examined showed any cracking either in the dark reaction rims or in the interstitial paste fractions, which are the common result of expansions from alkali-carbonate reactions. Therefore, the main visible cracks across various locations of pool through the plaster to noticeable depths into shotcrete, though structural in nature as opposed to surface cracks are judged not due to potentially deleterious expansion of shotcrete mass by ACR even though such a possibility exists especially during longer exposure to pool water than the time of this examination. Dark reaction rims and carbonation rims in adjacent paste indicate alkali-carbonate reaction (ACR, i.e., de-dolomitization reaction) but the reaction wasn't advanced enough to develop cracking in the interstitial paste fraction of shotcrete.

Alkali-Silica Reaction of Potentially Unsound Crushed Dolomitic Limestone Aggregate: Along with ACR, also detected are isotropic to birefringent alkali-silica reaction gel in the walls of main vertical cracks and in some coarse voids, which are judged to be the result of alkali-silica reaction (ASR) of reactive silica inclusions in some of crushed argillaceous dolomitic limestone particles and alkaline pore solutions in shotcrete. Despite its detection in rather meager amounts, similar to ACR, however no cracking was detected from ASR of reactive silica components in crushed dolomitic limestone aggregate. Like ACR, ASR too is present at a very early stage.

Potential Unsoundness and Wrong Choice of Argillaceous Dolomitic Limestone Aggregate – Therefore, despite the lack of direct evidence of distress (i.e., cracking) by either ACR or ASR of crushed argillaceous dolomitic limestone aggregates, their presence clearly showed the potential danger of bulk expansion of shotcrete by either or both reactions to cause cracking, which hasn't developed to advanced stage to show cracking of interstitial paste fractions of shotcrete. Missouri is well-known for many alkali-carbonate reactive rocks, which should have checked by petrographic examinations according to the procedures of ASTM C 295 prior to the incorporation of potentially reactive dolomitic limestone aggregate as the most voluminous component in the shotcrete mix.

Another more serious deleterious side effect of using ¼ in. (6.25 mm) crushed limestone-dolomitic limestone aggregate, beside the ACR potential, which is judged to have provided more direct role in promoting unaccomodative drying shrinkage of shotcrete is the increased paste volume of shotcrete from use of such crushed stone of high specific surface with the increased potential for drying shrinkage of high cement content shotcrete mix. Since the water-cement ratio was low (0.40 to 0.44), cement content has to be higher than usual at a given water content to increase the paste volume to adequately coat these aggregates during wet mixing process.

Shrinkage Cracking of Shotcrete – Based on detailed petrographic examinations, e.g., from (a) use of ¼ in. size crushed limestone-dolomite aggregate to increase the paste volume, to (b) configuration of paths of main vertical cracks through depth, from (c) evidence such as trapped paste and aggregate in between crack walls to (d) cracking of some crushed stone particles situated along the crack paths most of the visible cracks in the pool, at least at the locations of examined cores are judged to be due to unaccommodative shrinkage of shotcrete, where a portion of cracks may have formed at an early stage of shotcrete placement (i.e., plastic shrinkage) whereas a portion may have developed at a later hardening stage (i.e., as drying shrinkage) during the aerated stage prior to the filling of pool with water.

Three Potential Stresses for Development and Advancement of Cracks – Based on the present study, there are at least three different stresses detected at aerated and immersed states, which have the potential to cause cracking – (a) drying shrinkage of pool plaster at aerated states to develop extensive fine hairline microcracking in the cement paste fraction of plaster that are well-documented from optical microscopy and SEM studies here, (b) overall shrinkage of shotcrete body at aerated states from use of high paste volume at low water-cement ratio wet mix, which is also well-documented here, and (c) potential expansion of shotcrete body at immersed states by deleterious expansions from ACR and ASR where only evidence of such reactions are well documented here (e.g., from dark reaction rims, carbonation rims in paste, and ASR products in cracks and voids) but not the resultant cracking due to rather early stages of such reactions. Therefore, there might be two opposing forces acted – (1) one from overall bulk shrinkage of shotcrete body, which has developed the main vertical cracks where pool plaster simply reflected the cracks from shotcrete body (along with a potential contribution from shrinkage cracking of plaster itself, which might have opened additional pathways for pool water penetration through plaster), and (2) another from overall bulk expansion of shotcrete from ACR and ASR. Amongst these two opposing forces, shrinkage clearly won over expansion here for development of visible cracks since expansion mechanisms are found to be at early stages.

Other Factors to Consider For a Comprehensive Investigation of Pool Cracking – Despite finding the shotcrete itself, e.g., from its reactive argillaceous dolomitic limestone aggregate to high paste volume for one of the prime candidates for cracking mainly by shrinkage, however, the present study does not exclude investigation of other common causes of pool cracking, e.g., (1) stability and load-bearing capacity of soil subbase, (2) presence of potentially expansive soil, (3) subbase settlement, (4) incorporating high-sand rebound shotcrete, (5) failure to adequately tie the rebar in place when placing the rebar, (6) not keeping the pool sufficiently moist after shotcrete is sprayed on especially in hot-dry-sunny day, (7) absence of expansion/contraction joint on the pool deck allowing movement to occur between the deck and pool, etc. and other design and construction related errors all of which can contribute a noticeable role for cracking, which are beyond the scope of this study. Along with all these potential factors, the present study added a materials' reason from the shotcrete mix for potential early and late shrinkage and late expansion of shotcrete.

INTRODUCTION

Extensive cracking and subsequent water leaking of an in-ground exterior swimming pool in Columbia, Missouri has prompted this study. Constructed around 2017, the pool has developed extensive cracking through the walls and steps to the floor to reportedly cause almost a foot depth of water leakage per day.

FIELD PHOTOS AND BACKGROUND INFORMATION

Figures 1 to 8 show field photos of the pool and cracking inside the pool.

Cracks are:

- Short, discontinuous at the edges of steps – see Figure 5,
- Long, continuous on the interior walls – see Figures 3, 4, and 6,
- Long continuous from the walls that have traversed though the steps to floor – see Figures 4, 5, 6, and 8,
- Long continuous on the floor – see Figures 3 and 8,
- X-shaped intersecting cracks at the corners of steps – see Figures 6 and 8.

In order to investigate the reasons for extensive cracking, four composite cores (Nos. 1 to 4) were provided from four different locations across the pool. Figure 8 shows locations of four cores received for this study.

- Core 1 was drilled from a step from a visually crack-free surface but adjacent to short, discontinuous cracks along the edge of the step.
- Core 2 was drilled over a long-continuous crack on the step.
- Core 3 was drilled over an intersecting X-shaped cracks at the corner of steps.
- Core 4 was drilled over long, continuous crack on the floor.

All these cores were drilled after removal of pool water, which has helped visualization of cracks at the core locations as well as at other locations.

PURPOSES OF PRESENT INVESTIGATION

Based on the background information and field photos provided, the purposes of the present investigation are to determine:

- The condition, composition, and quality of pool plaster and shotcrete body in the cores; and
- Evidence of any chemical and/or physical deterioration of plaster and/or shotcrete, which have caused the visible cracking of pool.

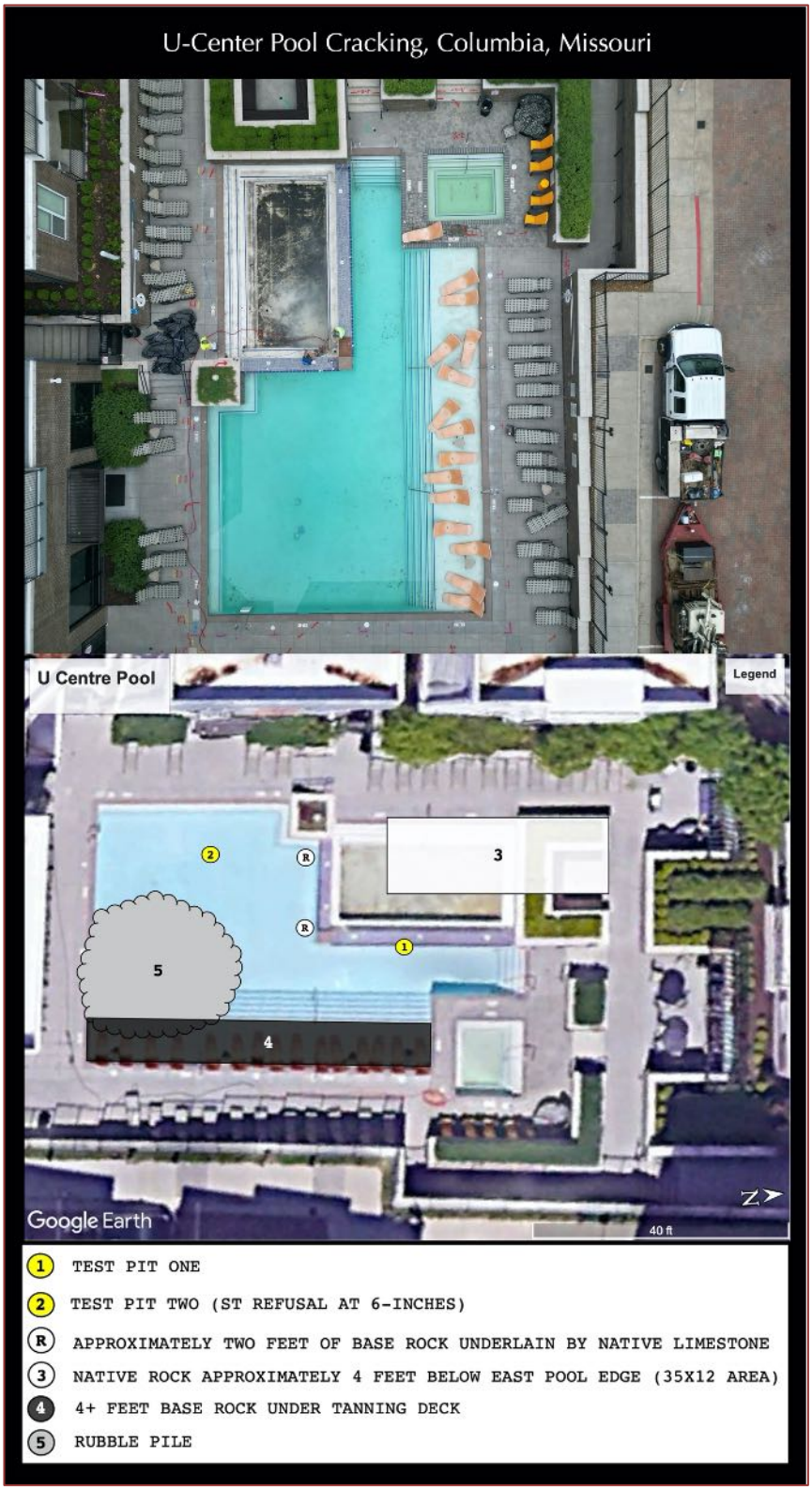

Figure 1: Drone-captured (top) and schematic (bottom) drawing of the pool showing locations of test pits, and other components.

Figure 2: Field photos of pool from where four composite cores of pool plaster and shotcrete were retrieved.

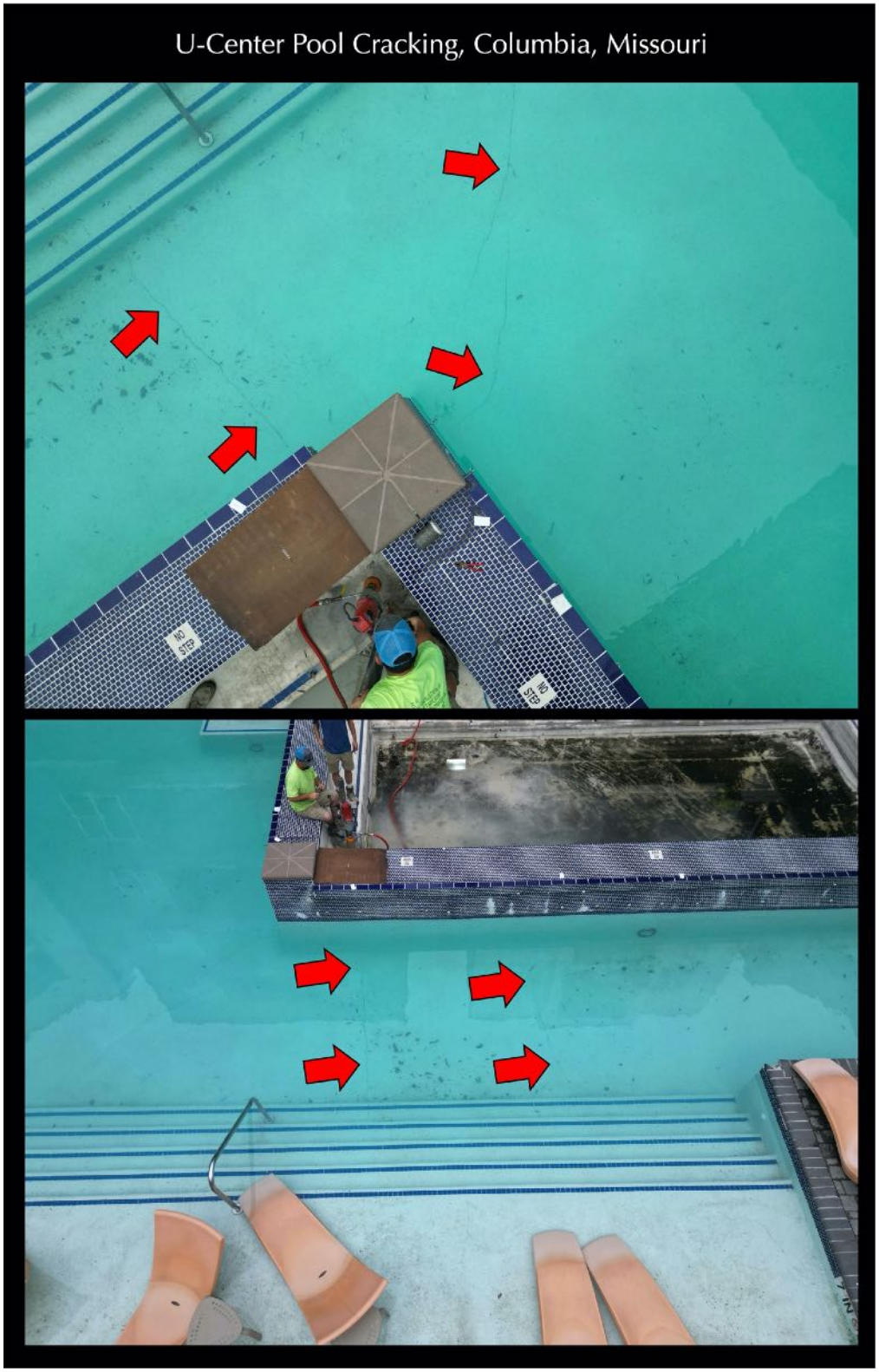

Figure 3: Cracks (marked by red arrows) on pool floor seen under water. Cracks are long, continuous and occurred at various locations as shown in subsequent field photos.

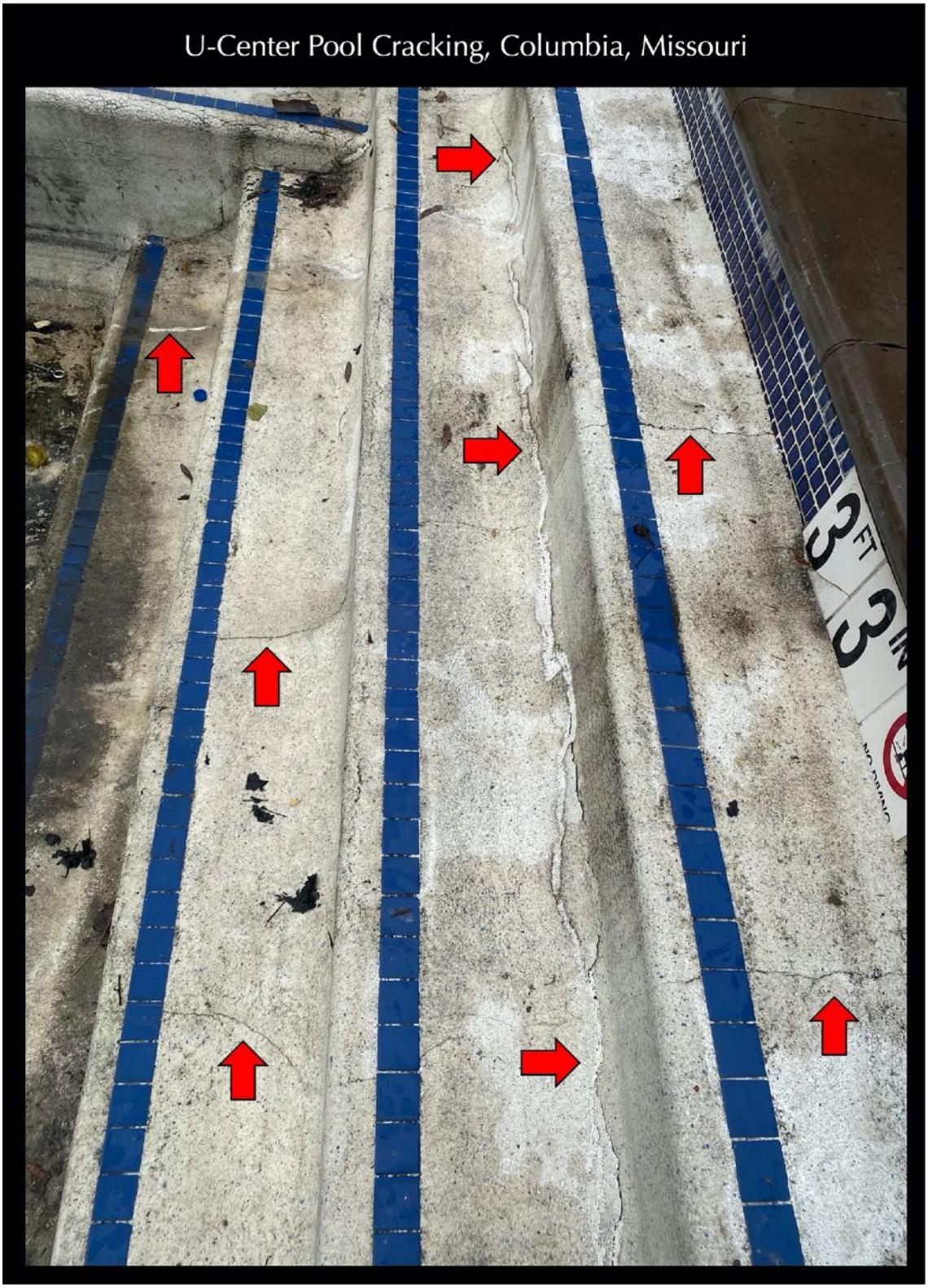

Figure 4: Long, parallel longitudinal and transverse through-steps cracks marked by red arrows. Notice many wider cracks were previously attempted to seal with elastomeric crack sealant, yet further development of finer-width unsealed cracks for steady penetration of pool water into the shotcrete.

Figure 5: Both long, continuous, and short discontinuous cracks marked by red arrows. Many cracks have traversed through the steps and walls to the floor.

Figure 6: X-shaped intersecting cracks at the corners (top) along with long, vertical cracks on the plaster walls (bottom) marked by red arrows.

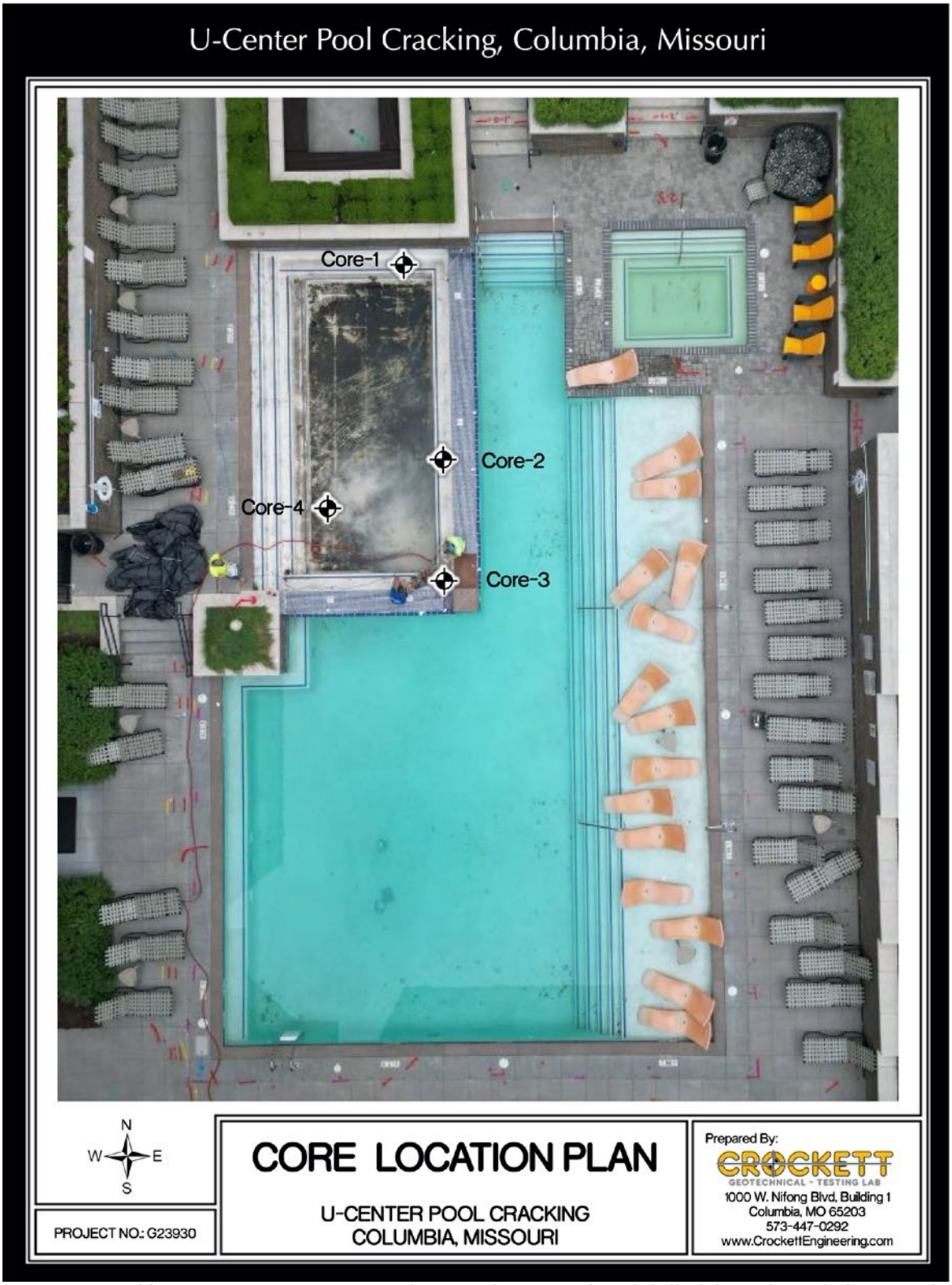

Figure 7: Locations of four cores Nos. 1 to 4 around various location of pool drilled through pool plaster to shotcrete and provided for detailed petrographic examinations.

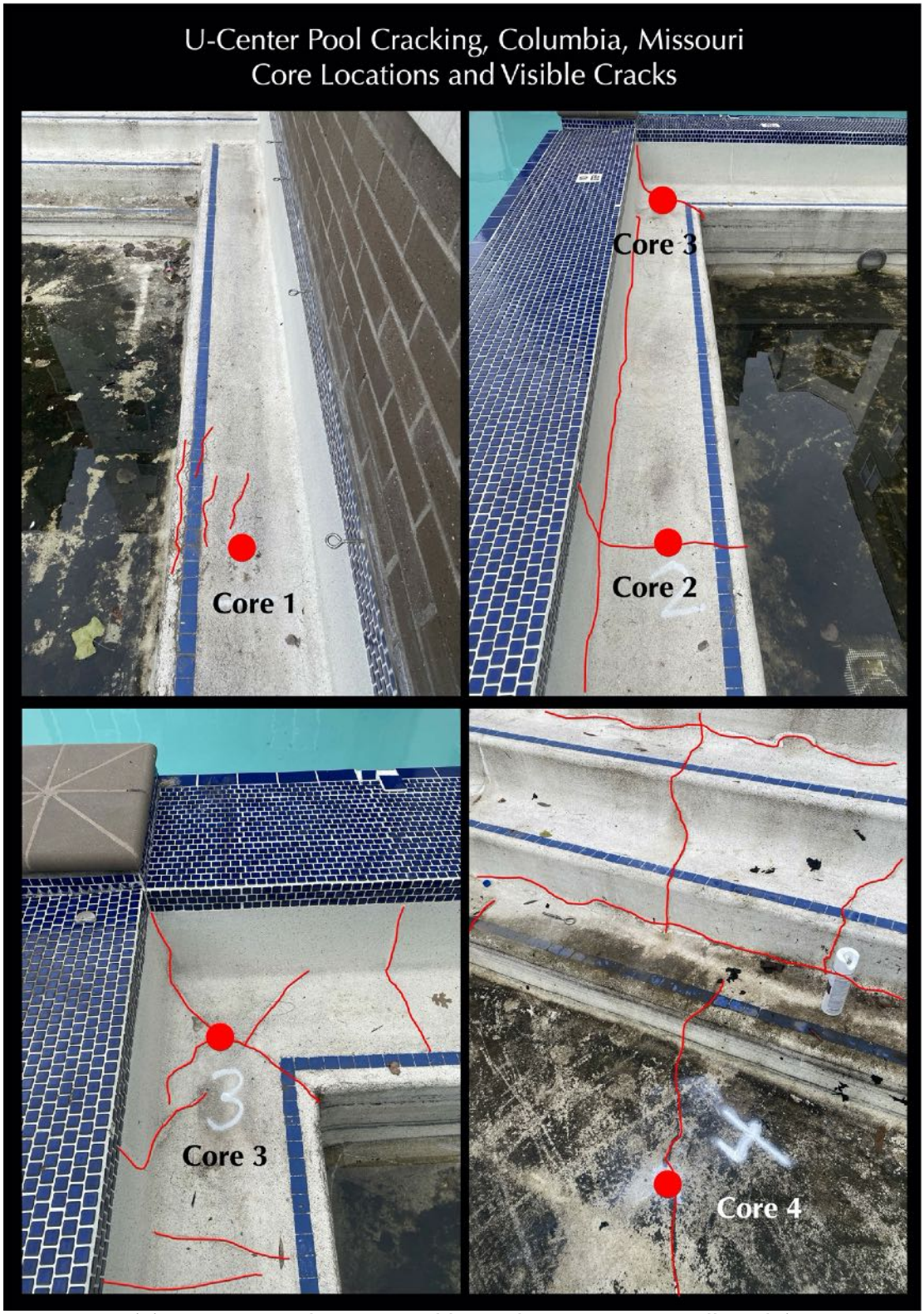

Figure 8: Locations of four cores in relation to visible cracks. Core 1 was collected from an area of short, discontinuous cracks where the core itself showed no visible cracks on the plaster's exposed surface, when received. Core 2 was over a long, continuous crack that has traversed through the pool wall and steps to the floor. Core 3 was from X-shaped intersecting cracks at a corner. Core 4 was from a visible crack on the floor.

SAMPLES

PHOTOGRAPHS, IDENTIFICATION, INTEGRITY, AND DIMENSIONS

Core ID	Diameter	Length	Exterior Surface	Interior Surface	Cracking	Embedded Items	Plaster Thickness Max. measured on cross section, and Bond	Coarse Voids	Integrity
1	3¾ in. (90 mm)	14 in. (350 mm)	Sound plaster surface	Fresh Fracture	No visible cracking on the cylindrical surface	None	15 mm, well-bonded to Shotcrete with an intermediate leveling course	Mostly at the bottom/ interior end of core (Fig.10)	Intact, Dry, Ring-sounded resonance
2	3¾ in. (90 mm)	14 in. (350 mm)	Plaster surface with a visible crack that has been sealed	Fresh Fracture	Crack extended to a depth of 10.5 in. having a surface width of 1.5 mm	No. 4 at 4 in. depth (Fig. 16)	9 mm, well-bonded to Shotcrete with an intermediate leveling course	Mostly at mid-depth location (Fig. 13)	Broken into by a diagonal crack at 6 in. depth, Dry, Ring-sounded resonance
3	3¾ in. (90 mm)	14 in. (350 mm)	Plaster surface with a visible crack that has been sealed	Fresh Fracture	Crack extended to a depth of 5.25 in. having a surface width of 1.5 mm	No. 4 at 5.25 in. depth where the core has broken into two parts (Fig. 16)	11 mm, well-bonded to Shotcrete with an intermediate leveling course	Both at top and bottom halves have zones rich in coarse voids (Fig. 16)	Broken into two halves by a crack beneath a rebar at 5.25 in. depth, Dry, Ring-sounded resonance
4	3¾ in. (90 mm)	11 in. (270 mm)	Plaster surface with a visible crack that has been sealed	Bottom surface of pool floor slab with adhered tone	Crack through the entire 11 in. depth having a surface width of 1.5 mm, which broken the core into two longitudinal halves	None	8-11 mm, well-bonded to Shotcrete	Most at bottom half (Fig. 18)	Broken into two longitudinal halves by through-depth crack, Dry, Ring-sounded resonance

Table 1: Dimensions and conditions of four plaster-shotcrete composite cores, as received.

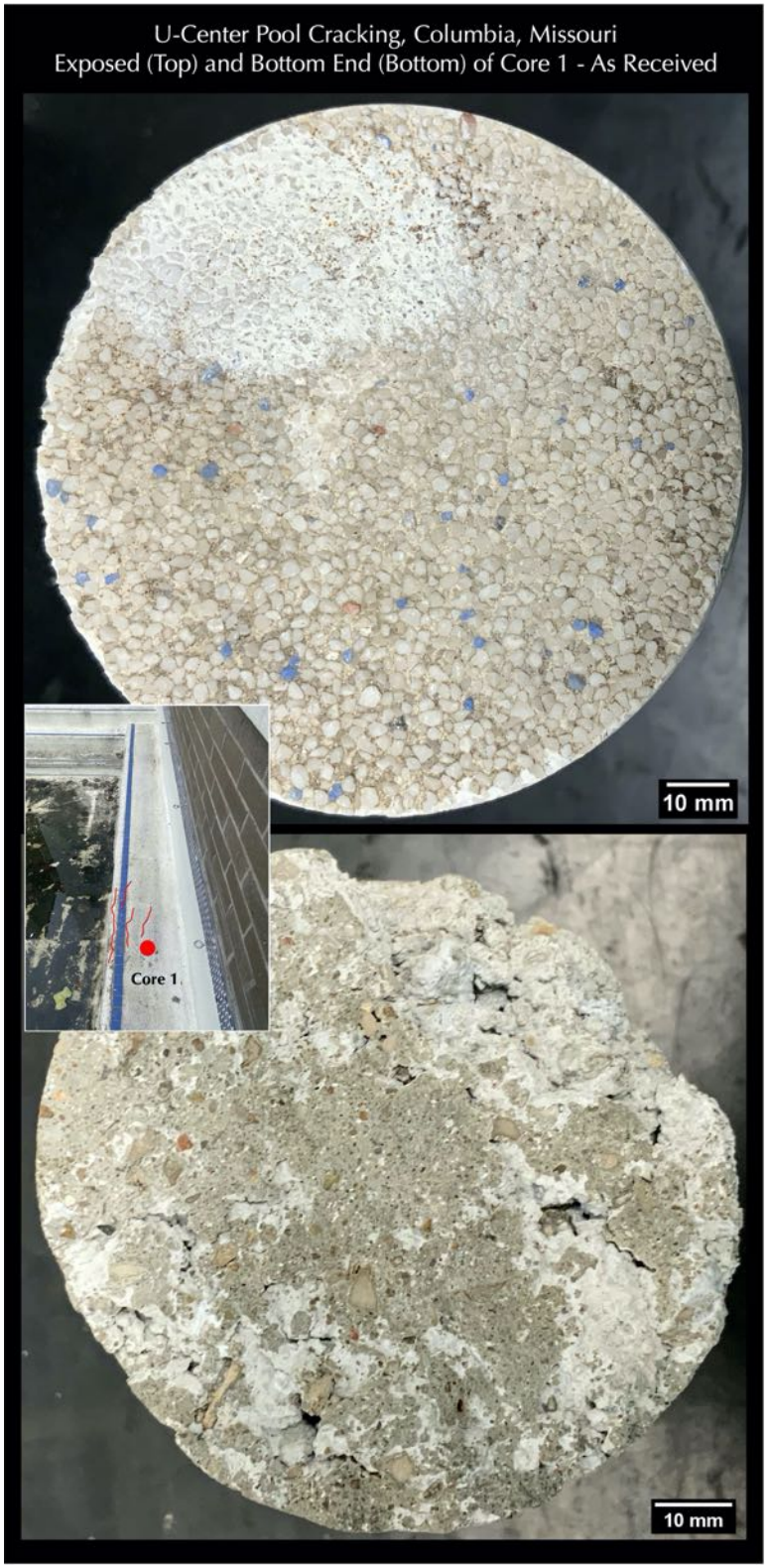

Figure 9: Shown are the top exposed surface of pool plaster without any visible cracks (top) and smooth flat formed base of shotcrete (bottom) in Core 1. Inset photo shows location of Core 1.

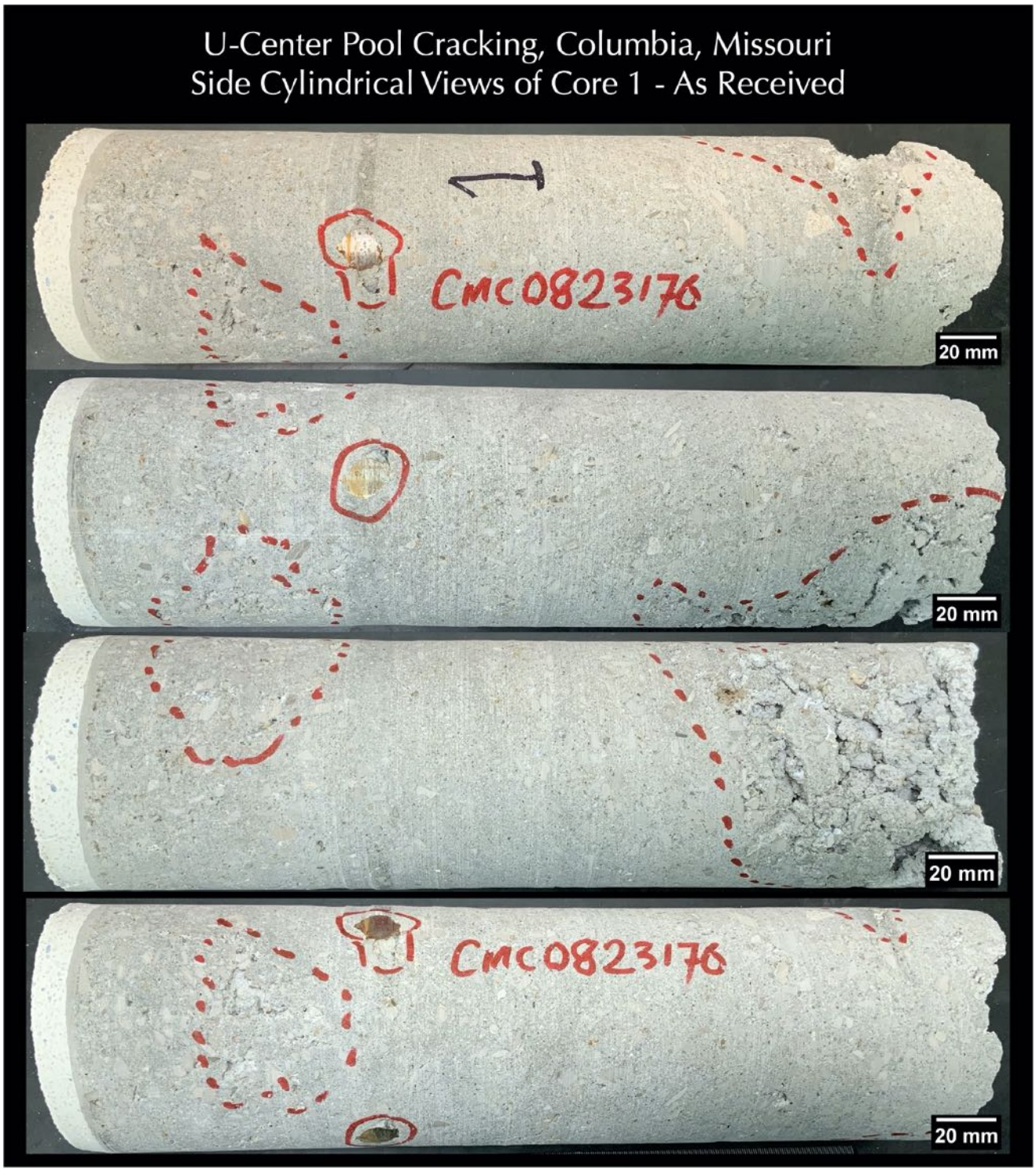

Figure 10: Shown are cylindrical surfaces of Core 1 where dotted lines enclose areas exhibiting coarse voids (honeycombing) and solid lines enclose steel reinforcement in shotcrete.

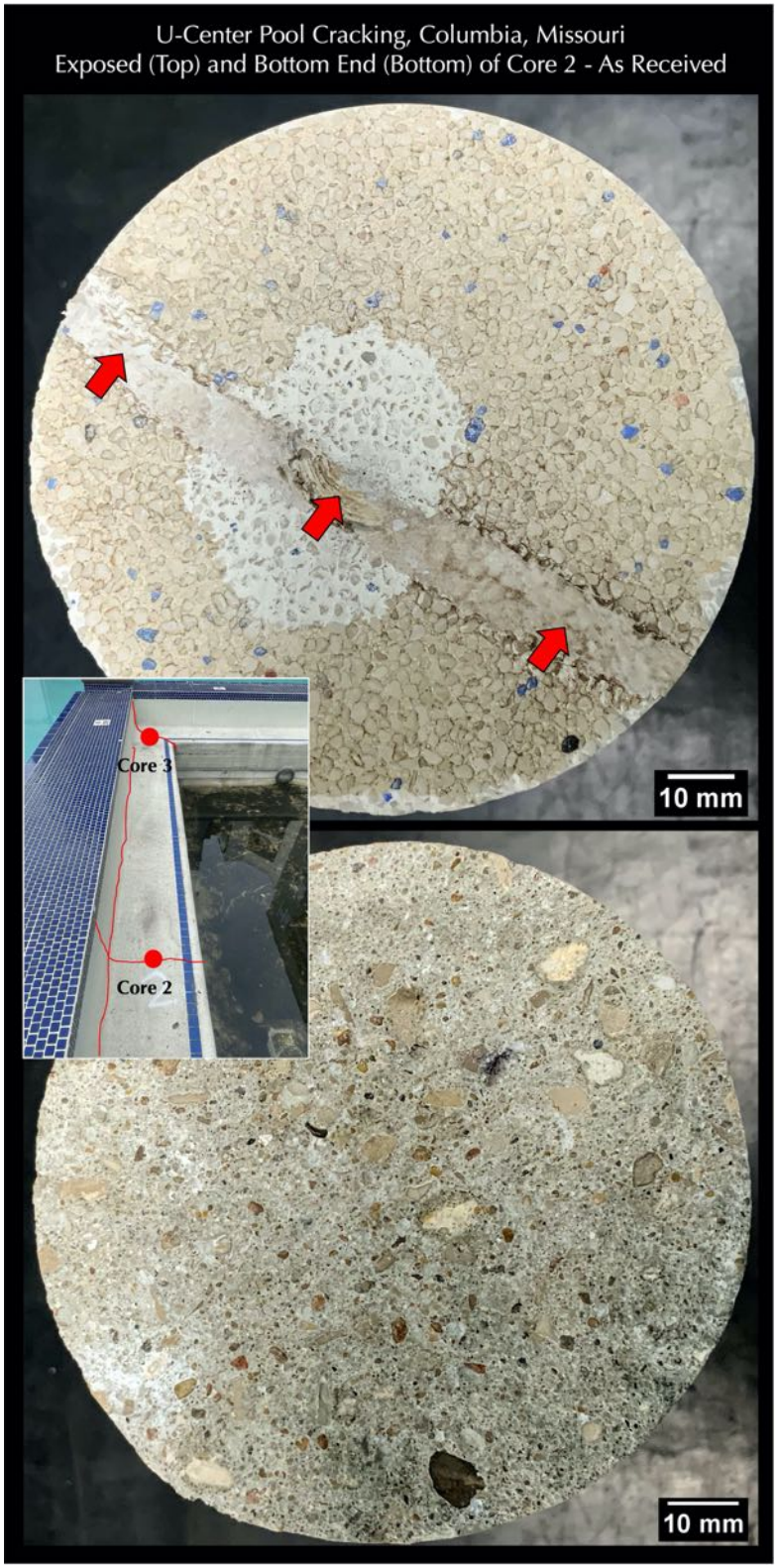

Figure 11: Shown are the top exposed surface of pool plaster with a crack that has been sealed with a repair caulk (top) and fresh fractured surface of shotcrete (bottom) in Core 2. Inset photo shows location of Core 2.

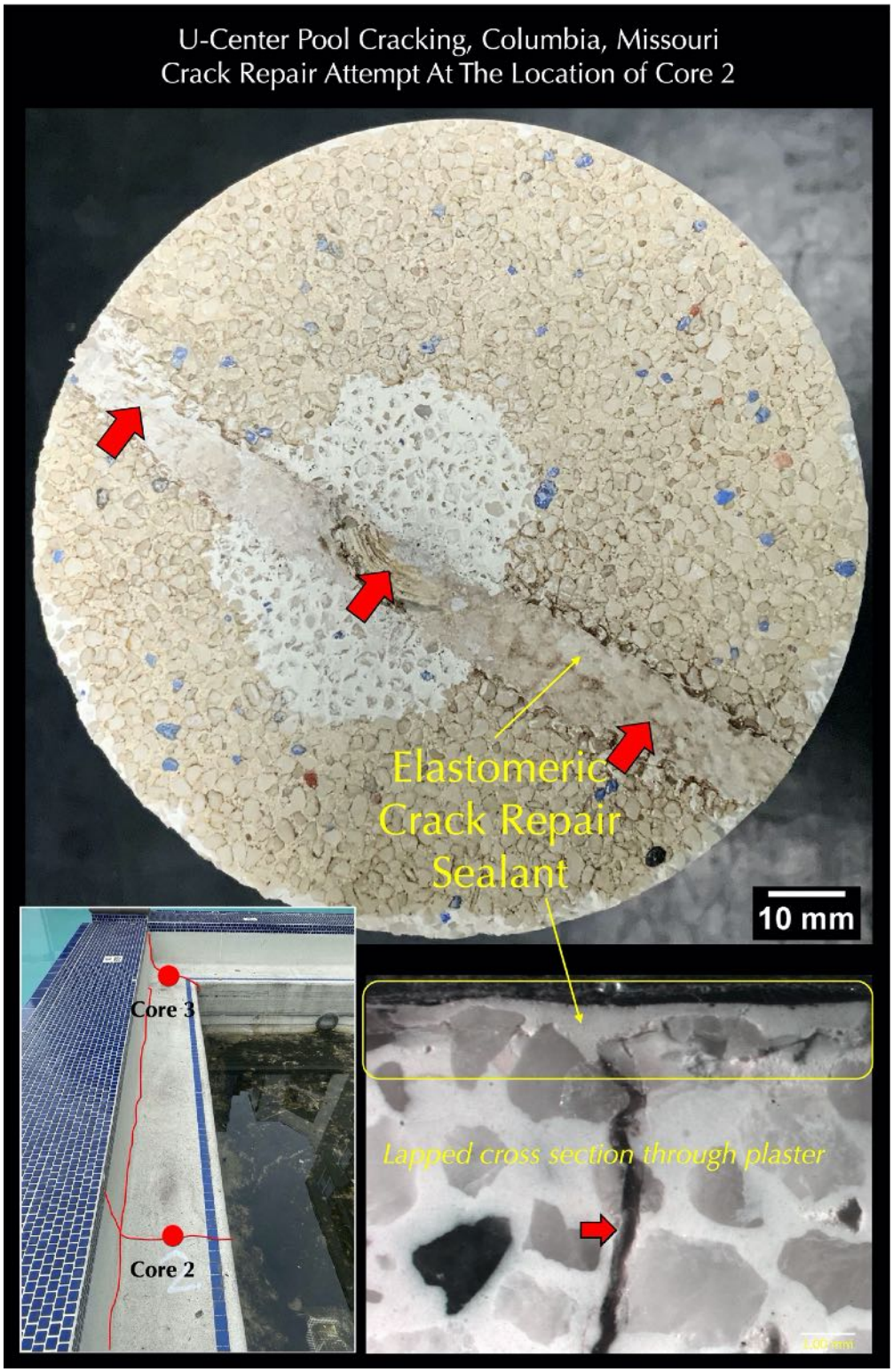

Figure 12: Elastomeric repair sealant on crack at the location of Core 2. Lapped cross section of plaster at the bottom right photo shows an apparent well bond of repair sealant to the plaster at the area of examination but ineffective penetration of crack filler into the crack where most of the crack beneath the sealant/filler is empty.

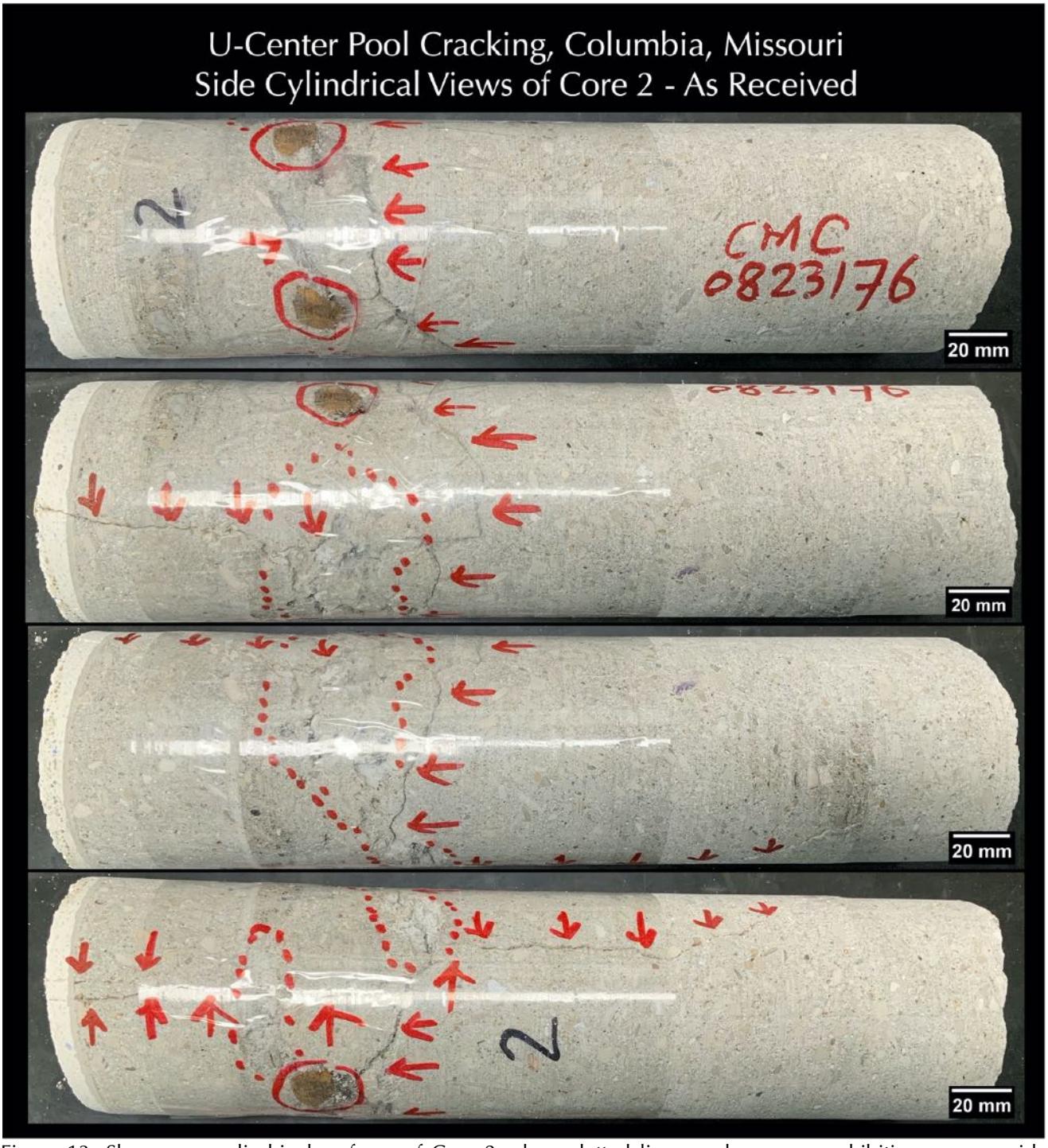

Figure 13: Shown are cylindrical surfaces of Core 2 where dotted lines enclose areas exhibiting coarse voids (honeycombing), solid lines enclose steel reinforcement in shotcrete, and arrows show visible cracks.

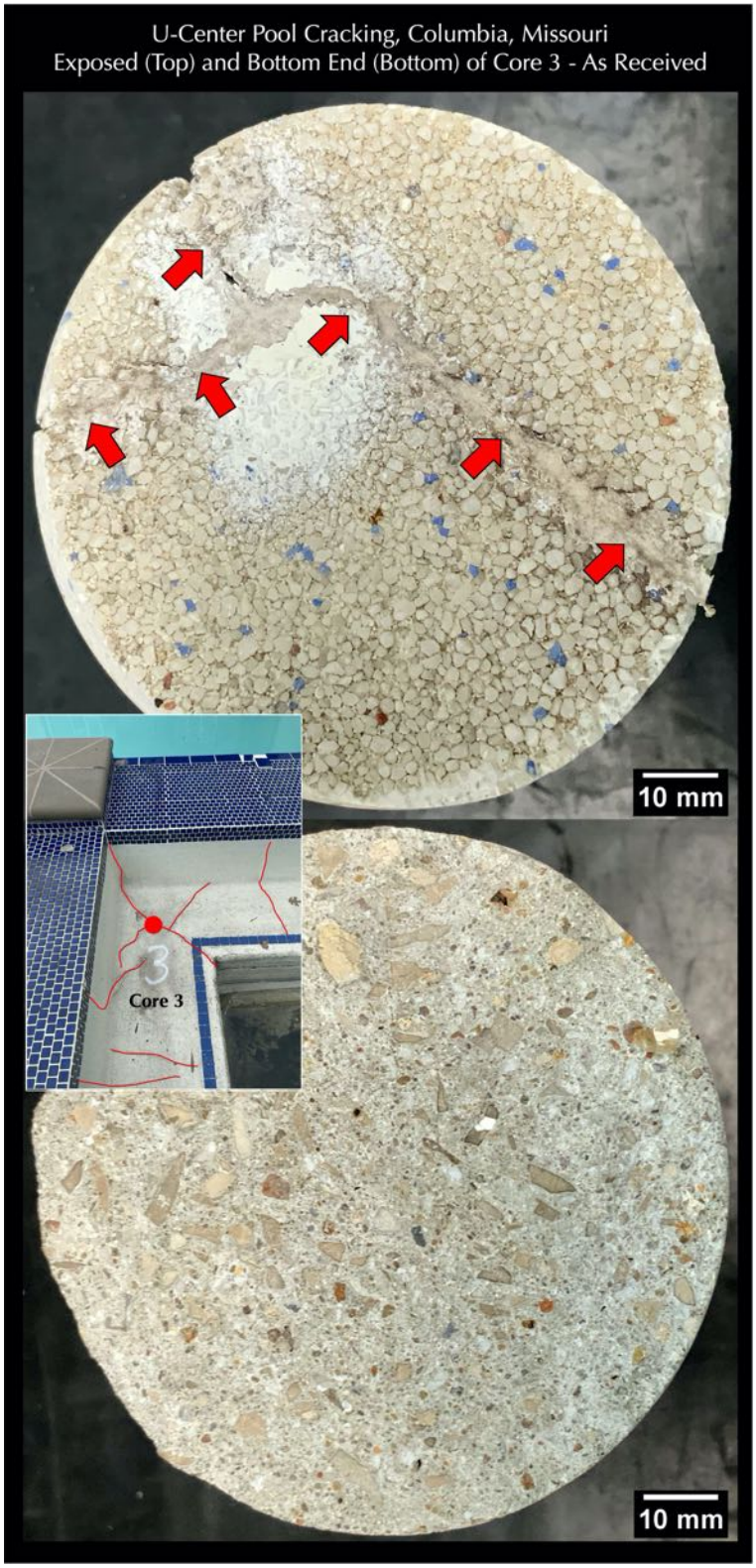

Figure 14: Shown are the top exposed surface of pool plaster with two intersecting X-shaped cracks seen at the corners that have been sealed with elastomeric repair caulk (top) and fresh fractured surface of shotcrete (bottom) in Core 3. Inset photo shows location of Core 3.

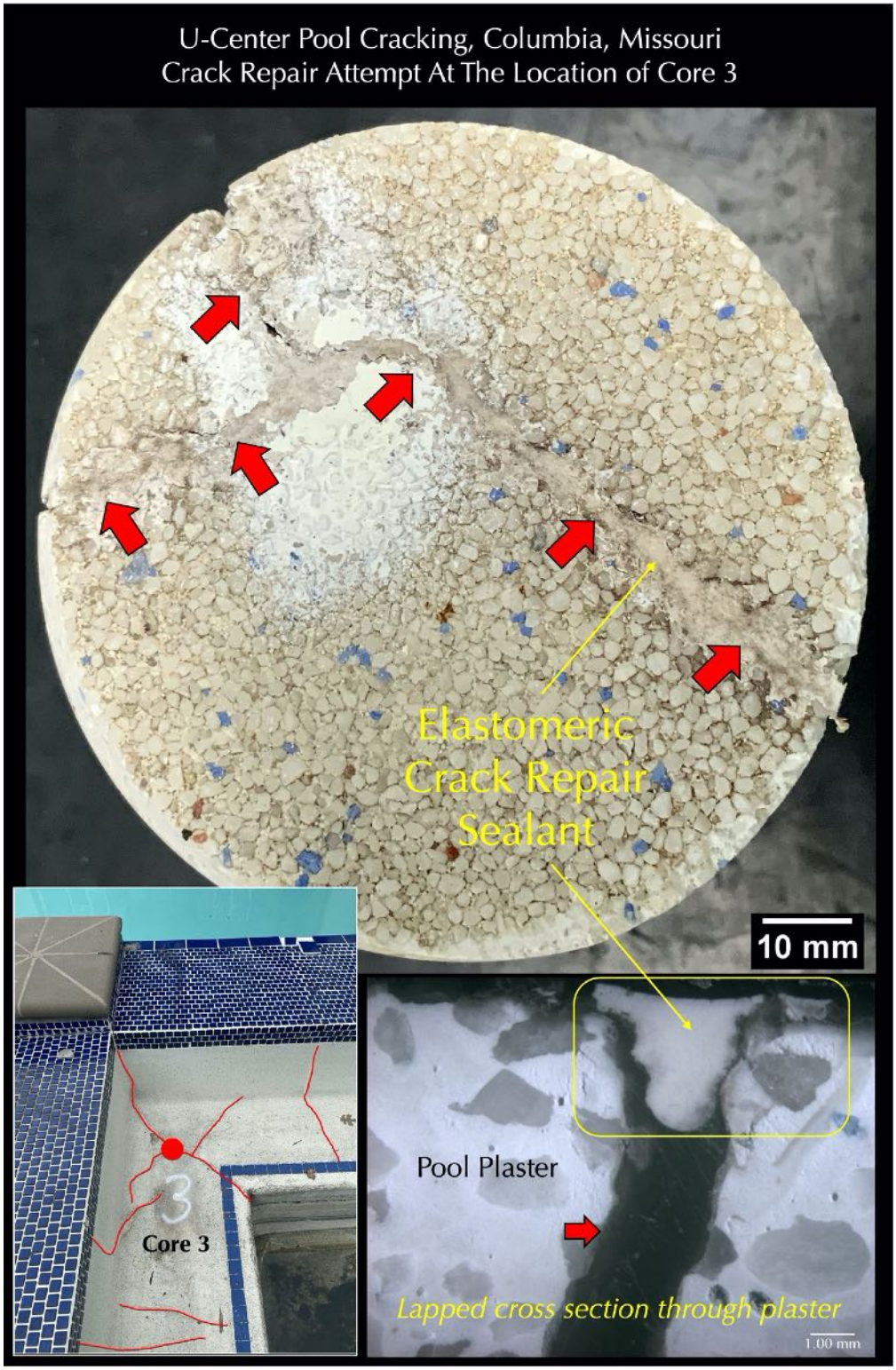

Figure 15: Elastomeric repair sealant on crack at the location of Core 3. Lapped cross section of plaster at the bottom right photo shows an apparent well bond of repair sealant to the plaster at the area of examination but ineffective penetration of crack filler into the crack where most of the crack beneath the sealant/filler is empty.

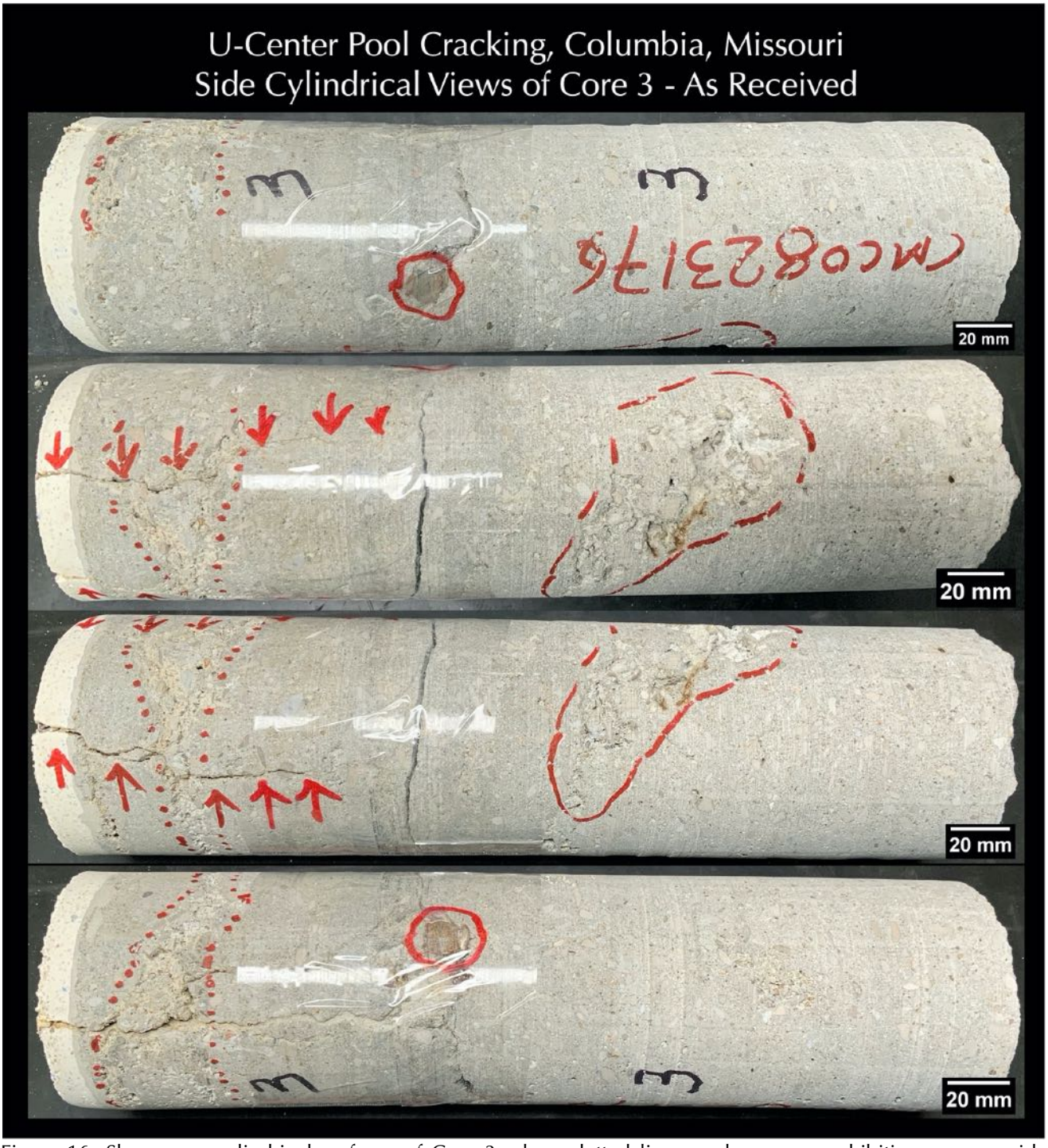

Figure 16: Shown are cylindrical surfaces of Core 3 where dotted lines enclose areas exhibiting coarse voids (honeycombing), solid lines enclose steel reinforcement in shotcrete, and arrows show visible cracks.

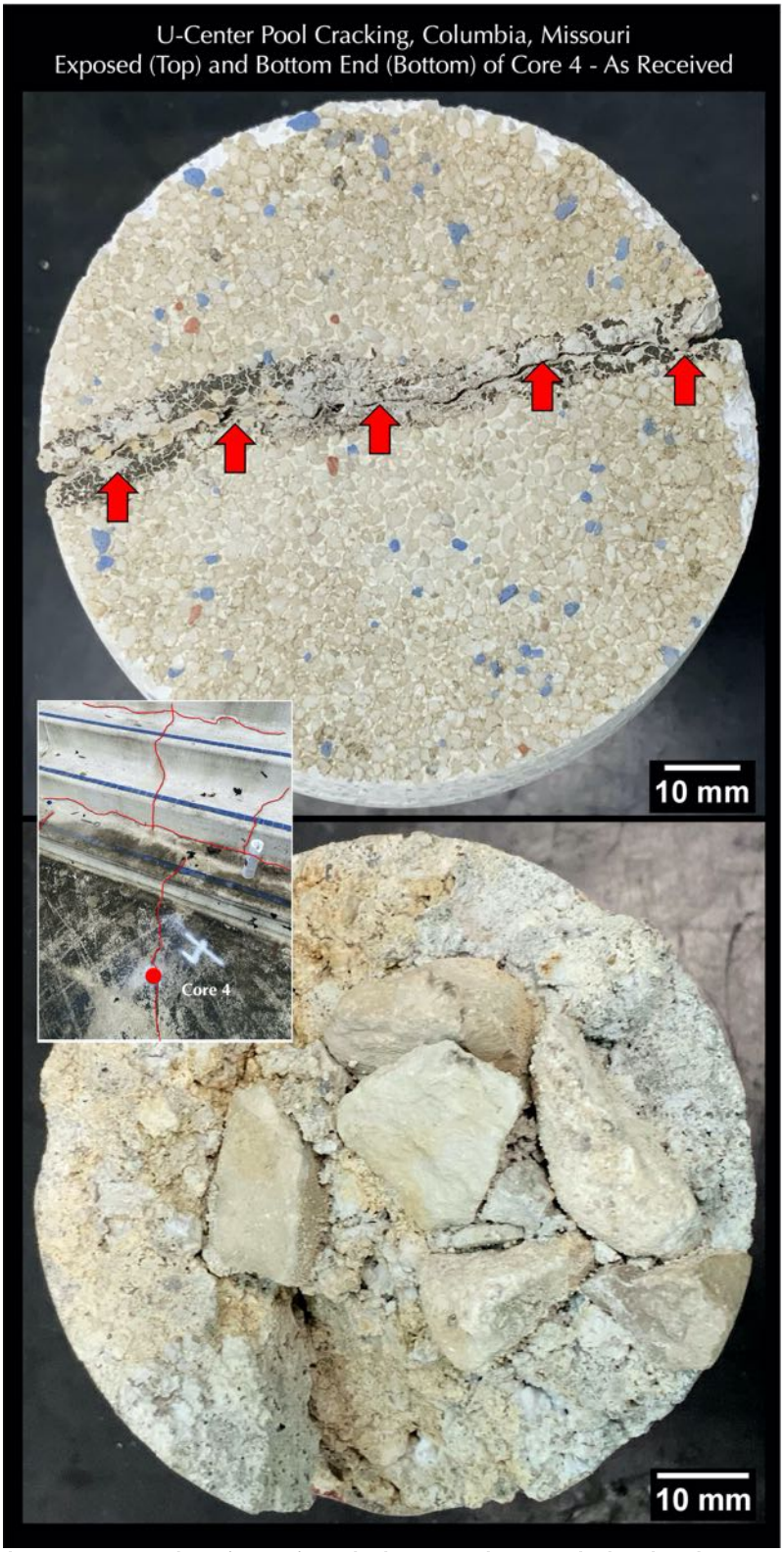

Figure 17: Shown are the top exposed surface of pool plaster with a crack that has been attempted to seal with a repair caulk but has cracked again through the seal (top) and underside of shotcrete with adhered crushed stone beneath the pool floor slab (bottom) in Core 4. Inset photo shows location of Core 4 on the floor of pool.

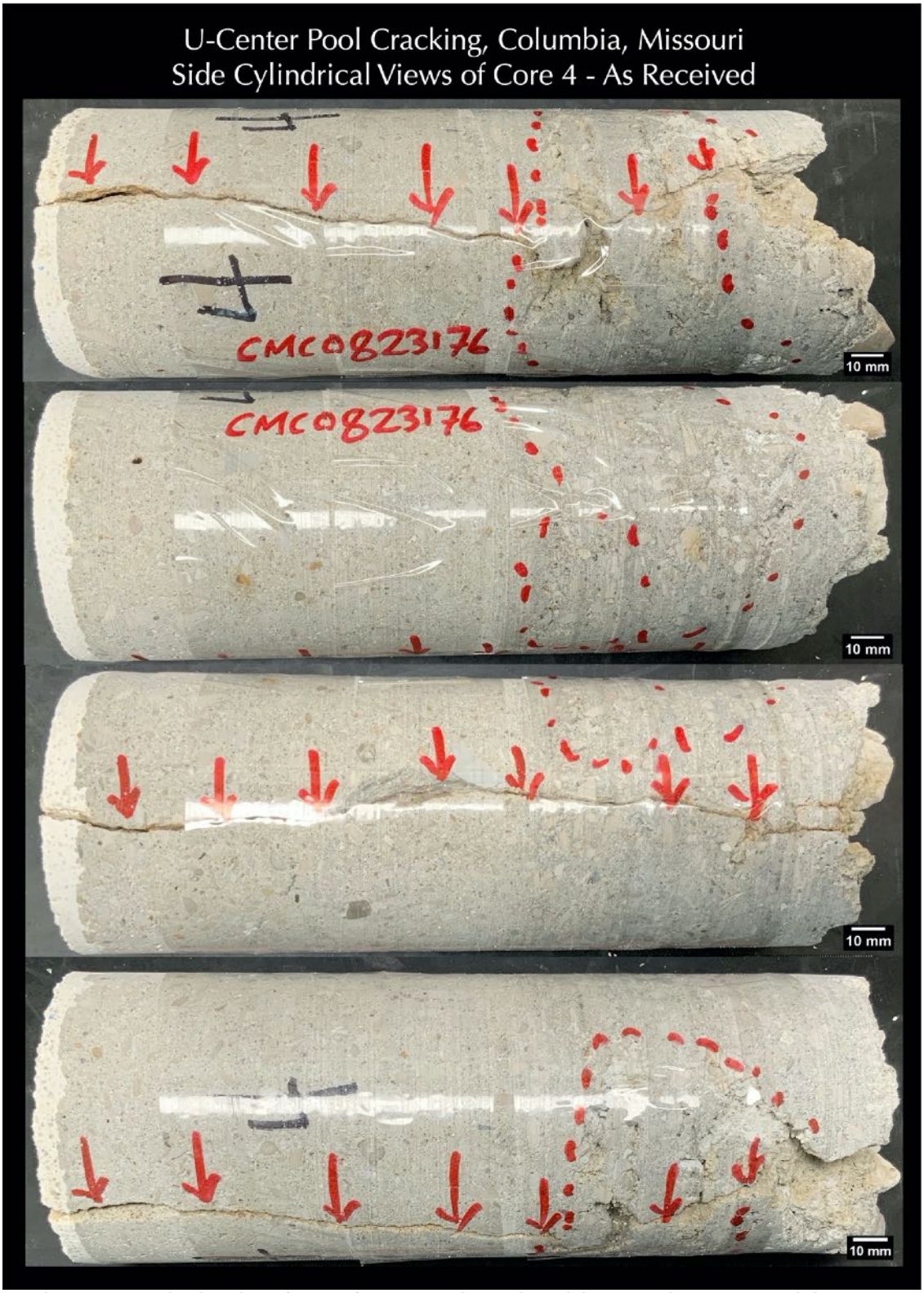

Figure 18: Shown are cylindrical surfaces of Core 4 where dotted lines enclose areas exhibiting coarse voids (honeycombing), and arrows show visible cracks.

METHODOLOGIES

PETROGRAPHIC EXAMINATIONS

The cores were examined by detailed petrographic (microscopical) examinations by following the methods of ASTM C 856 "Standard Practice for Petrographic Examination of Hardened Concrete." Details of concrete petrography, and sample preparation techniques for petrographic examinations of concrete are provided in Jana (2006).

Briefly, the steps followed during petrographic examinations of the cores include:

i. Visual examinations of cores, as received;
ii. Low-power stereo-microscopical examinations of as-received, saw-cut and freshly fractured sections, and lapped cross sections of cores for evaluation of textures, and compositions, and diagnosis of any distress;

Figure 19: Optical microscopy laboratory in CMC that houses various stereo-microscopes, and petrographic microscopes used in this study.

iii. Examinations of oil immersion mounts in a petrographic microscope for mineralogical compositions of specific areas of interest;
iv. Examinations of blue dye-mixed (to highlight open spaces, cracks, voids, etc.) epoxy-impregnated large area (50 mm × 75 mm) thin sections of plaster and shotcrete in a petrographic microscope for detailed compositional and microstructural analyses;
v. Determination of depths of carbonation and other alterations of paste from the exposed surface ends;
vi. Photographing the cores, as received and at various stages of preparation with digital camera and scanner;
vii. Micrographs of lapped cross sections and thin sections of cores taken with stereomicroscope and petrographic microscope, respectively, to provide detailed compositional and mineralogical information of plaster and shotcrete.
viii. Figure 19 shows the optical microscopy laboratory that houses various microscopes used for this study.

SCANNING ELECTRON MICROSCOPY AND X-RAY MICROANALYSES (SEM-EDS)

Figure 20: CamScan Series 2 scanning electron microscope used for examination of thin sections of cores for binder compositions of plaster and shotcrete.

After optical microscopy, thin sections of cores were further examined in a CamScan Series 2 scanning electron microscope (Figure 20) to investigate compositions of pool plaster, leveling course, and shotcrete. The instrument is equipped with a high-resolution column 40Å tungsten, 40 kV electron optics zoom condenser 75° focusing lens operating at 20 kV, equipped with a variable geometry secondary electron detector, backscatter electron detector, EDS detector for observations of microstructures at high-resolution, compositional analysis, and quantitative determinations of major element oxides from various areas of interest, respectively. Revolution 4Pi software is used for digital storage of secondary electron and backscatter electron images, elemental mapping, and analysis along a line, a point or an area of interest. 50 mm × 75 mm size thin sections of cores were polished, coated with a gold-palladium alloy, and used with a custom-made aluminum sample holder in the large multiported chamber with the eucentric 50 × 100 mm motorized stage. SEM-EDS studies were done by using the methods of ASTM C 1723.

PETROGRAPHIC EXAMINATIONS

SHOTCRETE (WET-MIX) VERSUS GUNITE (DRY-MIX)

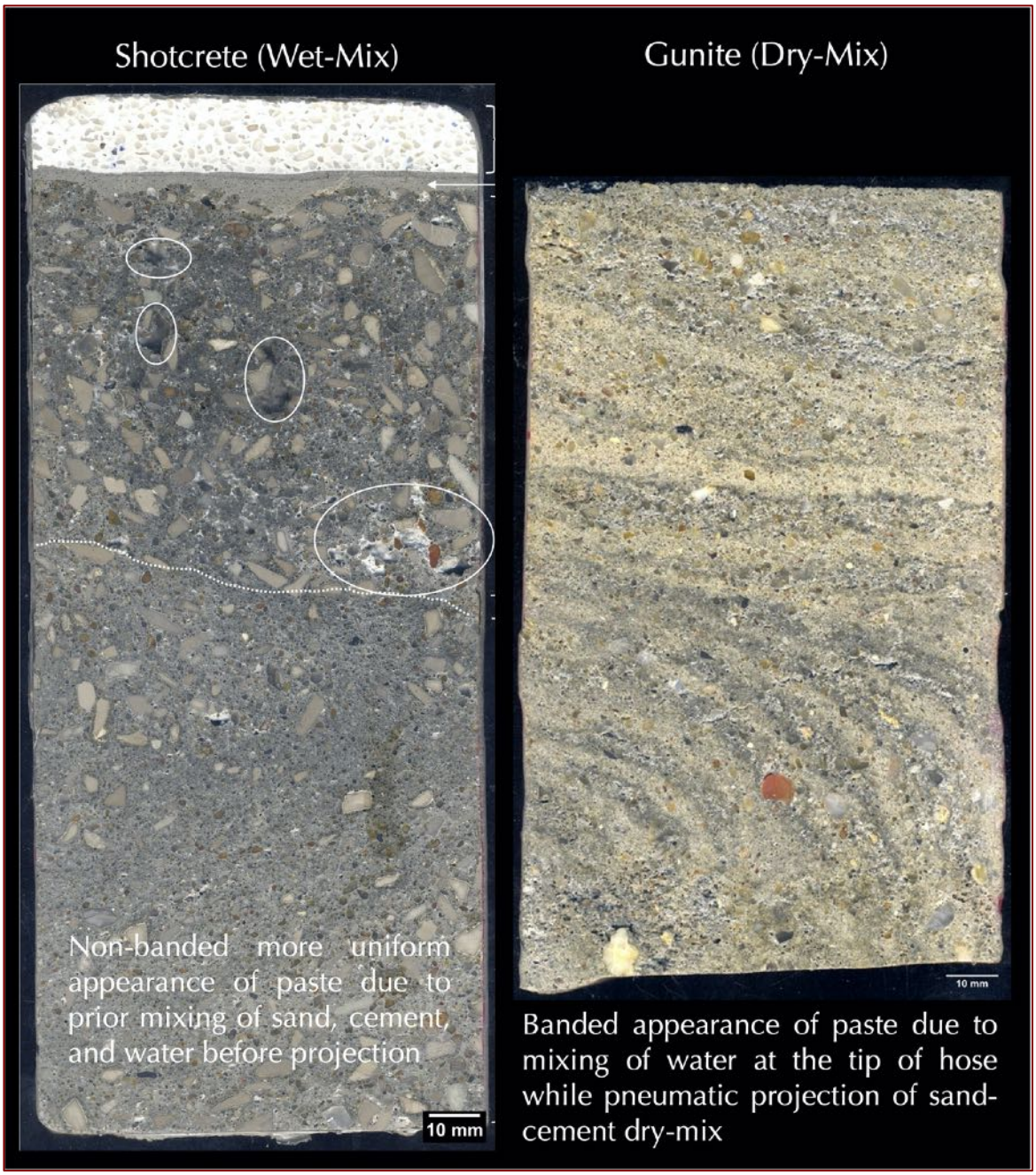

Figure 21: Shotcrete is a wet-mix of sand, cement, and water pneumatically projected onto the pool walls whereas gunite is a dry sand-cement mix where water is added during release of dry-mix at the tip of the hose. This basic difference in pre-mixing of ingredients in shotcrete versus mixing while release from hose usually creates a banded appearance of paste in the dry-mix gunite as alternating darker and lighter gray bands of paste as seen in the lapped cross section of a gunite core at right from a different project. Shotcrete usually lacks such a banded appearance, instead, shows a more uniform paste color for premixing of ingredients, except perhaps much wider zones of paste of slightly different color tones from projection of mix of slightly different water-cementitious materials ratios as seen in the lapped cross section of Core 1 from this project at left.

SAW-CUT AND LAPPED CROSS SECTIONS

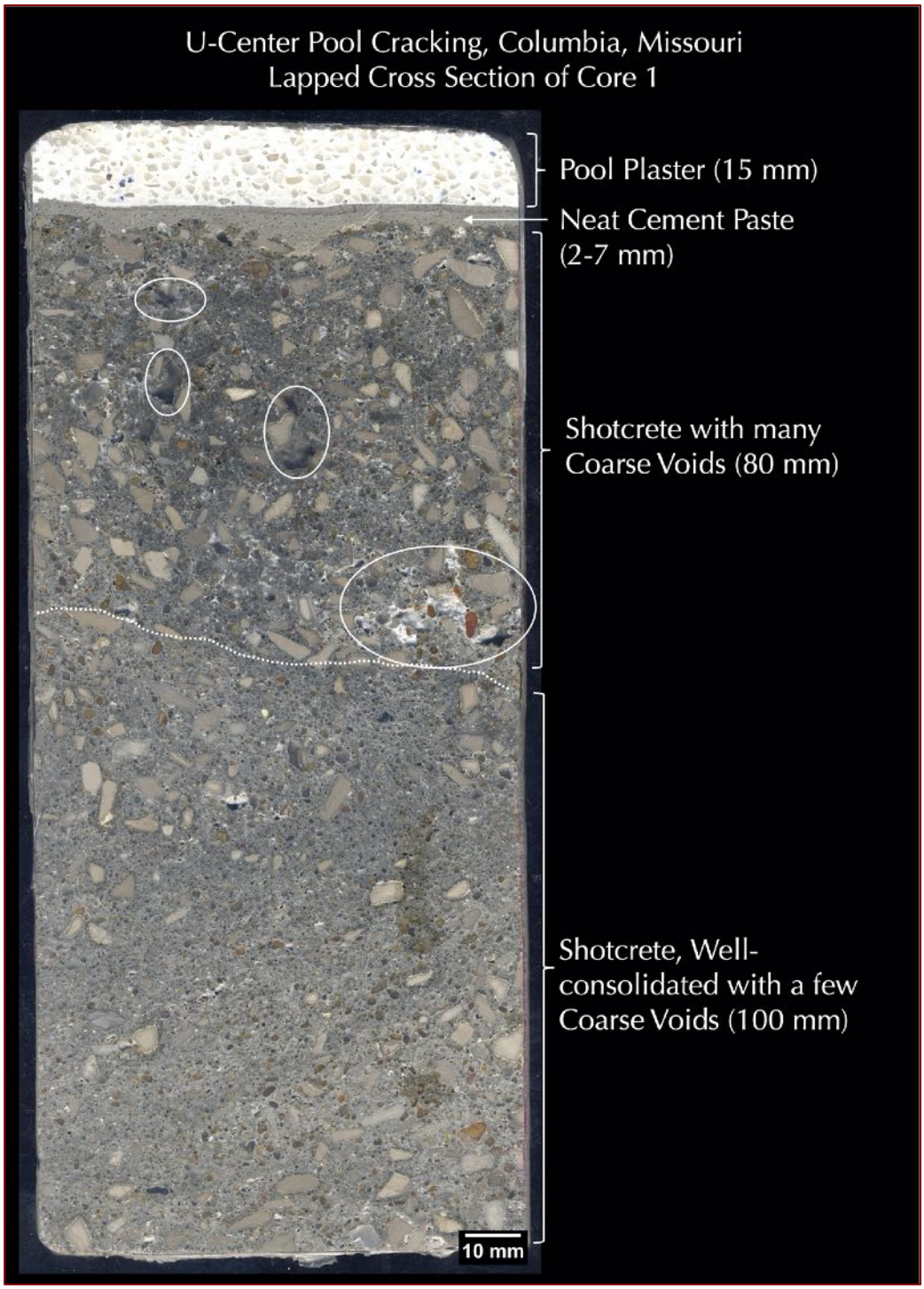

Figure 22: Lapped cross section of Core 1 showing: (a) 15 mm thick dense, white pool plaster, which is intimately bonded to (b) a medium to dark gray 2 to 7 mm thin paste-rich layer applied as a leveling coat on shotcrete prior to the installation of plaster, and (c) the main body of shotcrete consisting of areas rich in coarse voids as well as denser areas free of visible voids and have variable water-cementitious ratios due to the manner of pneumatic applications of shotcrete through a nozzle. Notice thin dark reaction rims around many crushed stone aggregate particles, which are described later.

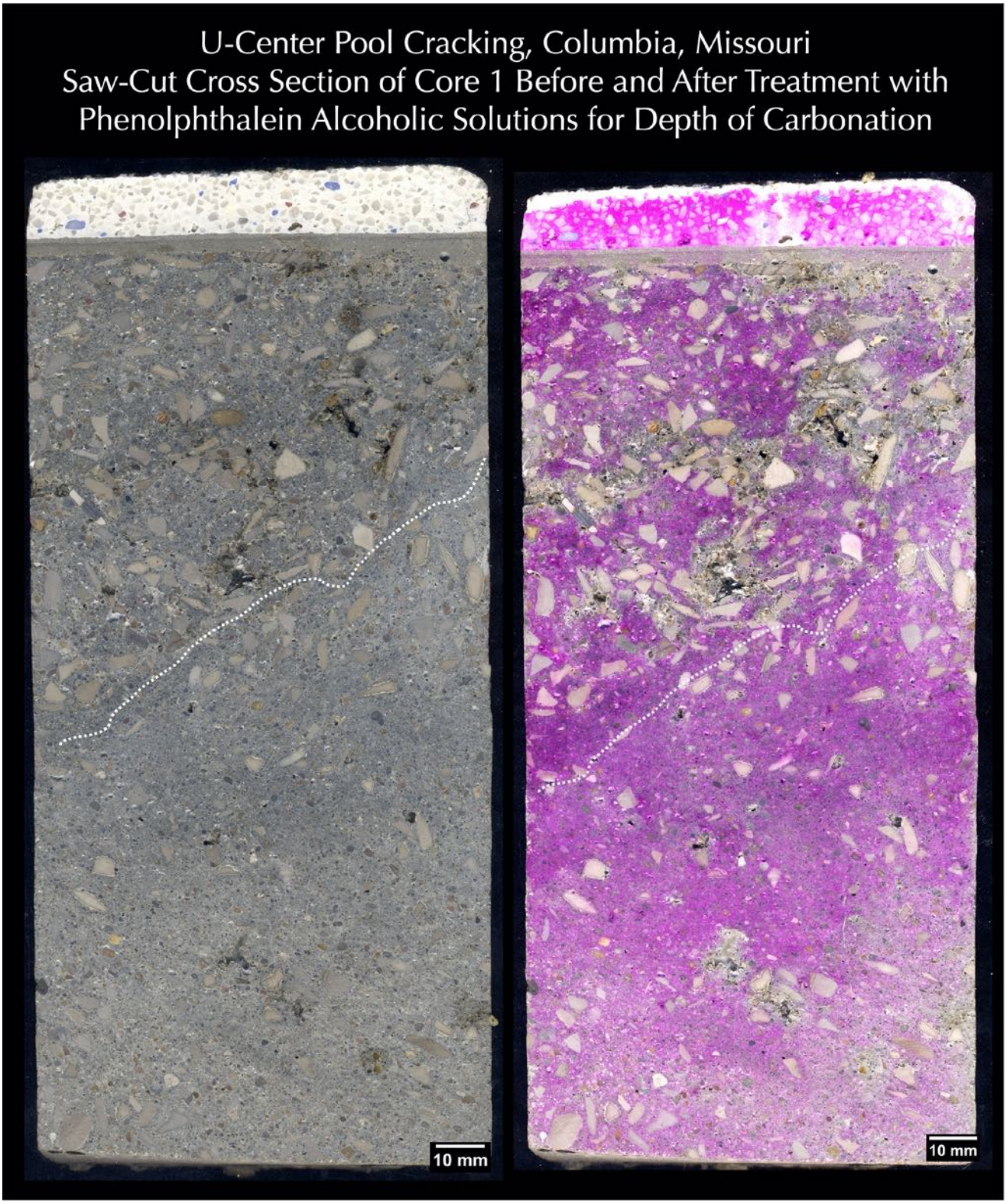

Figure 23: Sawcut cross section of Core 1 before (left) and after (right) treatment with phenolphthalein alcoholic solutions to show the depth and degree of carbonation of paste. Paste in both the pool plaster and most of the shotcrete (except in areas of coarse voids for ready penetration of atmospheric or dissolved CO_2) show lack of carbonation hence turned pink after phenolphthalein treatment whereas paste in medium to dark gray thin leveling coat shows some carbonation to remain in its inherent gray color tone after treatment due to a short exposure to atmospheric CO_2 prior to the installation of plaster.

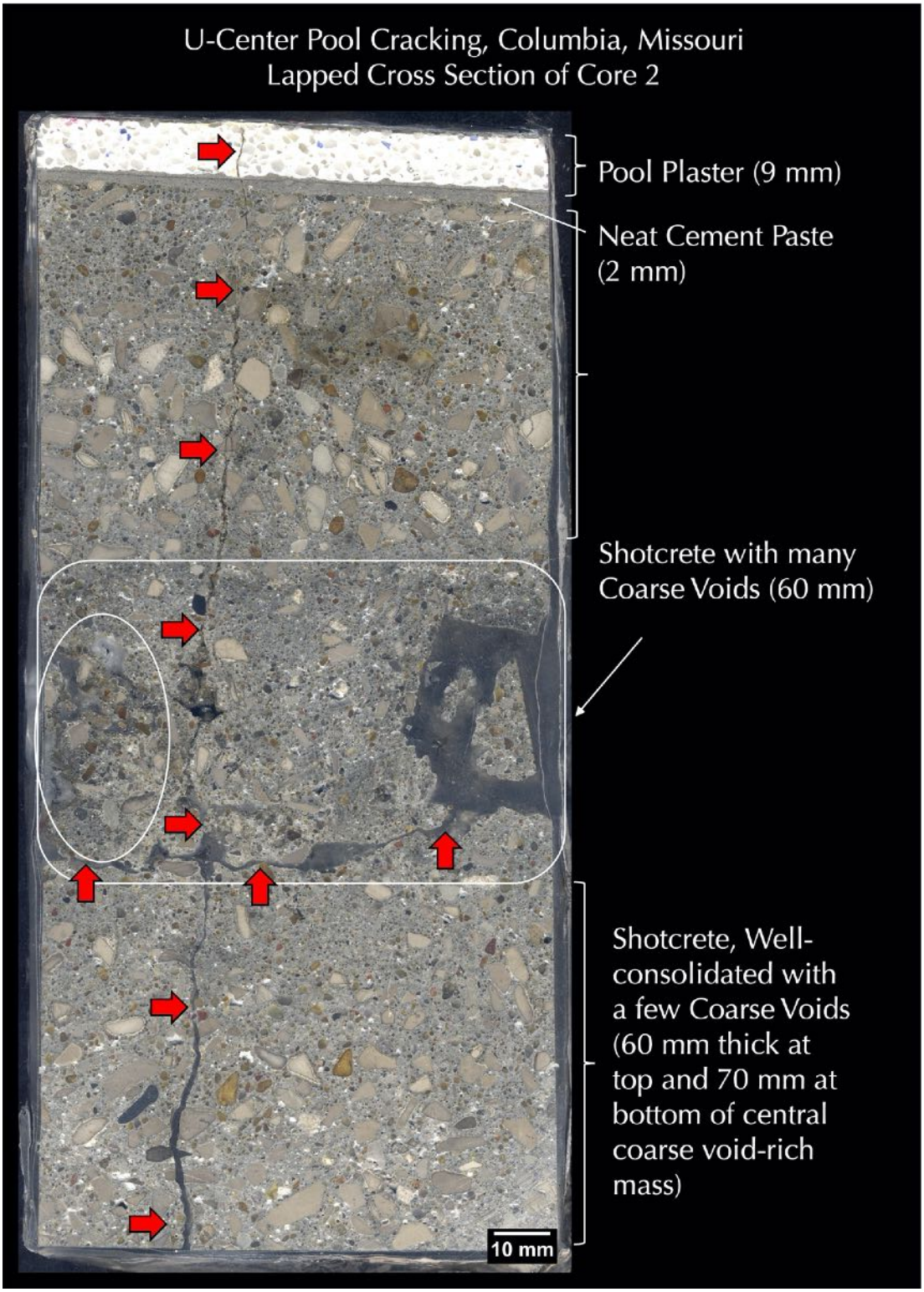

Figure 24: Lapped cross section of Core 2 showing: (a) 9 mm thick dense, white pool plaster, which is intimately bonded to (b) a medium to dark gray 2 mm thin paste-rich layer applied as a leveling coat on shotcrete prior to the installation of plaster, and (c) the main body of shotcrete consisting of areas rich in coarse voids as well as denser areas free of visible voids and have variable water-cementitious ratios due to the manner of pneumatic applications of shotcrete through a nozzle. Notice thin dark reaction rims around many crushed stone aggregate particles, which are described later. The entire core is transected through a major vertical crack that has transected and circumscribed the aggregate particles along path, as well as a surface-parallel crack in the body.

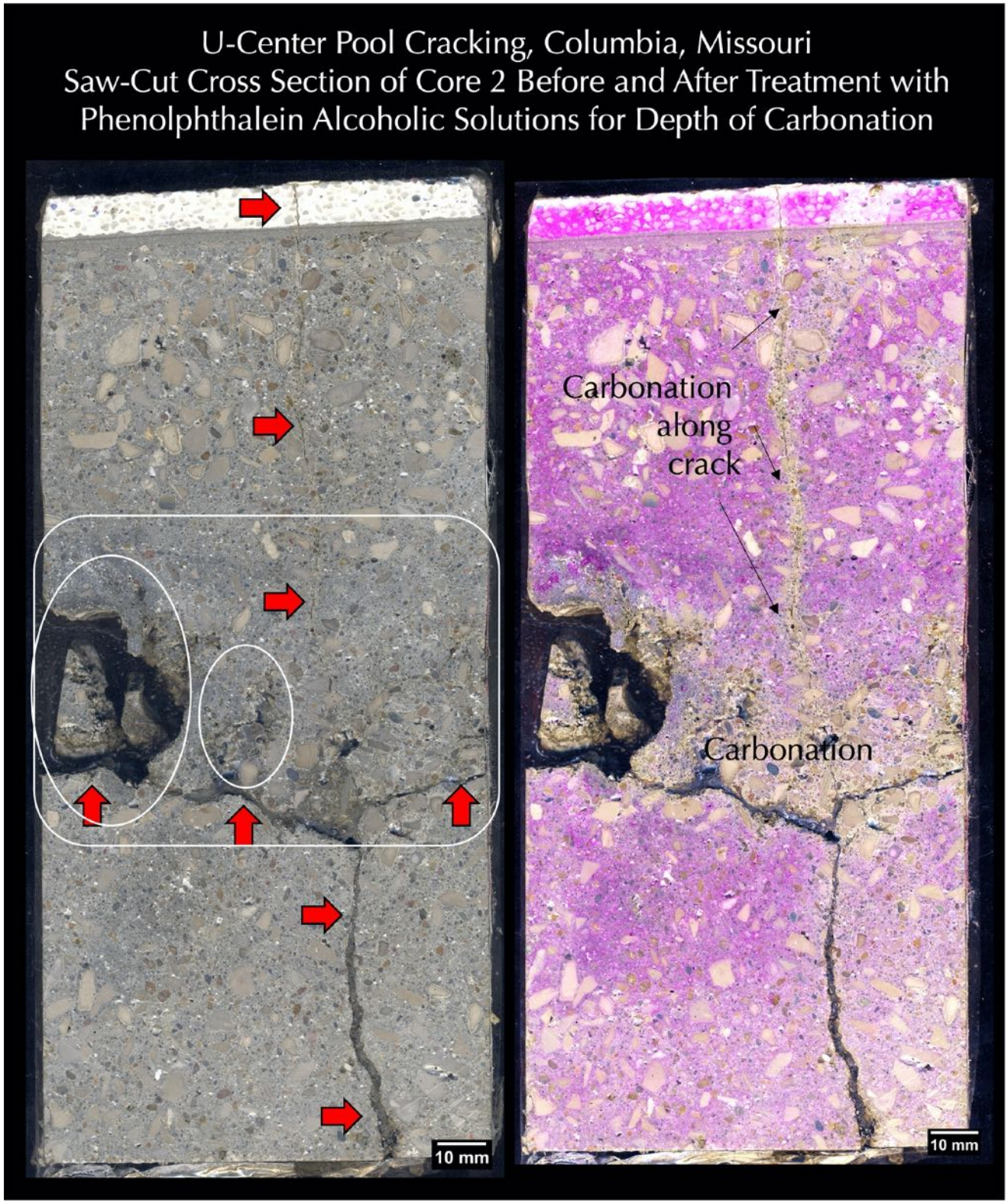

Figure 25: Sawcut cross section of Core 2 before (left) and after (right) treatment with phenolphthalein alcoholic solutions to show the depth and degree of carbonation of paste. Paste in both the pool plaster and most of the shotcrete (except along the major vertical crack and in areas of coarse voids for ready penetration of atmospheric or dissolved CO_2) show lack of carbonation hence turned pink after phenolphthalein treatment whereas paste in medium to dark gray thin leveling coat shows some carbonation to remain in its inherent gray color tone after treatment due to a short exposure to atmospheric CO_2 prior to the installation of plaster.

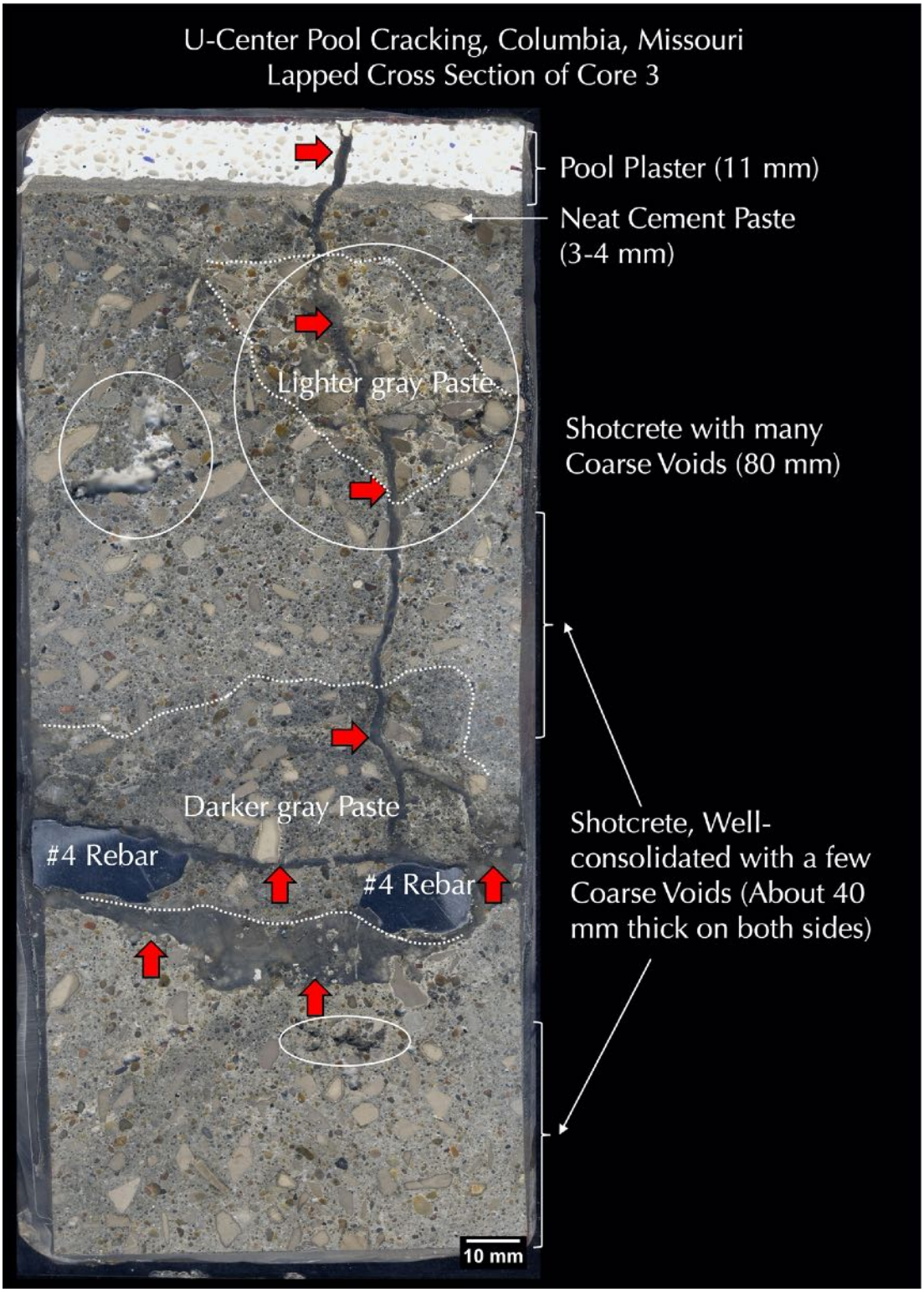

Figure 26: Lapped cross section of Core 3 showing: (a) 11 mm thick dense, white pool plaster, which is intimately bonded to (b) a medium to dark gray 3 to 4 mm thin paste-rich layer applied as a leveling coat on shotcrete prior to the installation of plaster, and (c) the main body of shotcrete consisting of areas rich in coarse voids as well as denser areas free of visible voids and have variable water-cementitious ratios due to the manner of pneumatic applications of shotcrete through a nozzle. Notice thin dark reaction rims around many crushed stone aggregate particles, which are described later. The entire core is transected through a major vertical crack that has transected and circumscribed the aggregate particles along path, as well as a surface-parallel crack in the body.

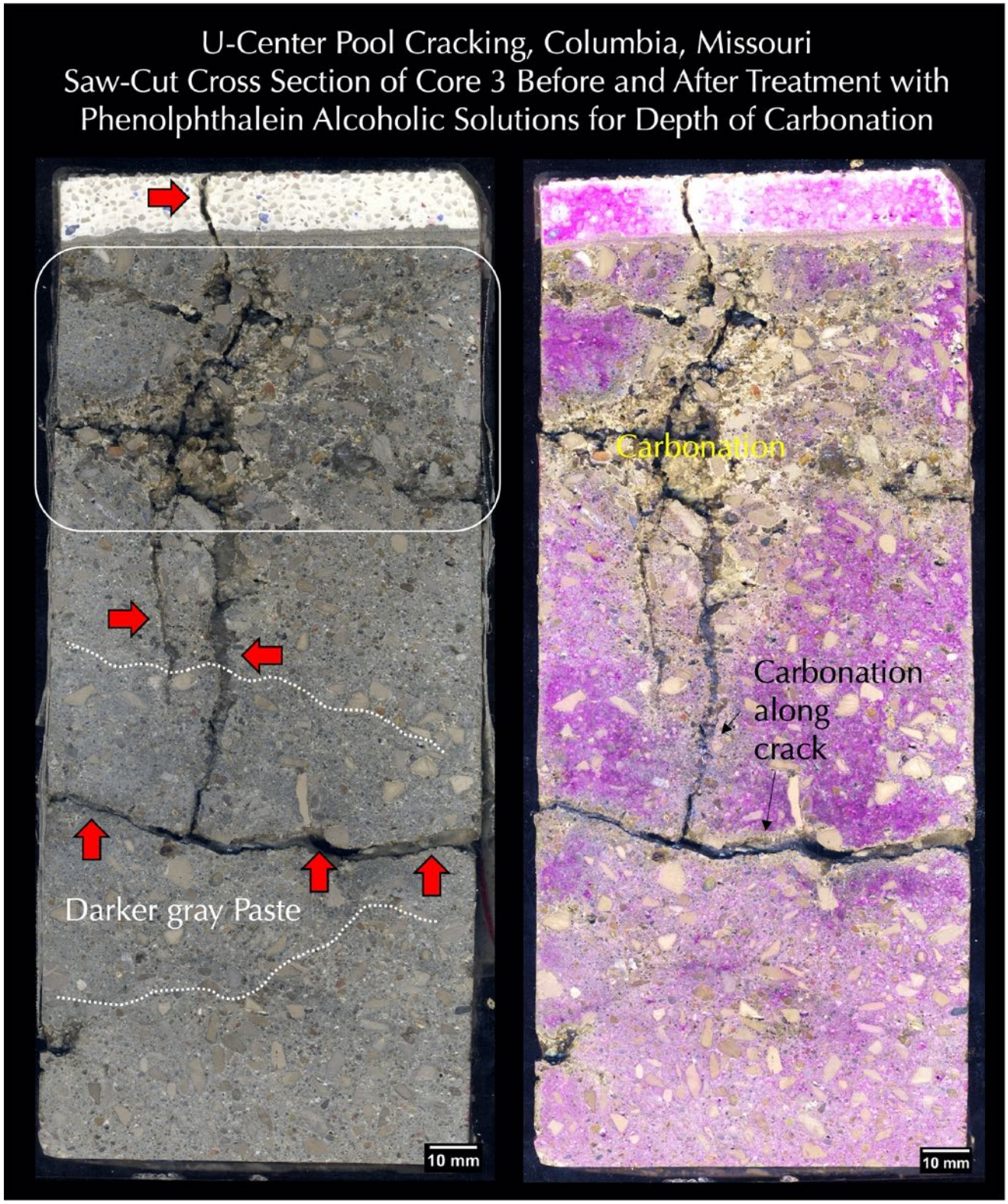

Figure 27: Sawcut cross section of Core 3 before (left) and after (right) treatment with phenolphthalein alcoholic solutions to show the depth and degree of carbonation of paste. Paste in both the pool plaster and most of the shotcrete (except along the major vertical crack and in areas of coarse voids for ready penetration of atmospheric or dissolved CO_2) show lack of carbonation hence turned pink after phenolphthalein treatment whereas paste in medium to dark gray thin leveling coat shows some carbonation to remain in its inherent gray color tone after treatment due to a short exposure to atmospheric CO_2 prior to the installation of plaster.

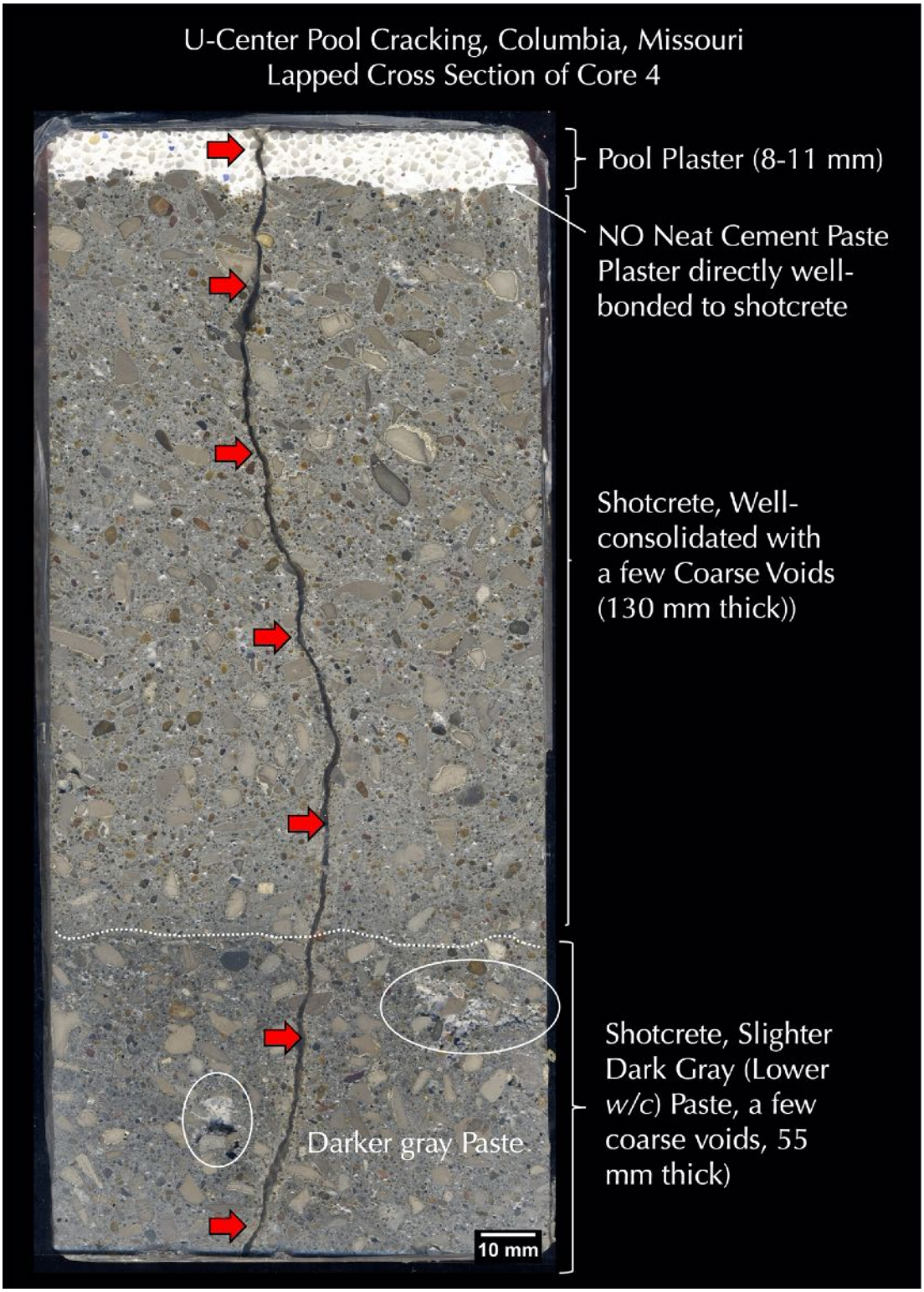

Figure 28: Lapped cross section of floor Core 4 showing: (a) 8 to 11 mm thick dense, white pool plaster, which is intimately bonded to (b) the main body of shotcrete without any intermediate leveling coat where shotcrete consists of areas rich in coarse voids as well as denser areas free of visible voids and have variable water-cementitious ratios due to the manner of pneumatic applications of shotcrete through a nozzle. Notice thin dark reaction rims around many crushed stone aggregate particles, which are described later. The entire core is transected through a major vertical crack that has transected and circumscribed the aggregate particles along its path.

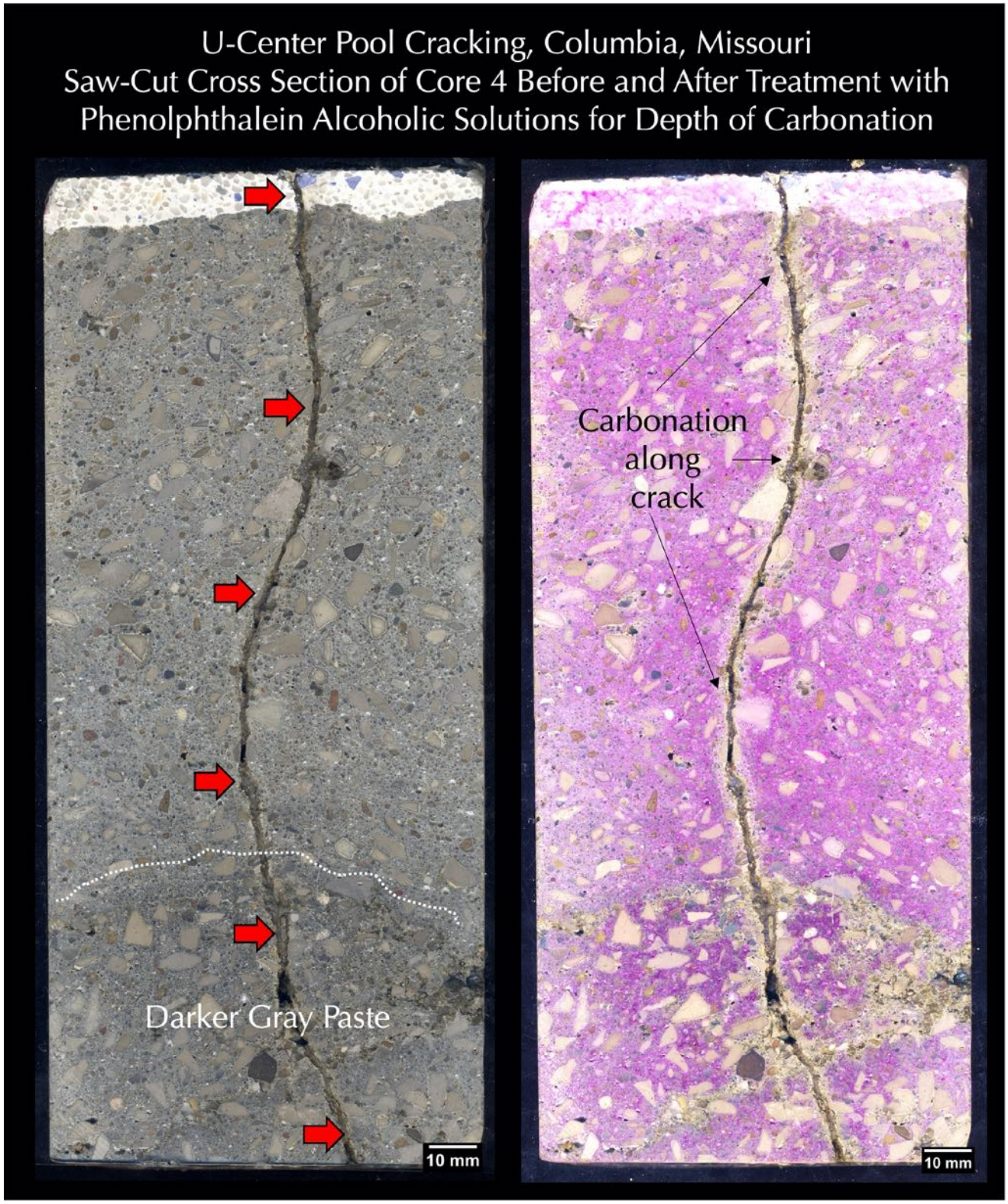

Figure 29: Sawcut cross section of Core 4 before (left) and after (right) treatment with phenolphthalein alcoholic solutions to show the depth and degree of carbonation of paste. Paste in both the pool plaster and most of the shotcrete (except along the major vertical crack and in areas of coarse voids for ready penetration of atmospheric or dissolved CO_2) show lack of carbonation hence turned pink after phenolphthalein treatment whereas paste in medium to dark gray thin leveling coat shows some carbonation to remain in its inherent gray color tone after treatment due to a short exposure to atmospheric CO_2 prior to the installation of plaster.

MICROGRAPHS OF LAPPED CROSS SECTIONS

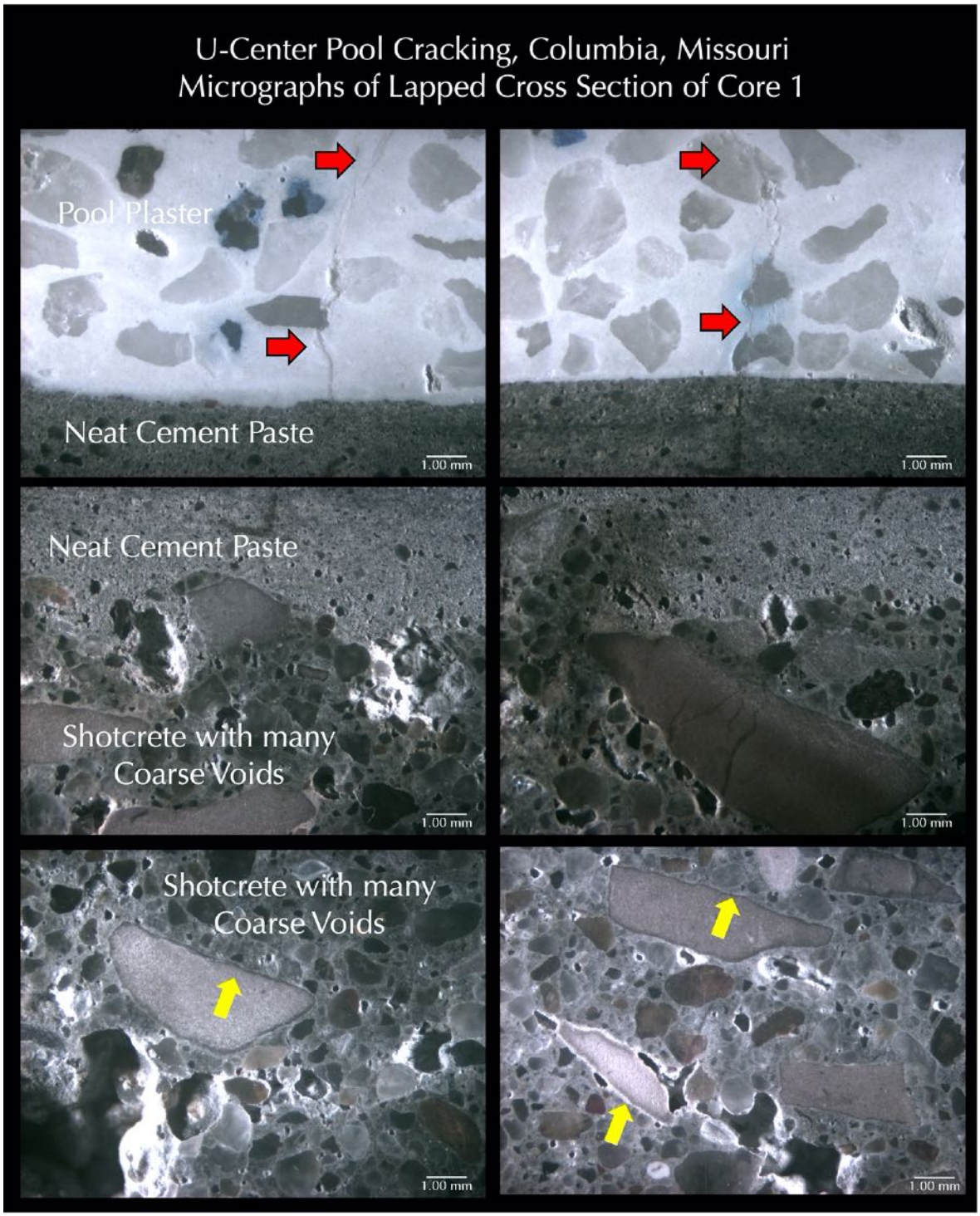

Figure 30: Micrographs of lapped cross section of Core 1 showing: (a) the dense, white, pool plaster with visible cracks extended into underlying leveling coat (top row, red arrows), (b) medium to dark gray thin neat cement paste leveling coat (middle row), (c) the shotcrete having crushed dolomitic limestone aggregate particles many with dark reaction rims followed by light cream-colored carbonated paste rims (yellow arrows), (d) overall non-air-entrained nature of shotcrete having many coarse voids, and (e) overall intimate bond between pool plaster, leveling coat, and shotcrete.

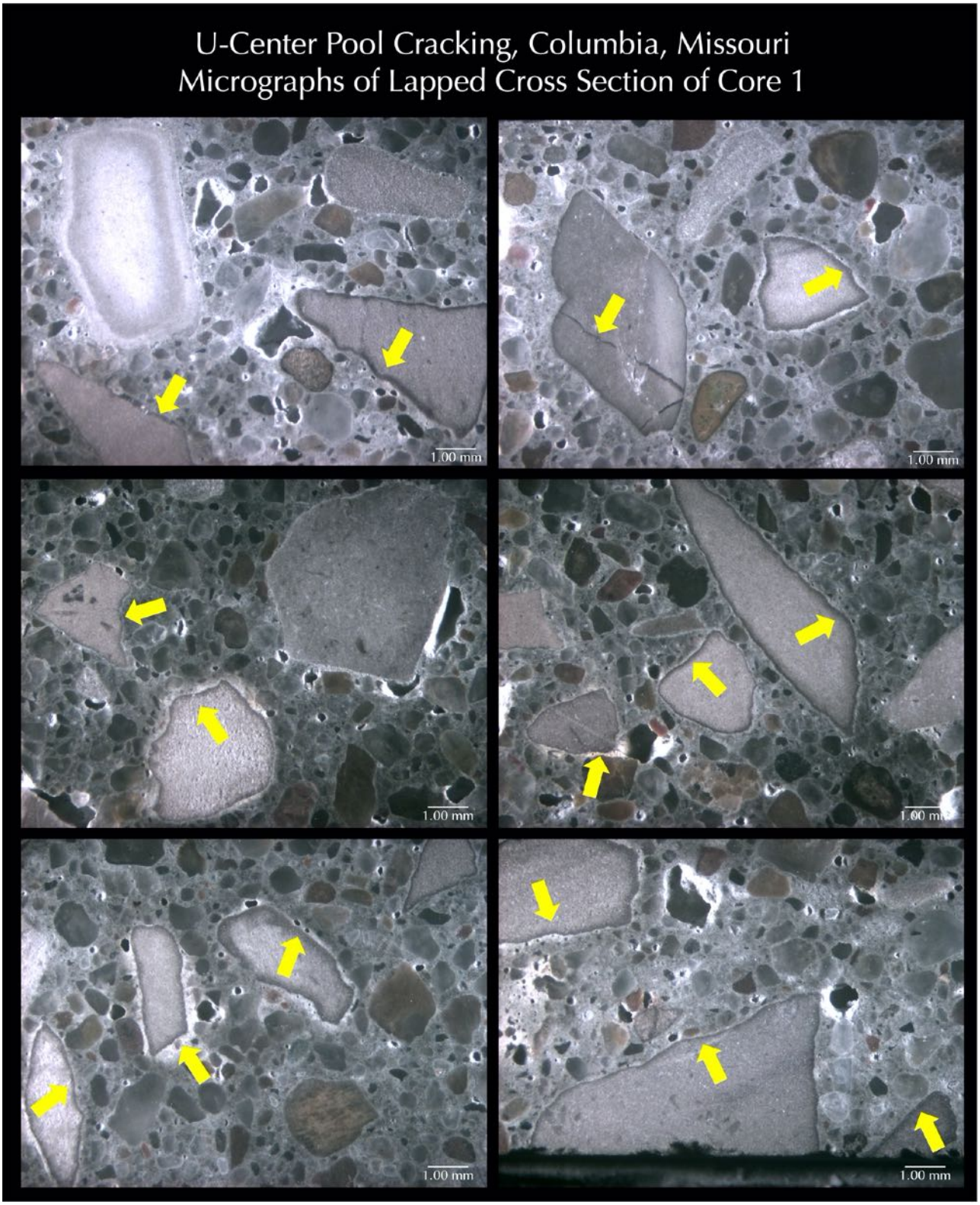

Figure 31: Micrographs of lapped cross section of Core 1 showing: (a) the shotcrete having crushed dolomitic limestone aggregate particles many with dark reaction rims followed by light cream-colored carbonated paste rims (yellow arrows), and (b) overall non-air-entrained nature of shotcrete having many coarse entrapped air voids.

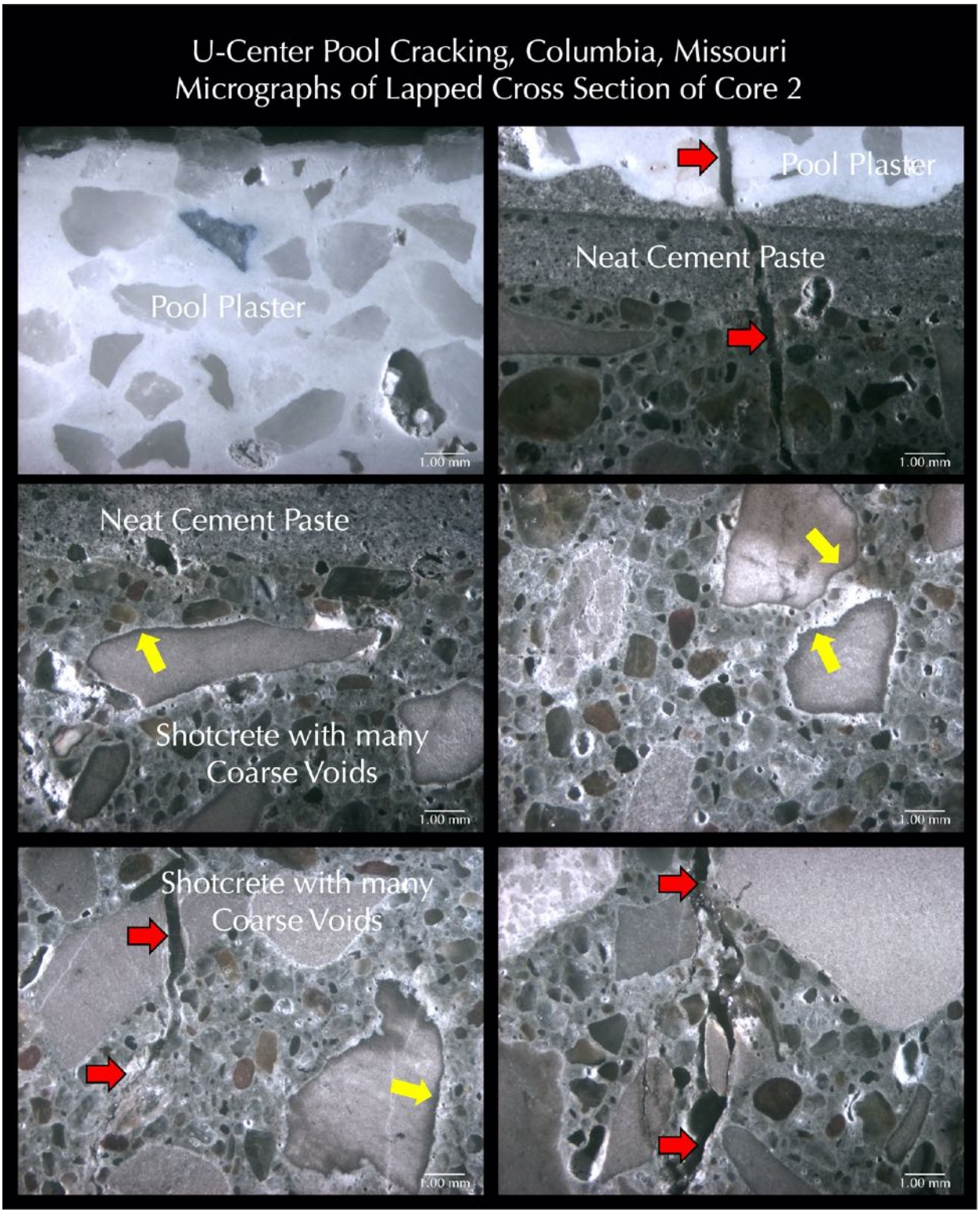

Figure 32: Micrographs of lapped cross section of Core 2 showing: (a) the dense, white, pool plaster with visible cracks extended into underlying leveling coat (top row right photo, red arrows), (b) medium to dark gray thin paste-rich layer of leveling coat (top right and middle row left photos), (c) the shotcrete having crushed dolomitic limestone aggregate particles many with dark reaction rims followed by light cream-colored carbonated paste rims (yellow arrows), (d) overall non-air-entrained nature of shotcrete having many coarse entrapped air voids, and (e) overall intimate bond between pool plaster, leveling coat, and shotcrete.

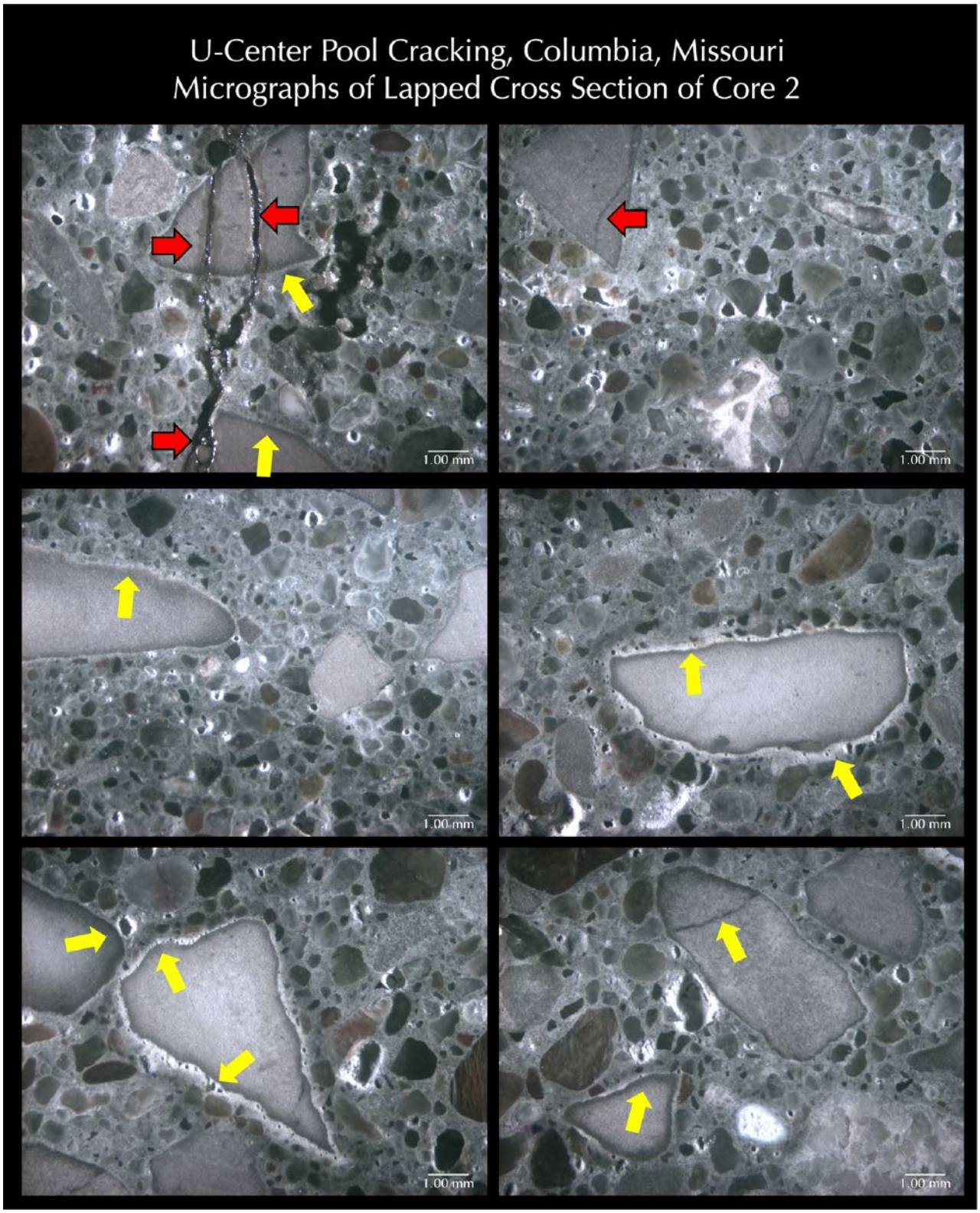

Figure 33: Micrographs of lapped cross section of Core 2 showing: (a) the shotcrete having crushed dolomitic limestone coarse aggregate particles many with dark reaction rims followed by light cream-colored carbonated paste rims (yellow arrows), and (b) overall non-air-entrained nature of shotcrete having many coarse entrapped air voids. The top row left photo shows a visible crack that has transected a crushed dolomtiic limestone aggregate particle.

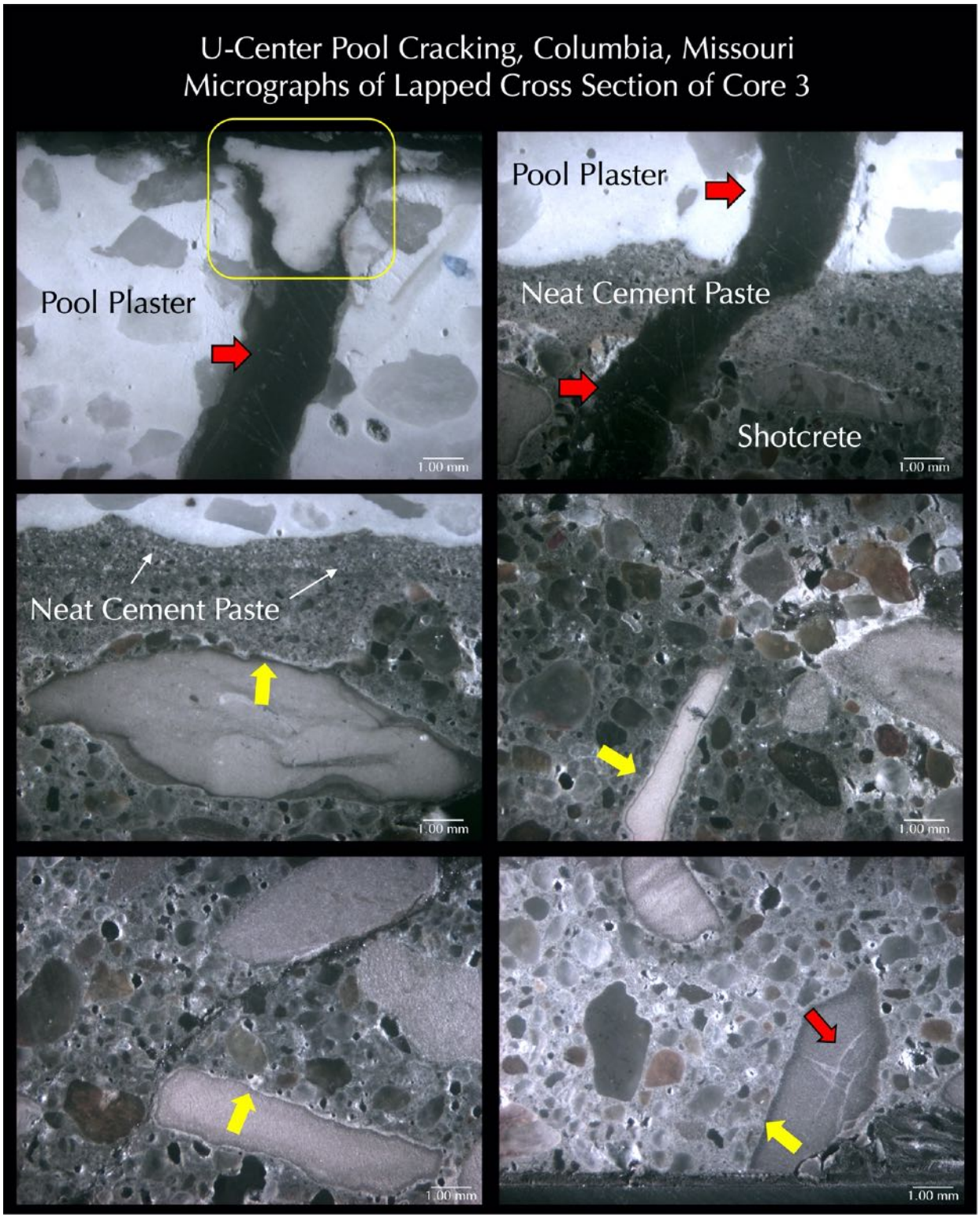

Figure 34: Micrographs of lapped cross section of Core 3 showing: (a) the dense, white, pool plaster with visible cracks extended into underlying leveling coat (top row, red arrows) and a crack seal caulk in the top left photo (boxed), (b) medium to dark gray thin paste-rich layer of leveling coat (top right and middle row left photos, thin white arrows), (c) the shotcrete having crushed dolomitic limestone aggregate particles many with dark reaction rims followed by light carbonated paste rims (yellow arrows), (d) overall non-air-entrained nature of shotcrete having many coarse entrapped air voids, and (e) overall intimate bond between pool plaster, leveling coat, and shotcrete.

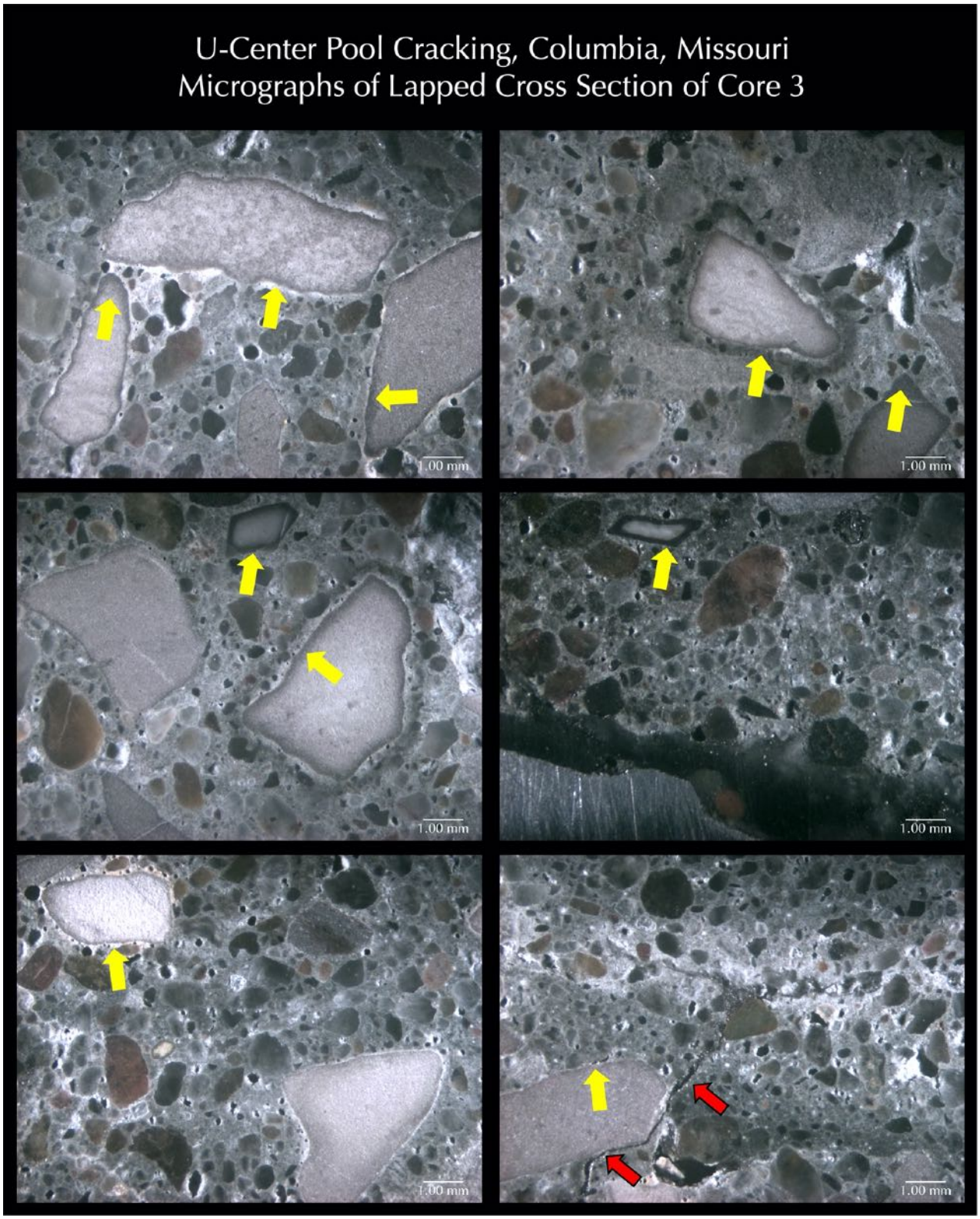

Figure 35: Micrographs of lapped cross section of Core 3 showing: (a) the shotcrete having crushed dolomitic limestone aggregate particles many with dark reaction rims followed by light cream-colored carbonated paste rims (yellow arrows), and (b) overall non-air-entrained nature of shotcrete having many coarse entrapped air voids.

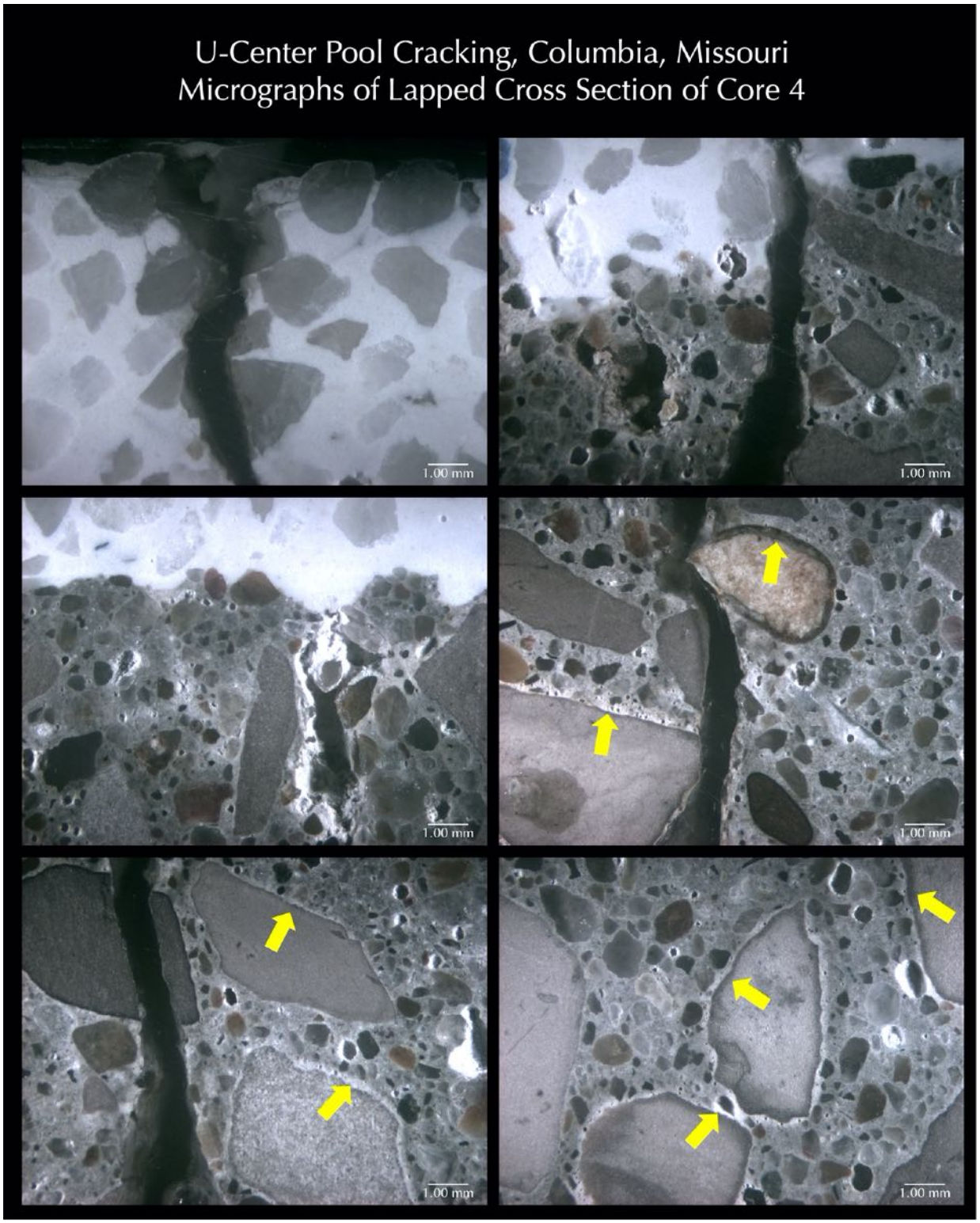

Figure 36: Micrographs of lapped cross section of Core 4 showing: (a) the dense, white, pool plaster with visible cracks extended into underlying leveling coat (top row), (b) no medium to dark gray leveling coat found in other 3 cores but not applied in the floor, (c) the shotcrete having crushed dolomitic limestone aggregate particles many with dark reaction rims followed by light cream-colored carbonated paste rims (yellow arrows), (d) overall non-air-entrained nature of shotcrete having many coarse entrapped air voids, and (e) overall intimate bond between pool plaster, leveling coat, and shotcrete. Major vertical crack through pool plaster and shotcrete are seen in four photos.

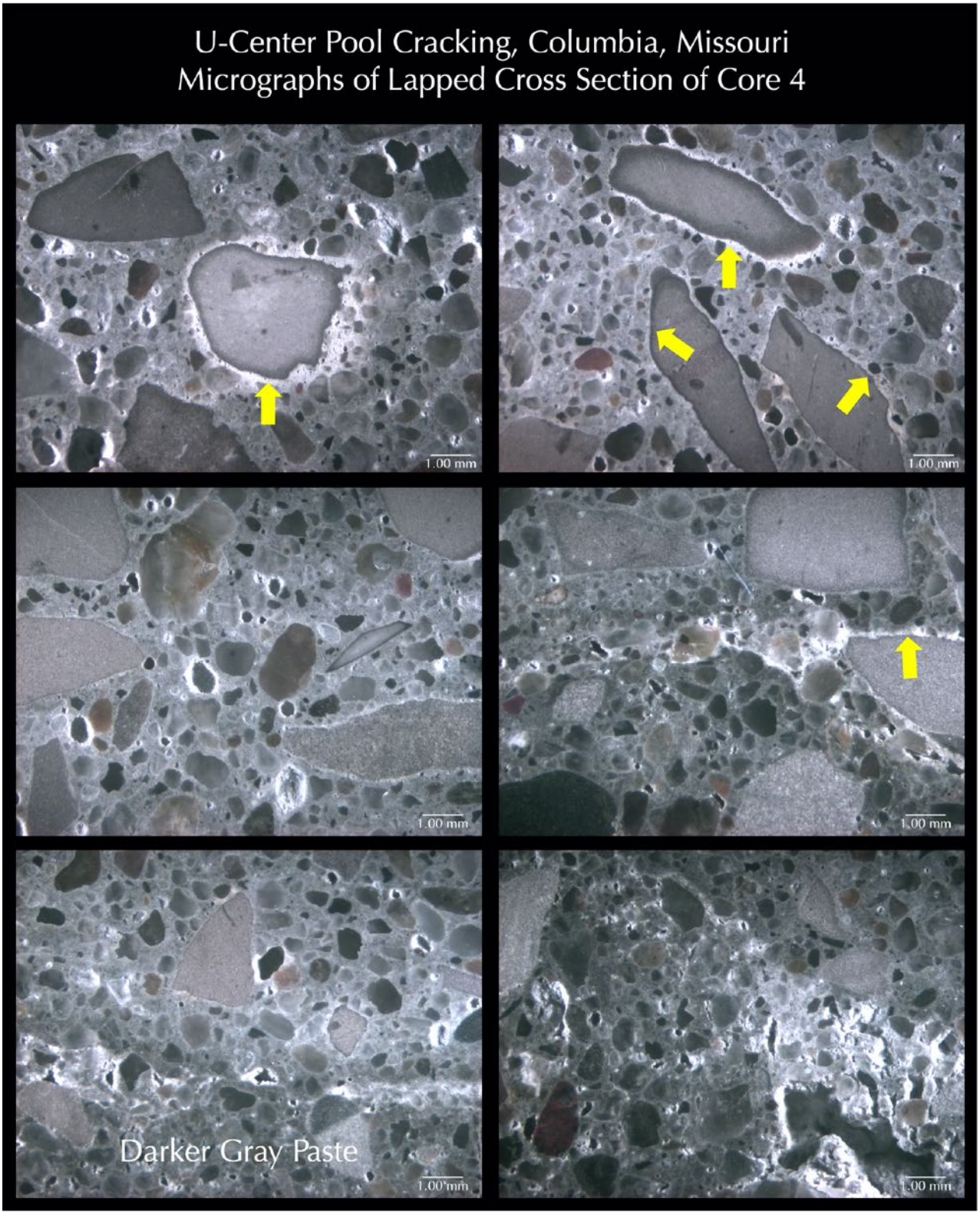

Figure 37: Micrographs of lapped cross section of Core 4 showing: (a) the shotcrete having crushed dolomitic limestone aggregate particles many with dark reaction rims followed by light cream-colored carbonated paste rims (yellow arrows), and (b) overall non-air-entrained nature of shotcrete having many coarse entrapped air voids.

BLUE DYE-MIXED EPOXY-IMPREGNATED THIN SECTIONS

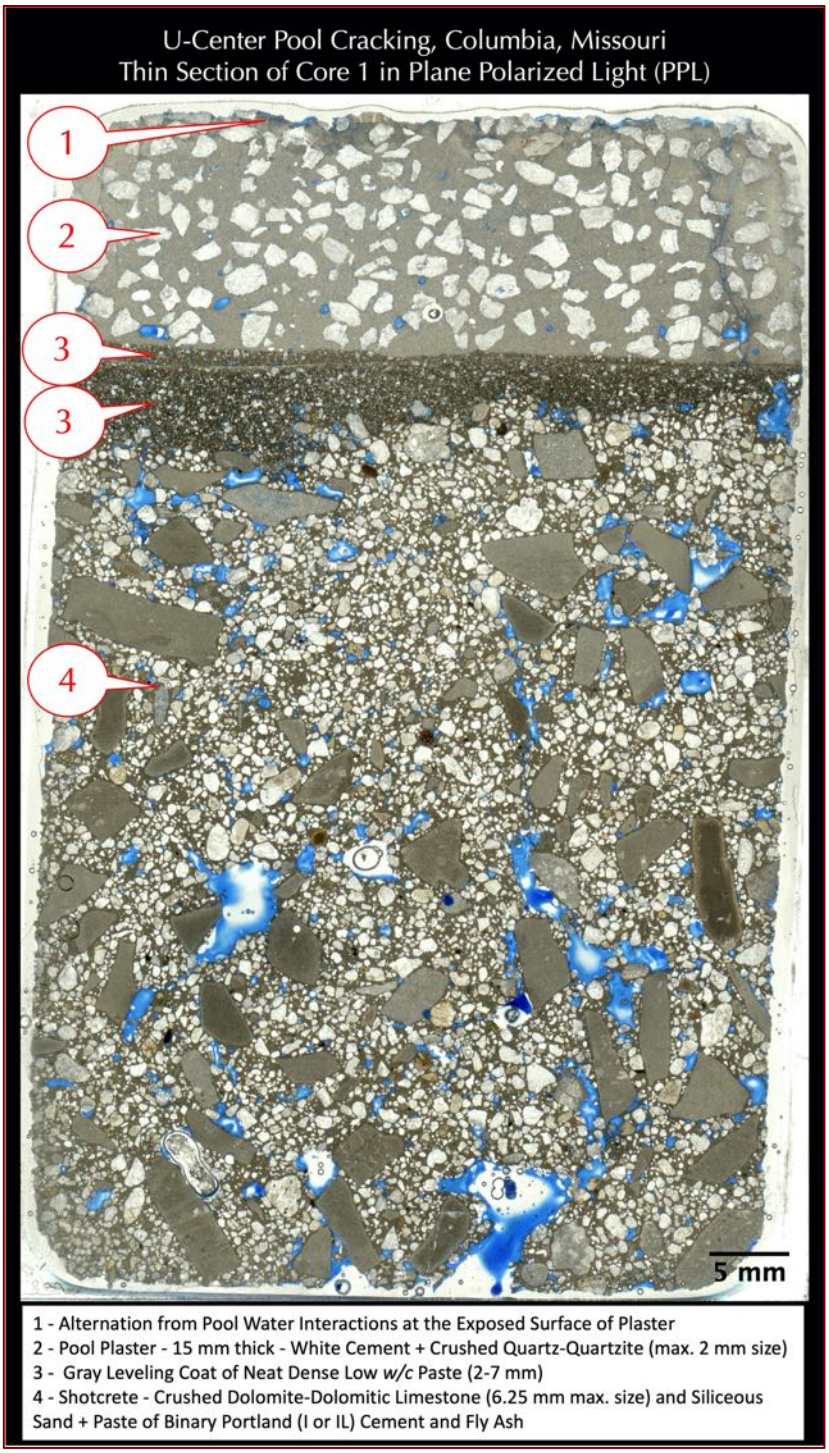

Figure 38: Blue dye-mixed epoxy-impregnated thin section of Core 1 showing: (a) a thin altered zone (Callout '1') from pool water interaction on the dense pool plaster (Callout '2') having many well-graded, well-distributed sub-rounded to angular (crushed) siliceous sand filler (2-3 mm size), (b) thin dark gray-toned paste of leveling coat (Callout '3'), and (c) the main shotcrete body (Callout '4') having crushed limestone and dolomitic limestone aggregate particles, natural siliceous sand aggregate, and interstitial paste with many coarse entrapped air voids highlighted by blue epoxy. The image was taken on a flatbed film scanner with a polarizing filter placed on the thin section to obtain plane polarized light view of polarizing microscope.

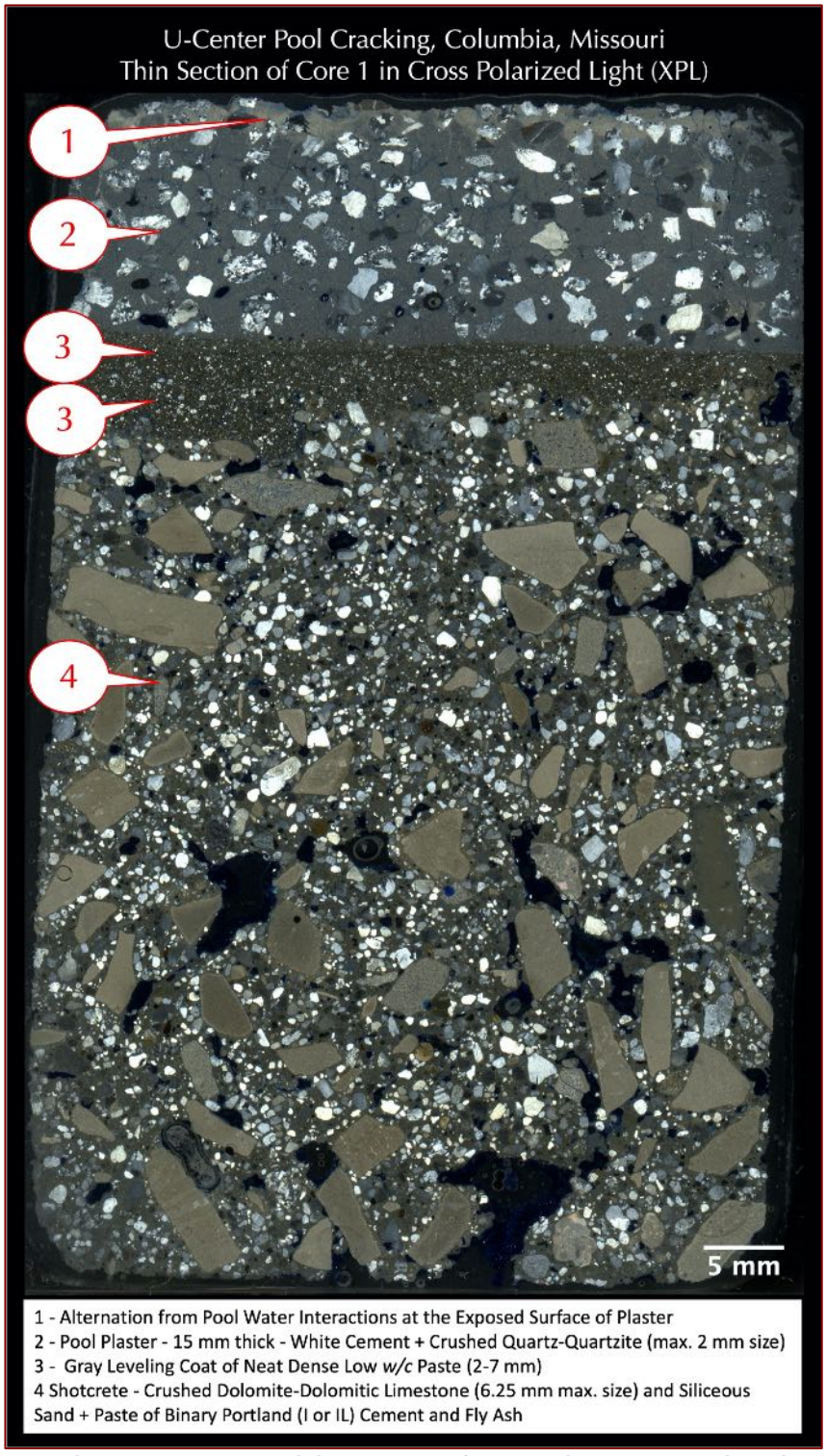

Figure 39: Blue dye-mixed epoxy-impregnated thin section of Core 1 showing: (a) a thin altered zone (Callout '1') from pool water interaction on the dense pool plaster (Callout '2') having many well-graded, well-distributed sub-rounded to angular (crushed) siliceous sand filler (2-3 mm size), (b) thin dark-toned paste of leveling coat (Callout '3'), and (c) the main shotcrete body (Callout '4') having crushed limestone and dolomitic limestone aggregate particles, natural siliceous sand aggregate, and interstitial paste with many coarse voids. The image was taken on a flatbed film scanner with two perpendicular polarizing filters placed on both sides of thin section to obtain cross polarized light view of polarizing microscope.

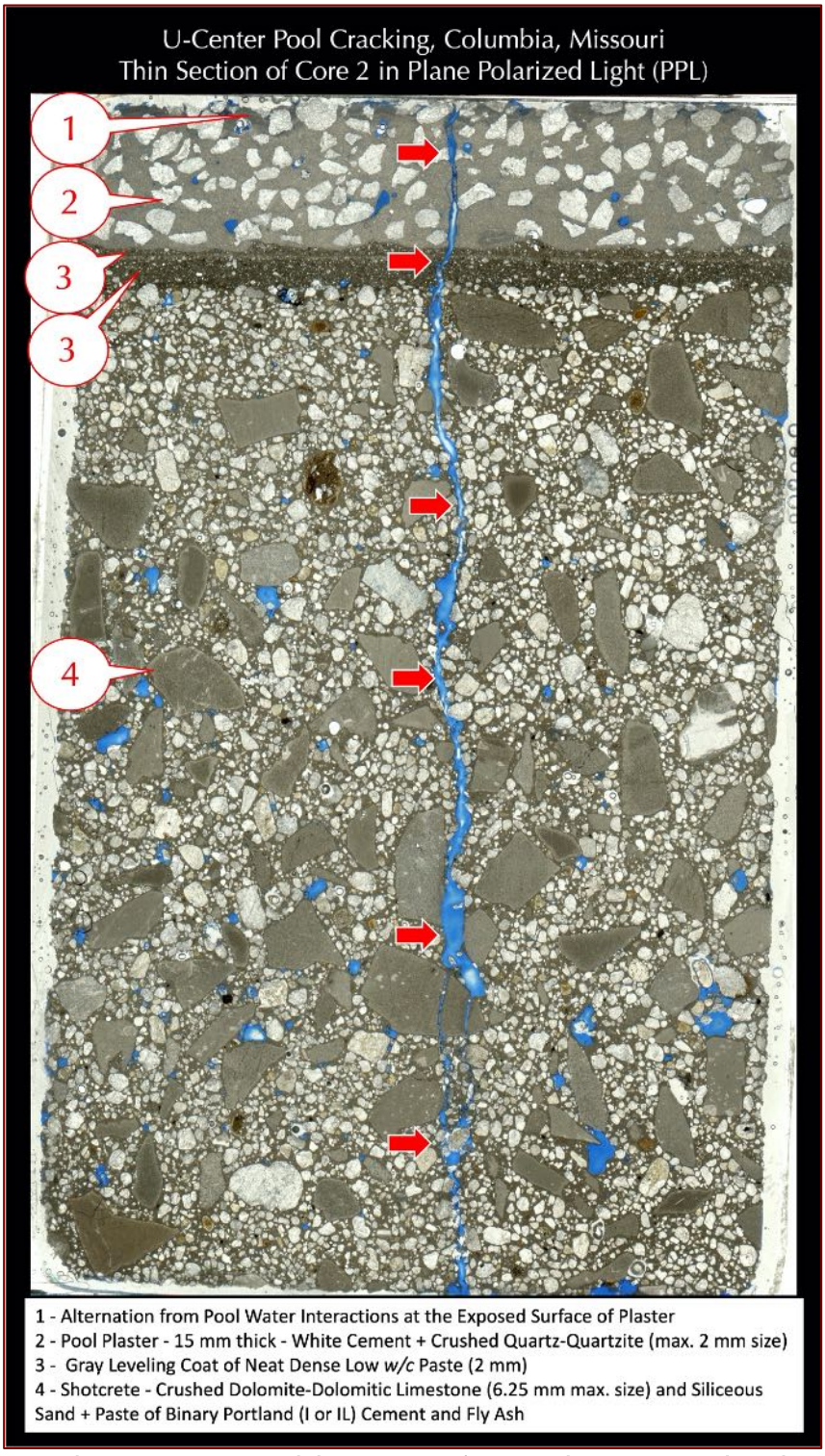

Figure 40: Blue dye-mixed epoxy-impregnated thin section of Core 2 showing: (a) a thin altered zone (Callout '1') from pool water interaction on the dense pool plaster (Callout '2') having many well-graded, well-distributed sub-rounded to angular (crushed) siliceous sand filler (2-3 mm size), (b) thin dark gray-toned paste of leveling coat (Callout '3'), and (c) the main shotcrete body (Callout '4') having crushed limestone and dolomitic limestone aggregate particles, natural siliceous sand aggregate, and interstitial paste with many coarse entrapped air voids highlighted by blue epoxy. The image was taken on a flatbed film scanner with a polarizing filter placed on the thin section to obtain plane polarized light view of polarizing microscope. The major vertical crack through pool plaster, leveling coat, and main shotcrete body is highlighted by blue epoxy and marked with red arrows.

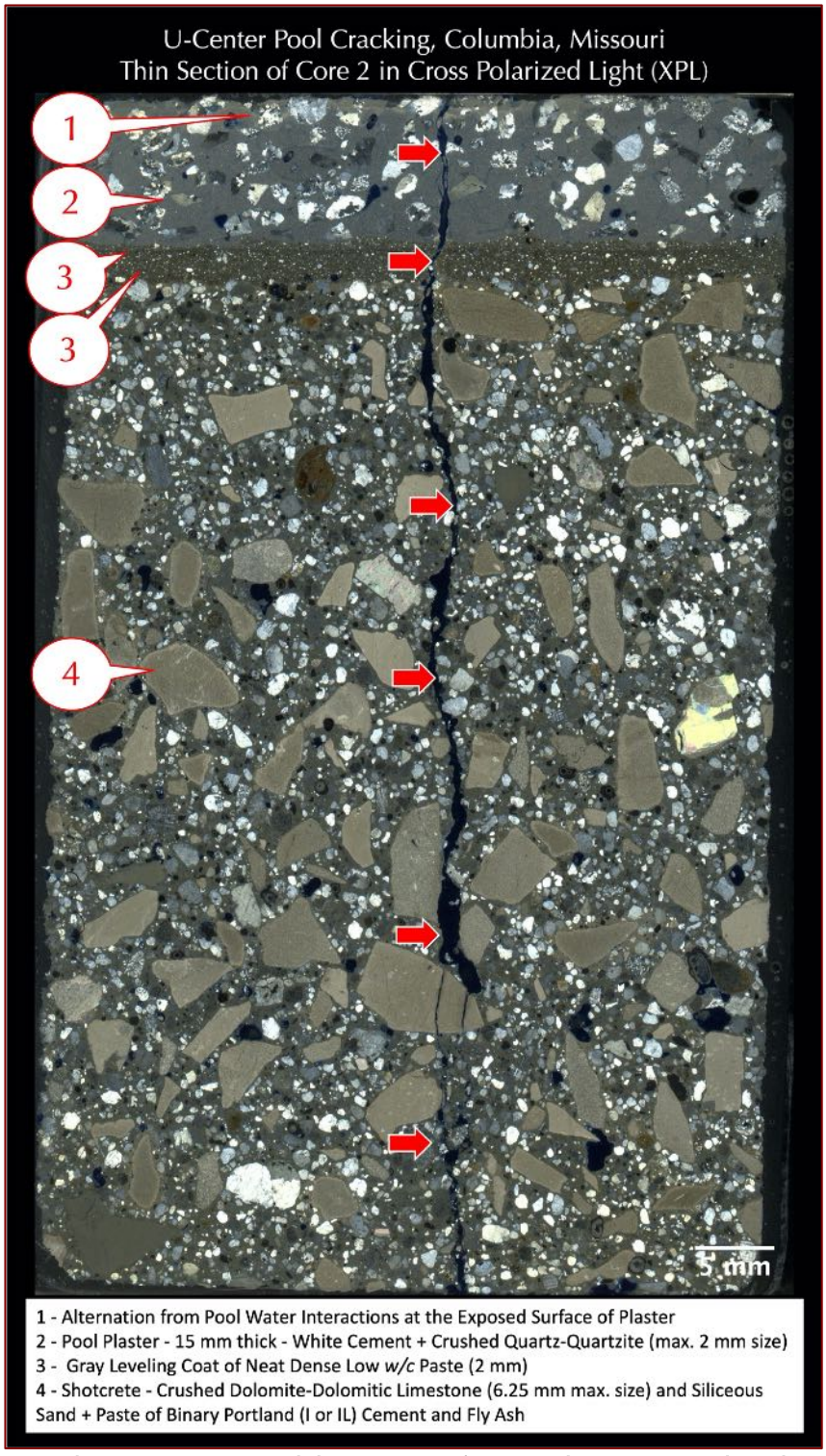

Figure 41: Blue dye-mixed epoxy-impregnated thin section of Core 2 showing: (a) a thin altered zone (Callout '1') from pool water interaction on the dense pool plaster (Callout '2') having many well-graded, well-distributed sub-rounded to angular (crushed) siliceous sand filler, (b) thin dark-toned paste of leveling coat (Callout '3'), and (c) the main shotcrete body (Callout '4') having crushed limestone and dolomitic limestone aggregate particles, natural siliceous sand aggregate, and interstitial paste with many coarse entrapped air voids. The image was taken on a flatbed film scanner with two perpendicular polarizing filters placed on both sides of thin section to obtain cross polarized light view of polarizing microscope. The major vertical crack through pool plaster, leveling coat, and main shotcrete body is highlighted with red arrows.

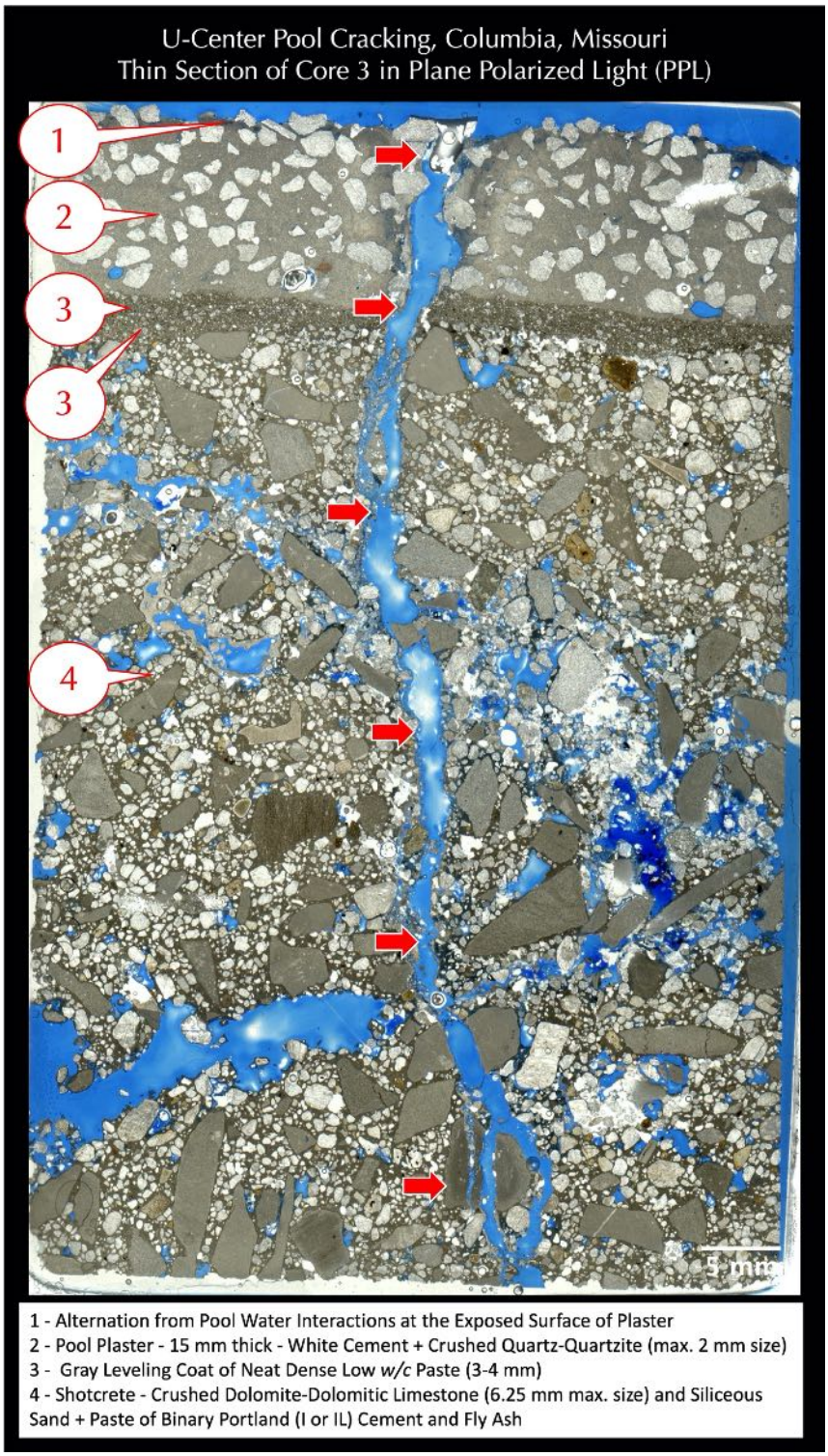

Figure 42: Blue dye-mixed epoxy-impregnated thin section of Core 3 showing: (a) a thin altered zone (Callout '1') from pool water interaction on the dense pool plaster (Callout '2') having many well-graded, well-distributed sub-rounded to angular (crushed) siliceous sand filler (2-3 mm size), (b) thin dark gray-toned paste of leveling coat (Callout '3'), and (c) the main shotcrete body (Callout '4') having crushed limestone and dolomitic limestone aggregate particles, natural siliceous sand aggregate, and interstitial paste with many coarse voids highlighted by blue epoxy. The image was taken on a flatbed film scanner with a polarizing filter placed on the thin section to obtain plane polarized light view of polarizing microscope. The major vertical crack through pool plaster, leveling coat, and main shotcrete body is highlighted by blue epoxy and marked with red arrows.

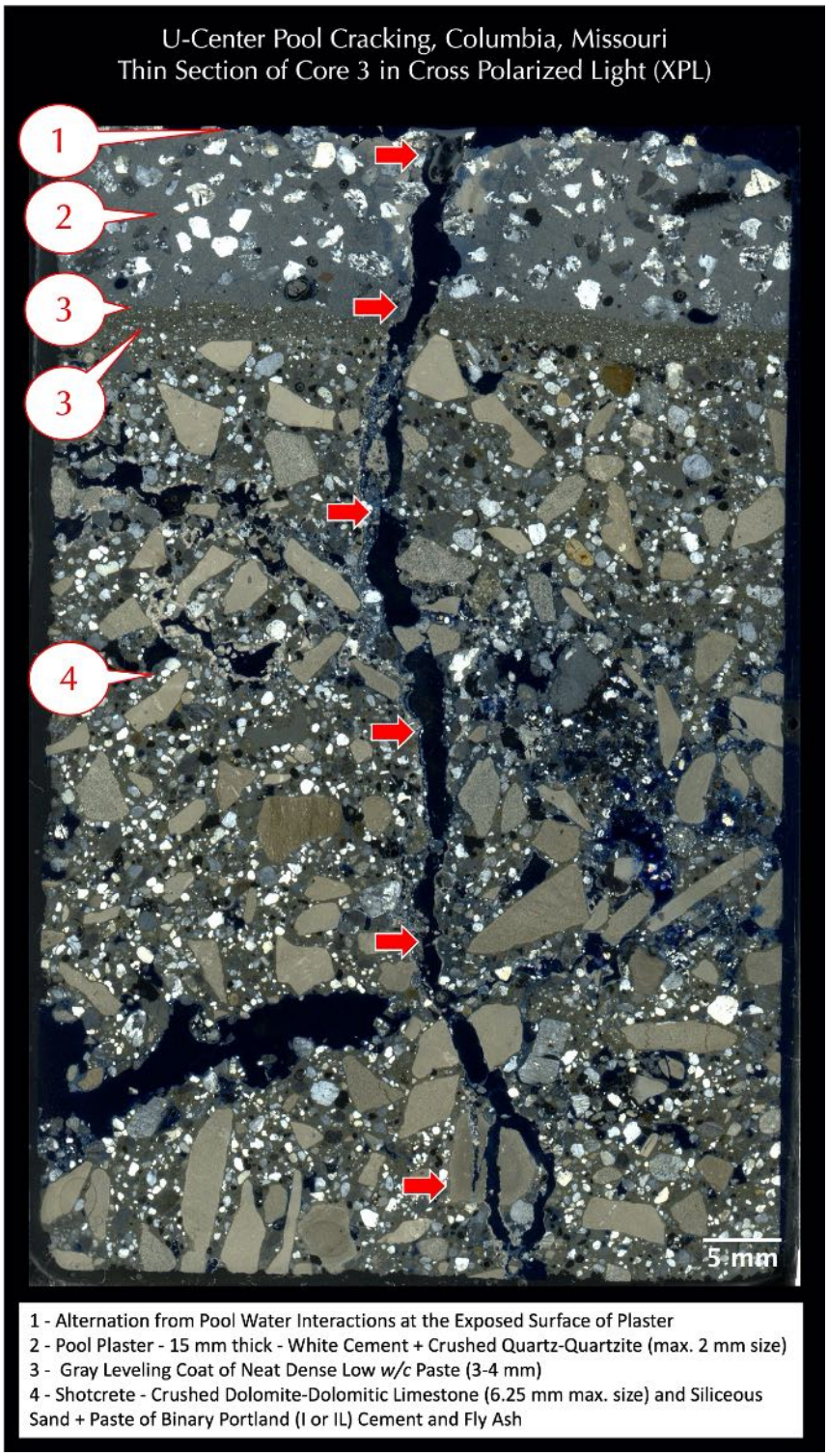

Figure 43: Blue dye-mixed epoxy-impregnated thin section of Core 3 showing: (a) a thin altered zone (Callout '1') from pool water interaction on the dense pool plaster (Callout '2') having many well-graded, well-distributed sub-rounded to angular (crushed) siliceous sand filler (2-3 mm size), (b) thin dark-toned paste of leveling coat (Callout '3'), and (c) the main shotcrete body (Callout '4') having crushed limestone and dolomitic limestone aggregate particles, natural siliceous sand aggregate, and interstitial paste with many coarse voids. The image was taken on a flatbed film scanner with two perpendicular polarizing filters placed on both sides of thin section to obtain cross polarized light view of polarizing microscope. The major vertical crack through pool plaster, leveling coat, and main shotcrete body is highlighted with red arrows.

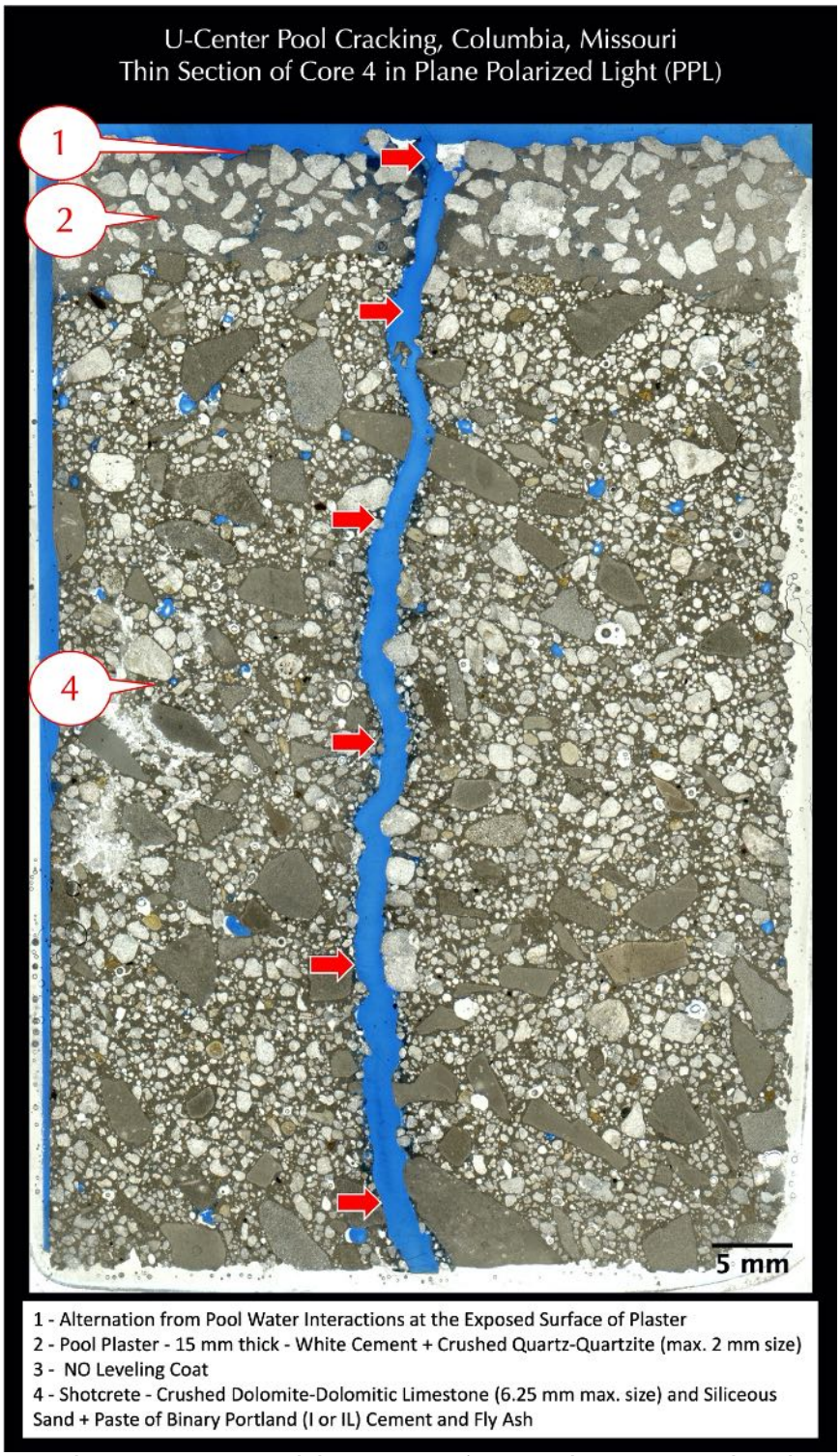

Figure 44: Blue dye-mixed epoxy-impregnated thin section of Core 4 showing: (a) a thin altered zone (Callout '1') from pool water interaction on the dense pool plaster (Callout '2') having many well-graded, well-distributed sub-rounded to angular (crushed) siliceous sand filler (2-3 mm size), (b) absence of the thin dark-toned paste of leveling coat found in other three cores, and (c) the main shotcrete body (Callout '4') having crushed limestone and dolomitic limestone aggregate particles, natural siliceous sand aggregate, and interstitial paste with many coarse voids. The image was taken on a flatbed film scanner with two perpendicular polarizing filters placed on both sides of thin section to obtain cross polarized light view of polarizing microscope. The major vertical crack through pool plaster, leveling coat, and main shotcrete body is highlighted with red arrows.

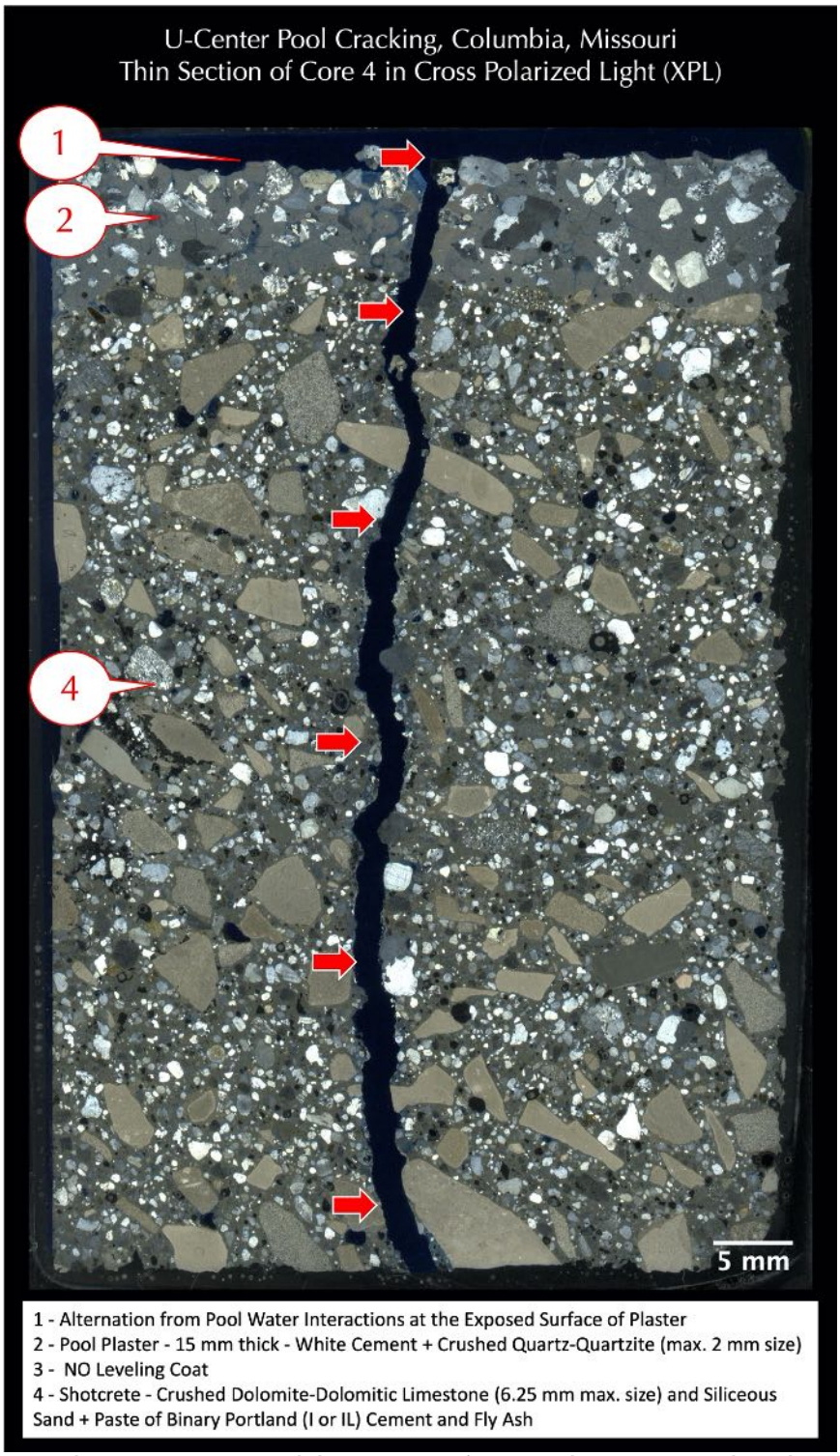

Figure 45: Blue dye-mixed epoxy-impregnated thin section of Core 4 showing: (a) a thin altered zone (Callout '1') from pool water interaction on the dense pool plaster (Callout '2') having many well-graded, well-distributed sub-rounded to angular (crushed) siliceous sand filler (2-3 mm size), (b) absence of thin dark-toned paste of leveling coat found in three other cores, and (c) the main shotcrete body (Callout '4') having crushed limestone and dolomitic limestone aggregate particles, natural siliceous sand aggregate, and interstitial paste with many coarse voids. The image was taken on a flatbed film scanner with two perpendicular polarizing filters placed on both sides of thin section to obtain cross polarized light view of polarizing microscope. The major vertical crack through pool plaster, leveling coat, and main shotcrete body is highlighted with red arrows.

MICROGRAPHS OF THIN SECTIONS

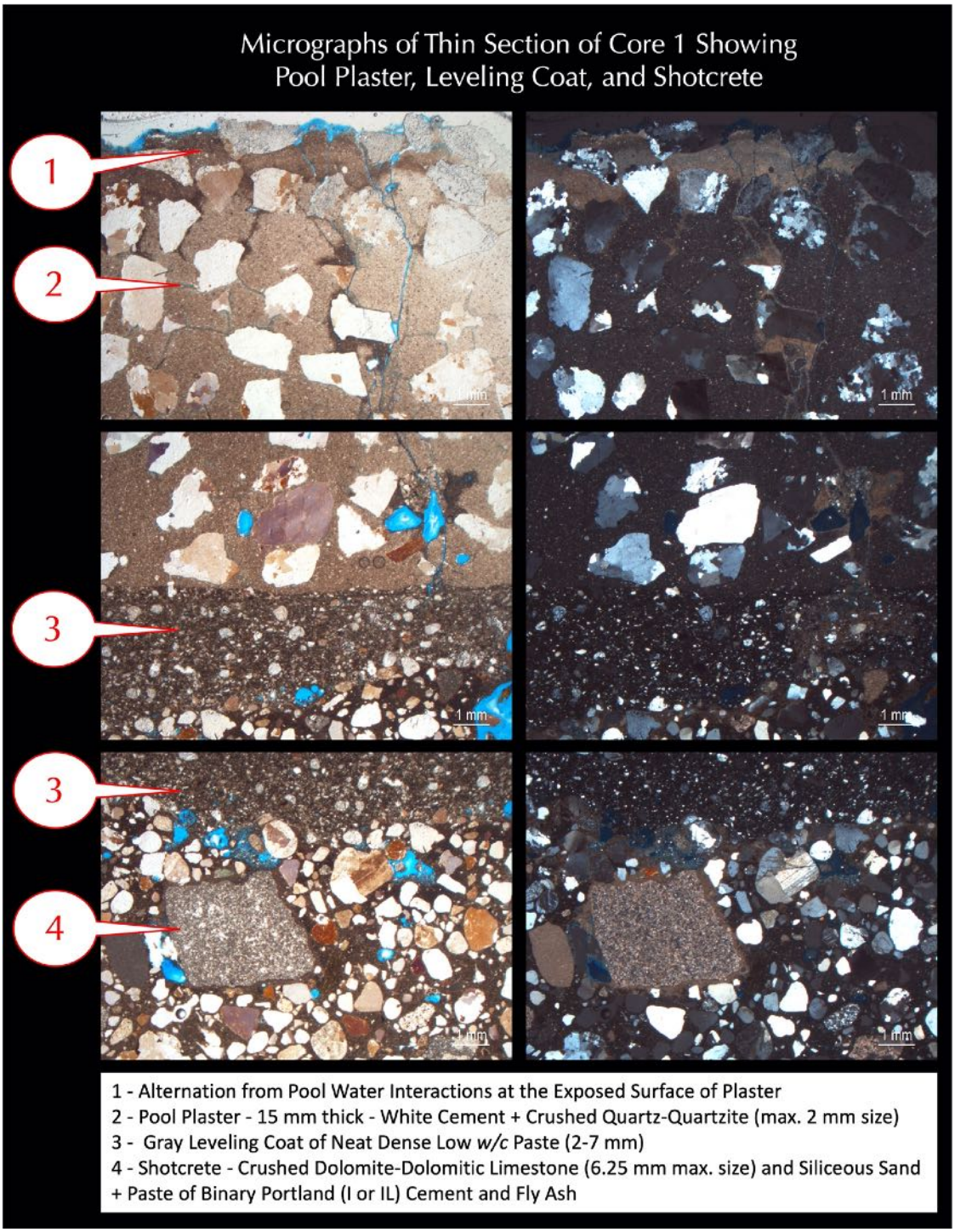

Figure 46: Micrographs of thin section of Core 1 showing: (a) a thin altered zone (Callout '1') from pool water interaction on the dense pool plaster (Callout '2') having many well-graded, well-distributed sub-rounded to angular (crushed) siliceous sand filler (2-3 mm size), (b) absence of thin dark-toned paste of leveling coat found in three other cores, and (c) the main shotcrete body (Callout '4') having crushed dolomitic limestone aggregate particles, natural siliceous sand aggregate, and interstitial paste with many coarse voids. Images were taken in plane (PPL, left) and corresponding cross (XPL, right) polarized light modes respectively, in a stereozoom microscope.

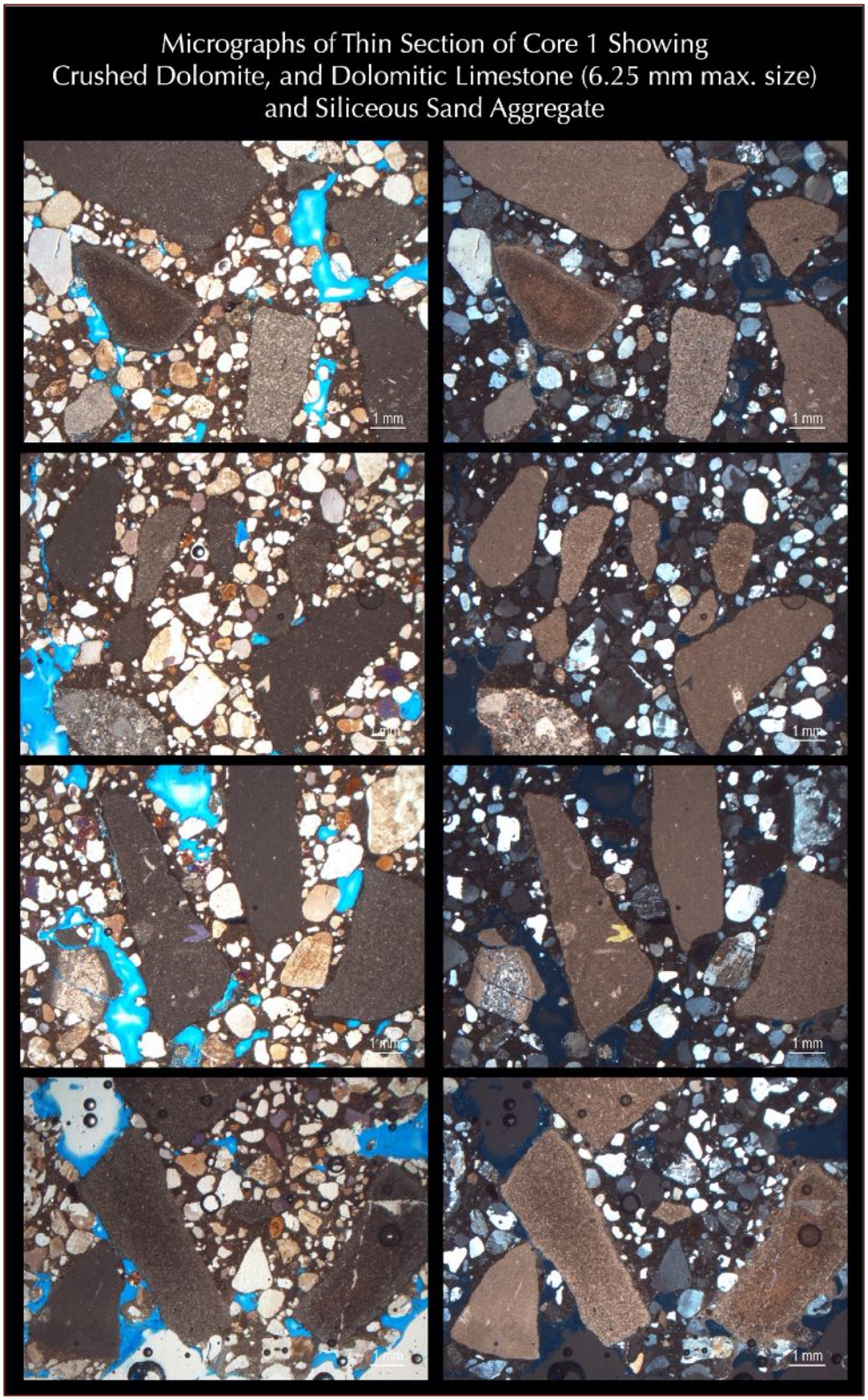

Figure 47: Micrographs of thin section of Core 1 showing: (a) the main shotcrete body having crushed limestone and dolomitic limestone aggregate particles, natural siliceous sand aggregate, and interstitial paste with many coarse voids. Images were taken in plane (PPL, left) and corresponding cross (XPL, right) polarized light modes respectively, in a stereozoom microscope.

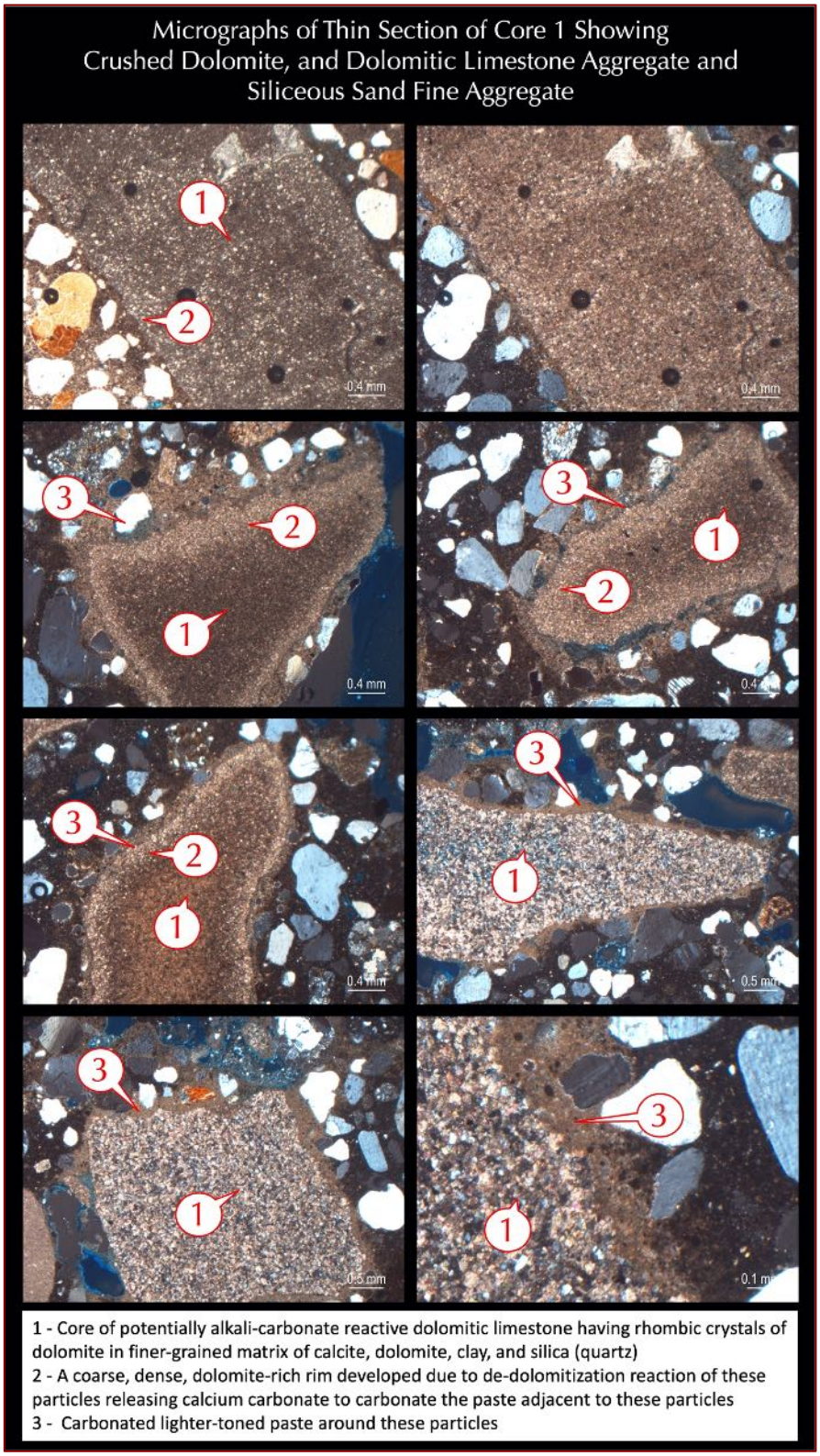

Figure 48: Micrographs of thin section of Core 1 showing many crushed dolomitic limestone aggregate particles having a core of rhombic crystals of dolomite in finer grains matrix of calcite, dolomite, clay, and quartz (Callout '1'), within a dense rim of coarse dolomite rhombs (Callout '2') and an outer lighter-toned carbonated paste rim (Callout '3'), which are potentially unsound alkali-carbonate reactive dolomitic limestone particles in aggregate. Images were taken in plane (PPL) or cross (XPL) polarized light modes in a stereozoom microscope.

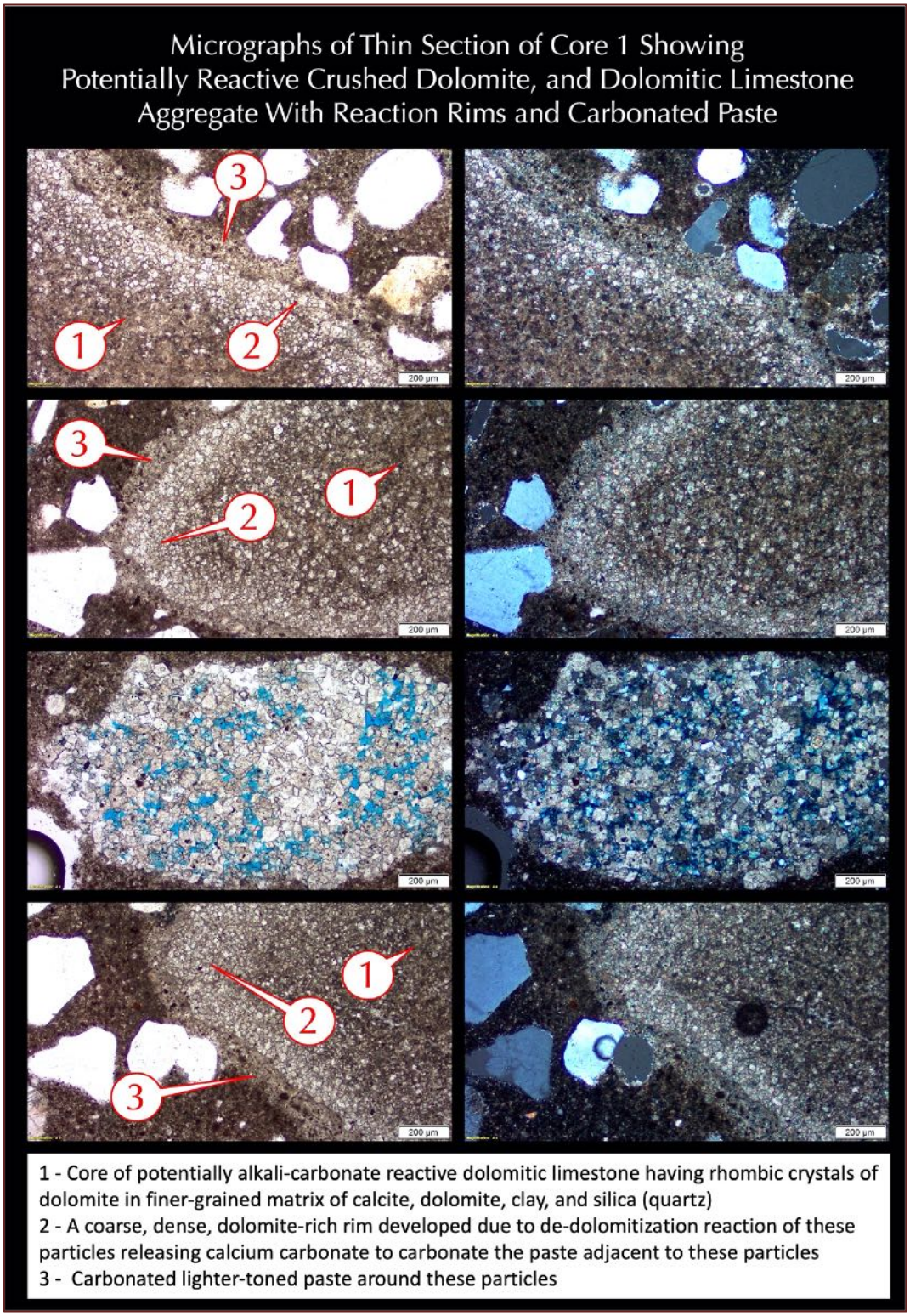

Figure 49: Micrographs of thin section of Core 1 showing many crushed dolomitic limestone aggregate particles having a core of rhombic crystals of dolomite in finer grains matrix of calcite, dolomite, clay, and quartz (Callout '1'), within a dense rim of coarse dolomite rhombs (Callout '2') and an outer lighter-toned carbonated paste rim (Callout '3'), which are potentially unsound alkali-carbonate reactive dolomitic limestone particles in aggregate. Images were taken in plane (PPL) or cross (XPL) polarized light modes in a petrographic microscope.

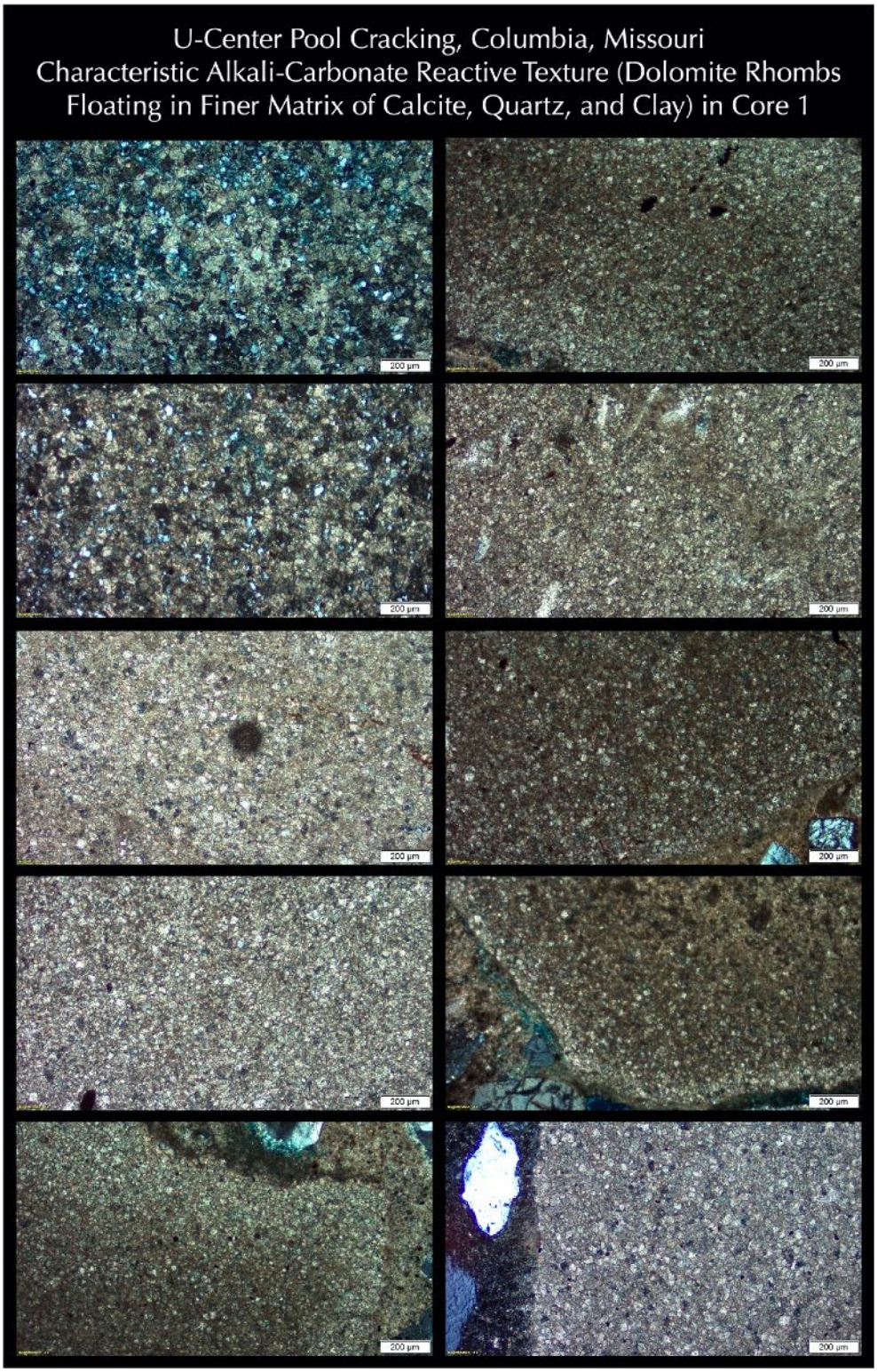

Figure 50: Micrographs of thin section of Core 1 showing characteristic texture of alkali-carbonate reactive (ACR) rocks in shotcrete in having dolomite rhombs floating in finer-grained matrix of calcite, quartz, and clay.

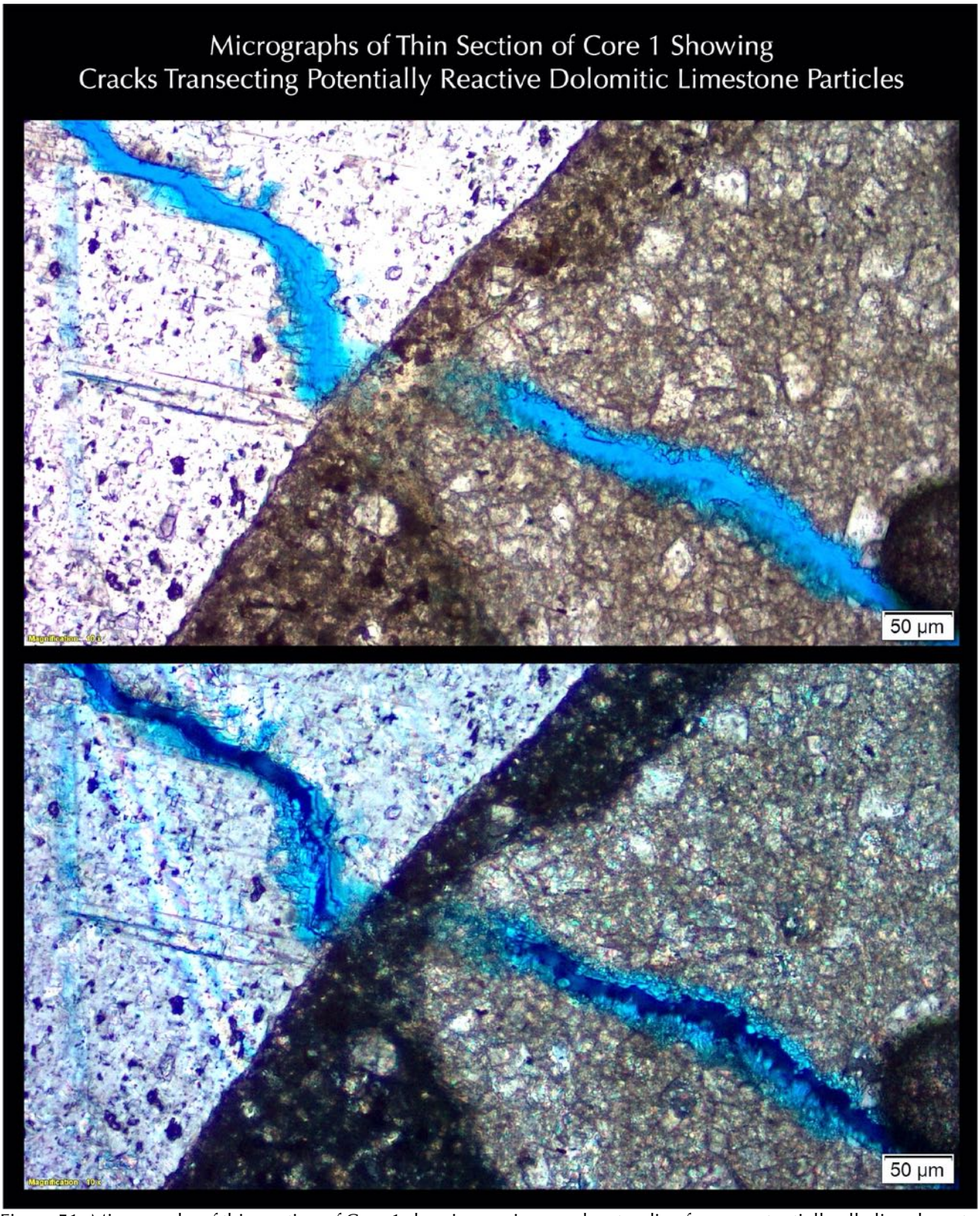

Figure 51: Micrographs of thin section of Core 1 showing a microcrack extending from a potentially alkali-carbonate reactive dolomitic limestone aggregate particle at right, through interstitial mortar fraction to another coarse calcite particle at left. Images were taken in plane (top, PPL) and corresponding cross (bottom, XPL) polarized light modes in a petrographic microscope.

Figure 52: Micrographs of thin section of Core 1 showing a microcrack from a potentially alkali-carbonate aggregate (having alkali-silica reactive inclusions within a dolomitic limestone aggregate particle) to neighboring paste. Notice many strained quartz particles in the core of dolomitic limestone aggregate are potentially alkali-silica reactive. Images were taken in plane (top, PPL) and corresponding cross (bottom, XPL) polarized light modes in a petrographic microscope.

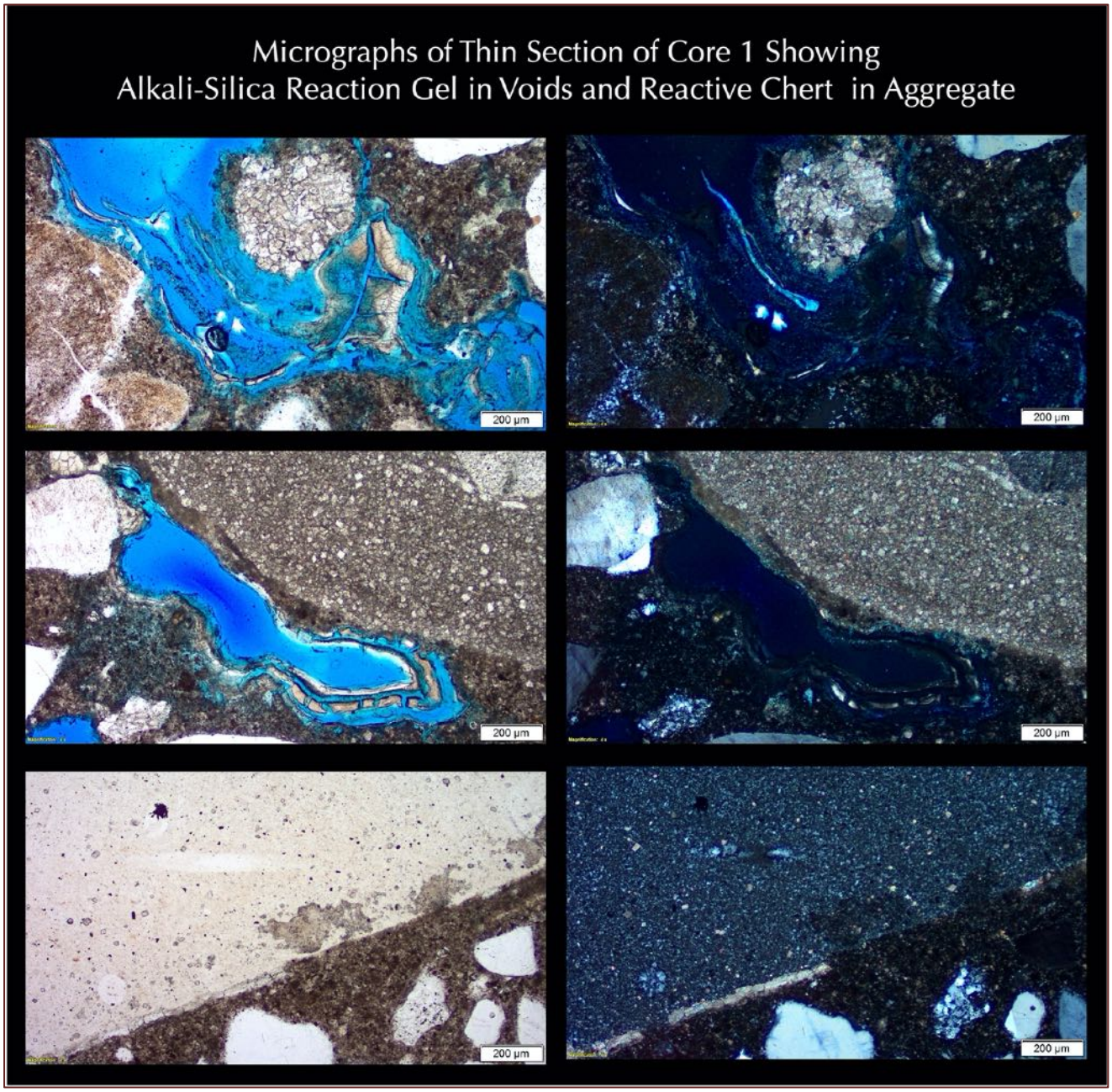

Figure 53: Evidence of alkali-silica reaction gel deposits lining walls of coarse voids where potentially reactive components may have derived from reactive silica particles within dolomitic limestone aggregate and/or reactive silica (chert, microcrystalline silica component in dolomitic limestone, strained quartzite, etc.) in fine aggregate. Images were taken in plane (PPL, left) and corresponding cross (XPL, right) polarized light modes respectively, in a petrographic microscope.

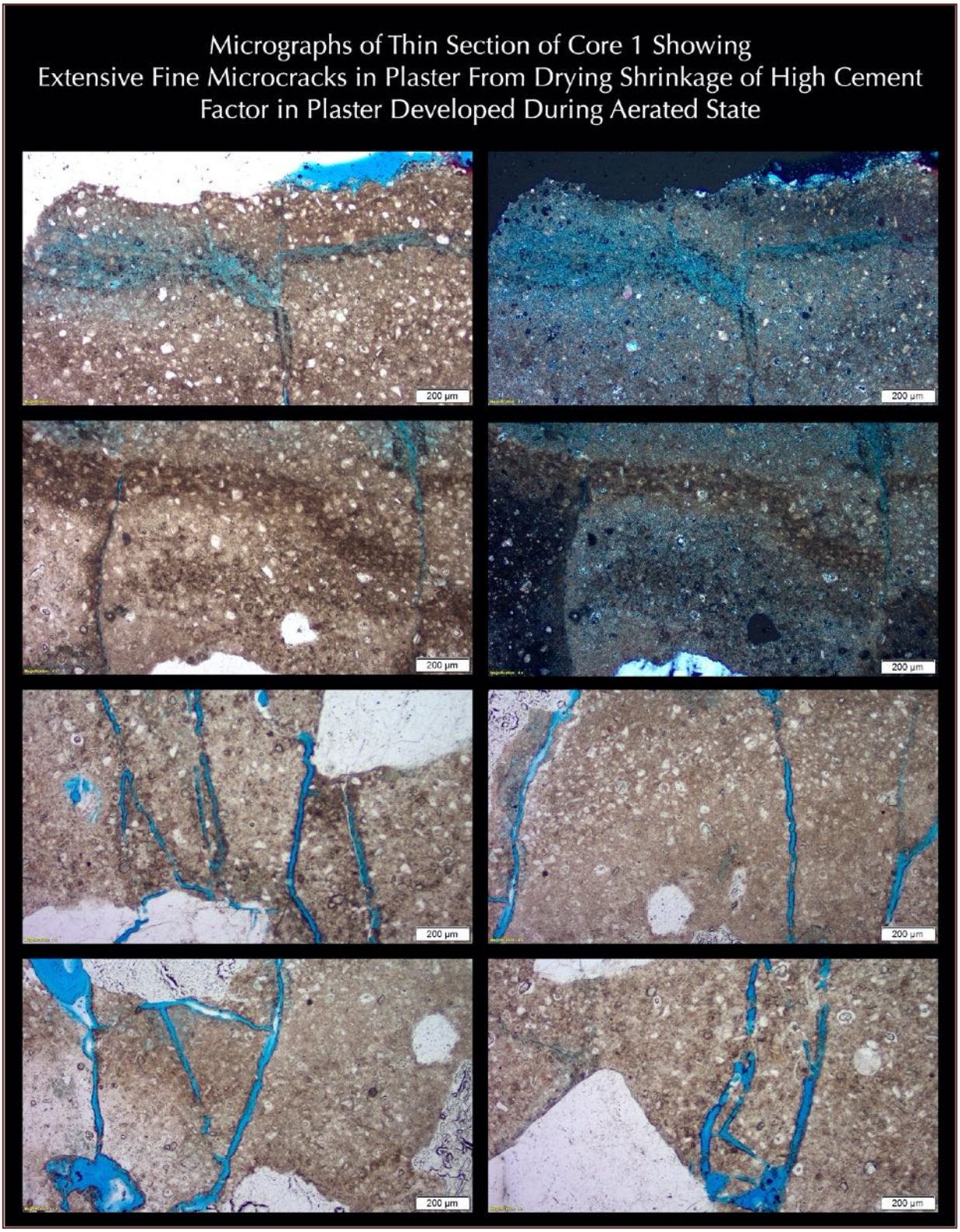

Figure 54: Micrographs of thin section of Core 1 showing: (a) extensive fine shrinkage microcracks within the white pool plaster, and (b) altered zone of plaster at the very top from interactions with pool water and air (top two rows). Images were taken in plane (PPL) and cross (XPL) polarized light modes in a petrographic microscope.

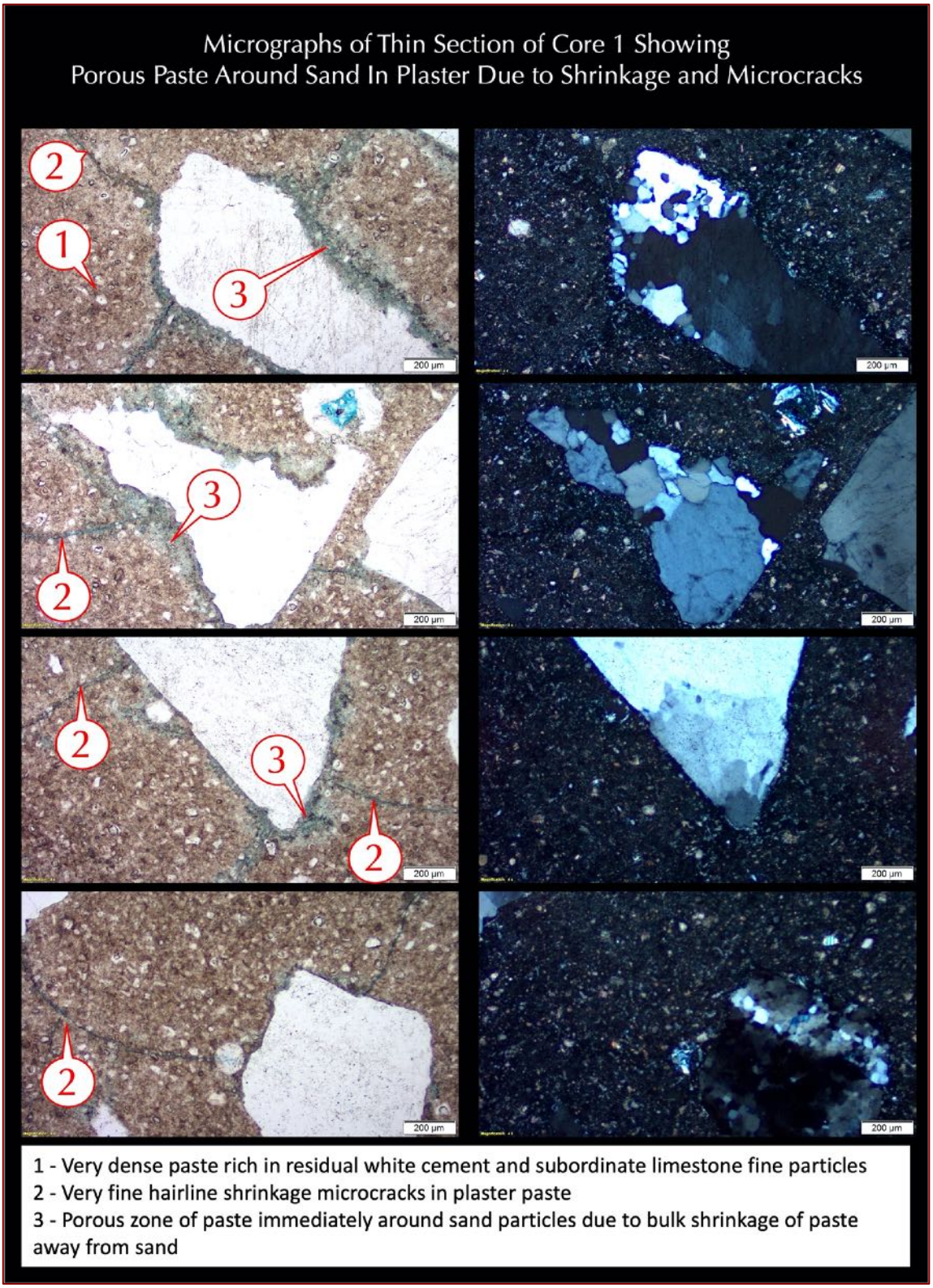

Figure 55: Micrographs of thin section of Core 1 showing: (a) dense white cement paste in pool plaster consisting of a dense matrix of cement hydration products and many very fine residual cement particles (Callout '1'), (b) extensive fine microcracks within the white pool plaster (Callout '2'), and (c) gaps or porous higher w/c zone of paste and associated microcracks around siliceous sand (quartz, quartzite) fillers in pool plaster (Callout '3'). Images were taken in plane (PPL) and cross (XPL) polarized light modes in a petrographic microscope.

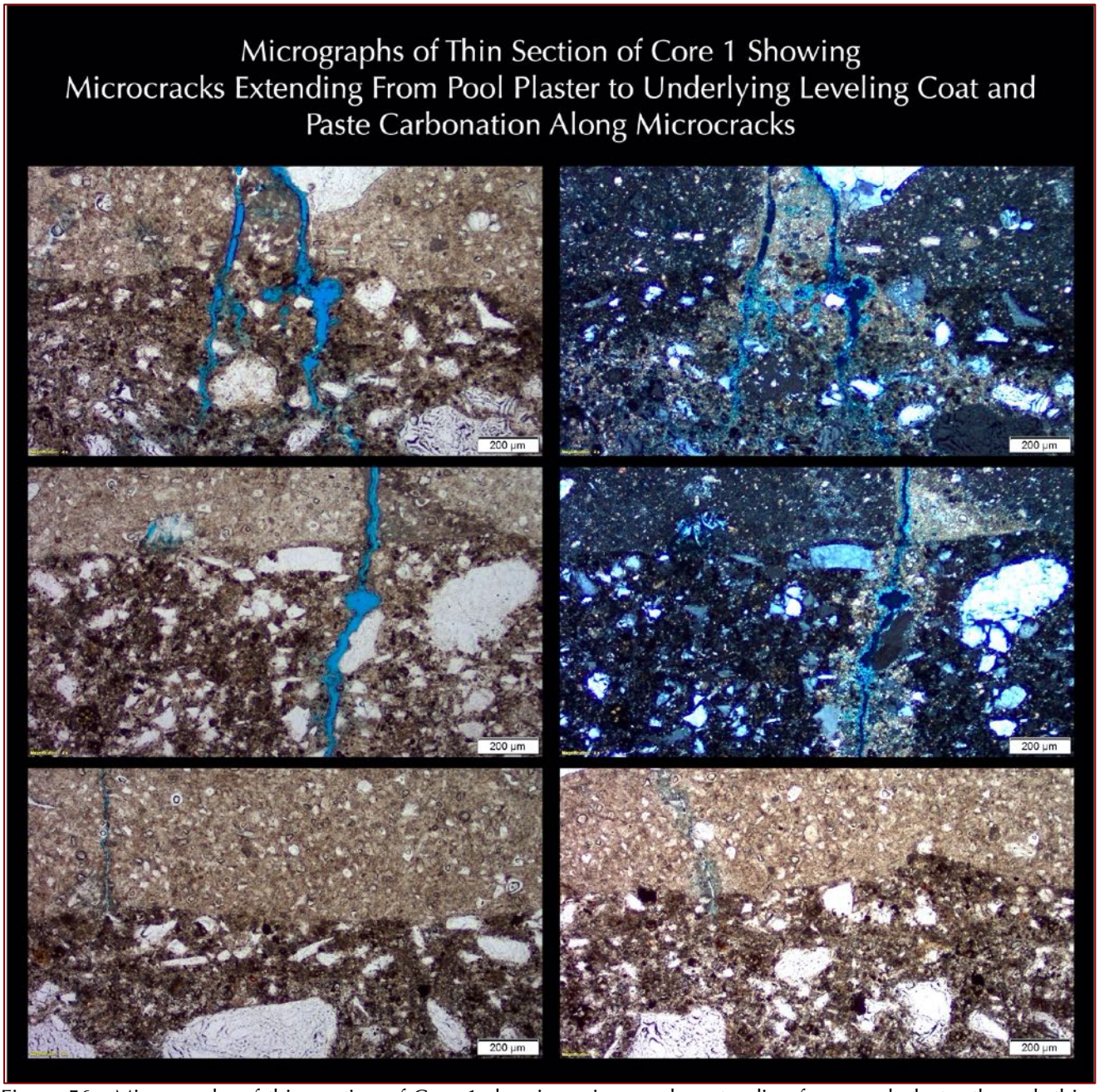

Figure 56: Micrographs of thin section of Core 1 showing microcracks extending from pool plaster through thin dark-toned intermediate leveling coat and carbonation of paste along the walls of microcracks indicating penetration of atmospheric and/or dissolved carbon dioxide from pool to shotcrete. Notice very different composition and microstructure of pool plaster and relatively darker brown thin calcium aluminate cement paste-rich layer of leveling coat where leveling coat have finely ground crushed quartz, quartzite particles and calcium aluminate-based cement (responsible for imparting the overall darker gray color tone). Images were taken in plane (PPL) and cross (XPL) polarized light modes in a petrographic microscope.

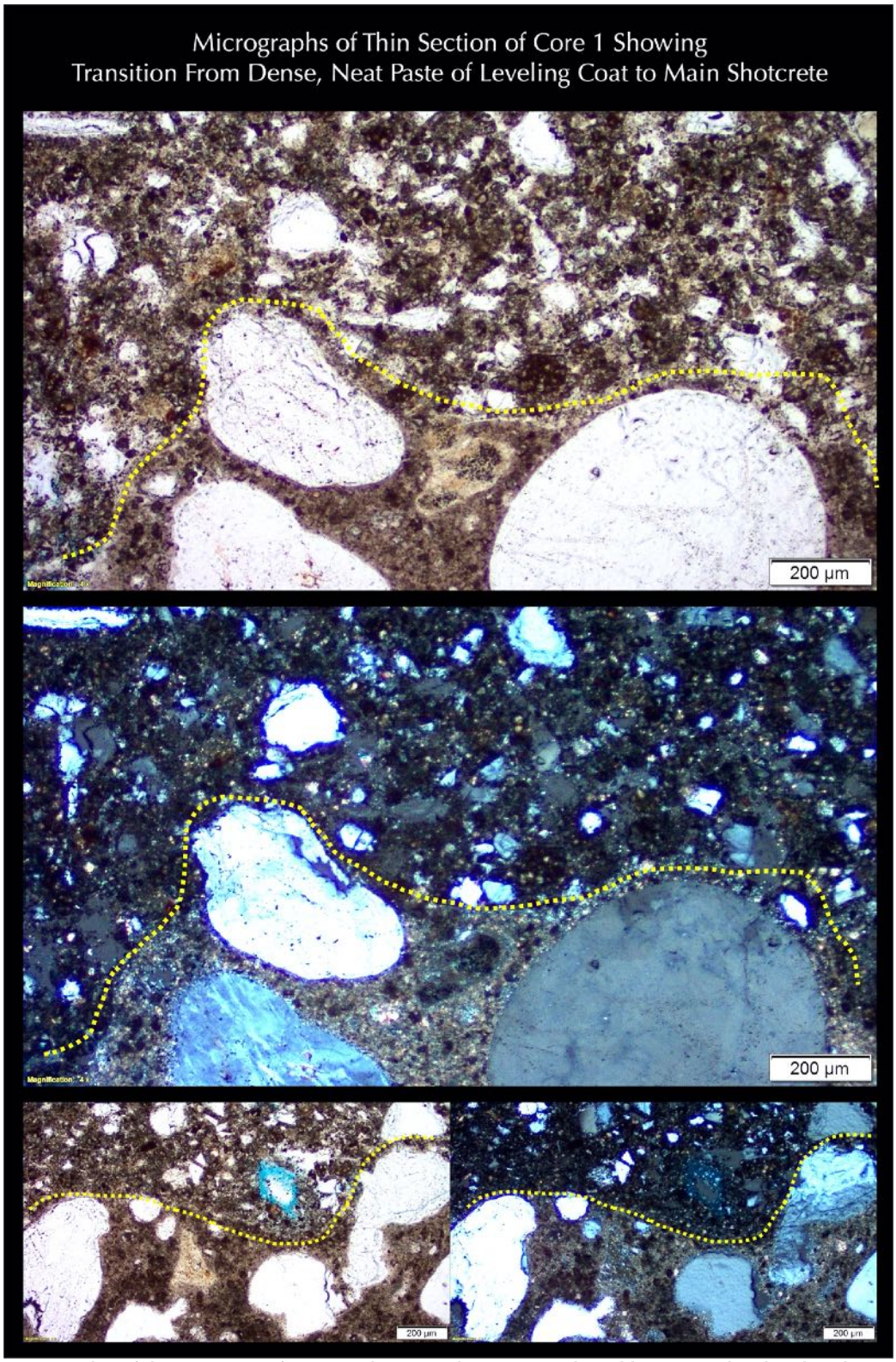

Figure 57: Micrographs of thin section of Core 1 showing the intimate bond between the thin leveling coat of dark-toned paste and very fine crushed quartz filler and underlying main shotcrete body. Notice carbonated paste of shotcrete immediately beneath the leveling coat in the middle row indicating an aerated exposure prior to the placement of leveling coat. Images were taken in plane (PPL) and cross (XPL) polarized light modes in a petrographic microscope.

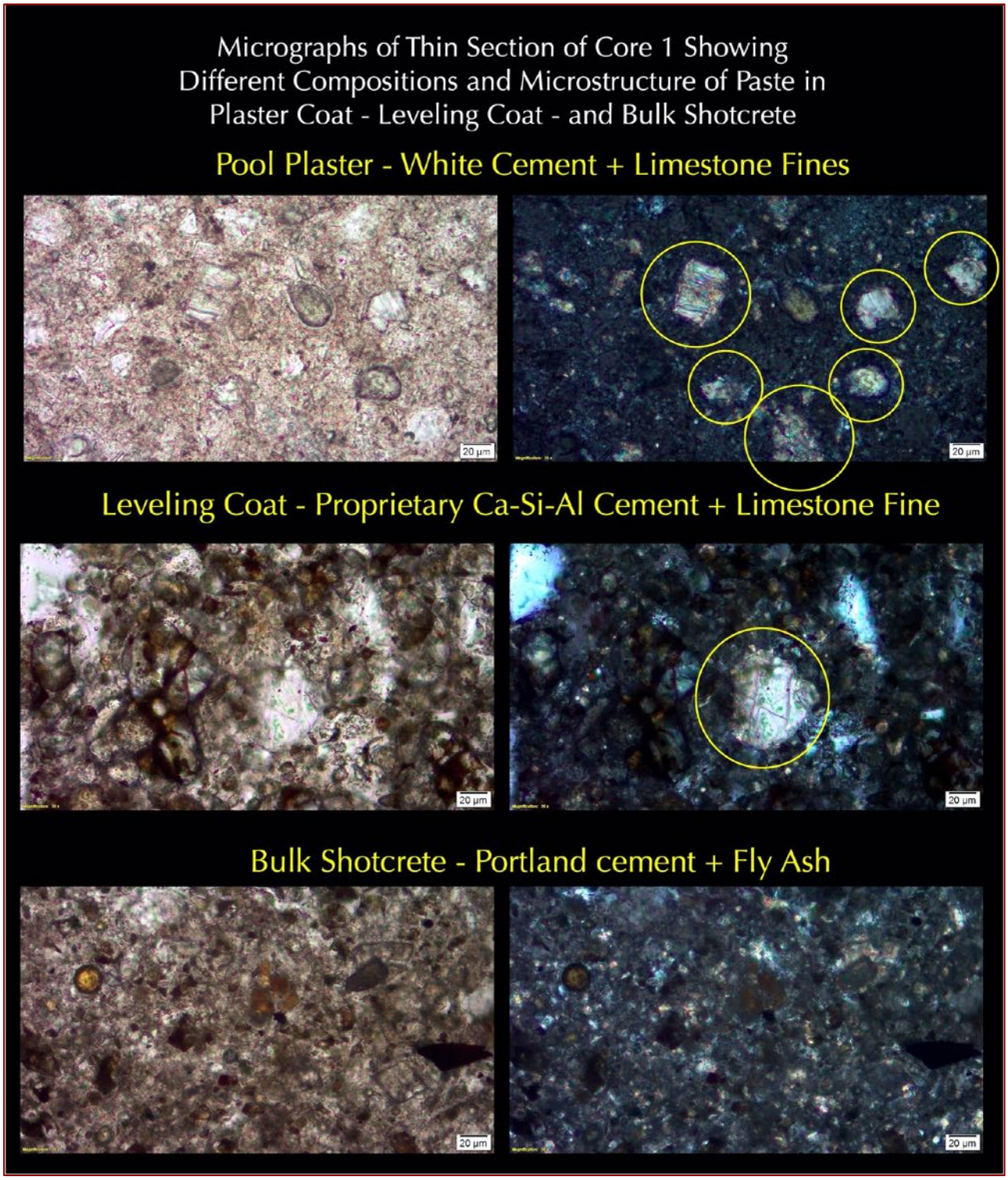

Figure 58: Micrographs of thin section of Core 1 showing the difference in compositions and microstructures of paste in: (a) pool plaster (top row) having white Portland cement and limestone fines scattered throughout a dense matrix of cement hydration products, (b) thin dark-toned leveling coat having dark brown calcium aluminoferrite phases with scattered finely crushed silica and occasional calcite fine particles (middle row), and (c) dense paste of finely ground Portland cement and minor fly ash having residual cement and spherical fly ash particles in the main shotcrete body (bottom row). Images were taken in plane (PPL, left) and corresponding cross (XPL, right) polarized light modes respectively, in a petrographic microscope.

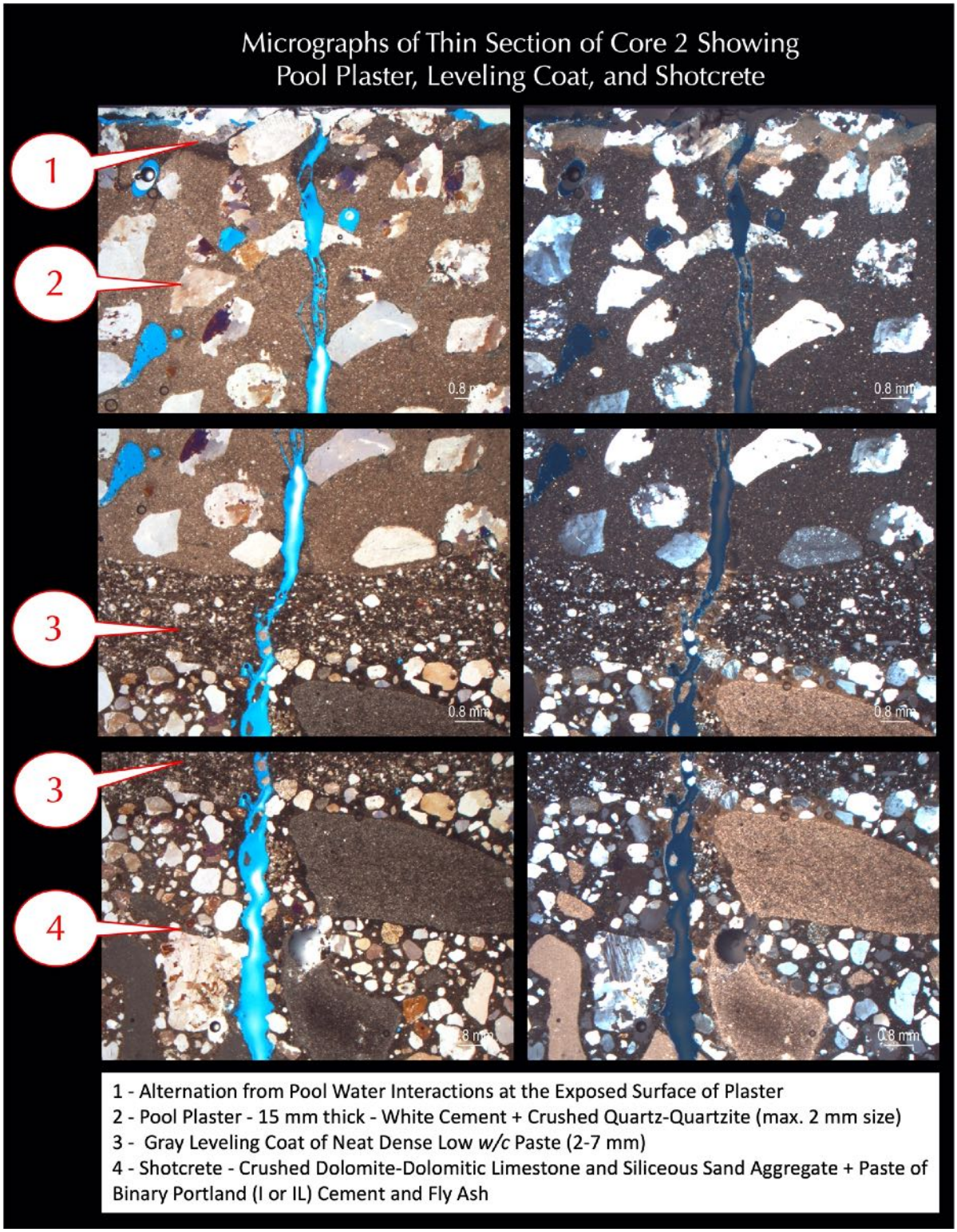

Figure 59: Micrographs of thin section of Core 2 showing: (a) a thin altered zone (Callout '1') from pool water interaction on the dense pool plaster (Callout '2') having many well-graded, well-distributed sub-rounded to angular (crushed) variably strained siliceous sand filler (2-3 mm size), (b) thin dark brown paste of leveling coat having very finely crushed silica sand and occasional limestone fines (Callout '3') in a calcium aluminate cement paste, and (c) the main shotcrete body (Callout '4') having crushed limestone and dolomitic limestone aggregate particles, natural siliceous sand aggregate, and interstitial paste with many coarse entrapped air voids. Images were taken in plane (PPL, left) and corresponding cross (XPL, right) polarized light modes respectively, in a stereozoom microscope.

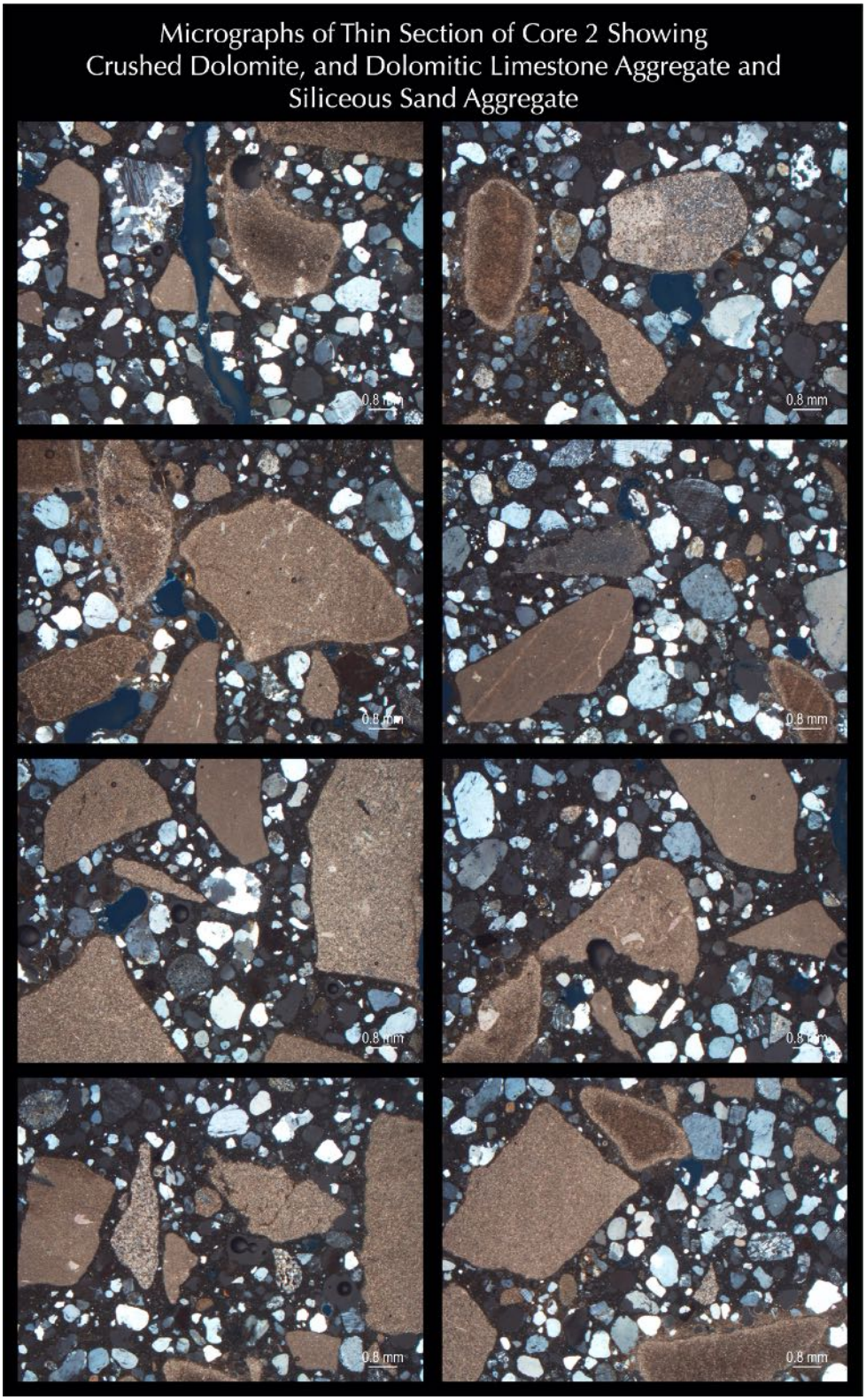

Figure 60: Micrographs of thin section of Core 2 showing: (a) the main shotcrete body having crushed limestone and dolomitic limestone aggregate particles, natural siliceous sand fine aggregate, and interstitial paste with many coarse entrapped air voids. Images were taken in cross (XPL) polarized light mode, in a stereozoom microscope.

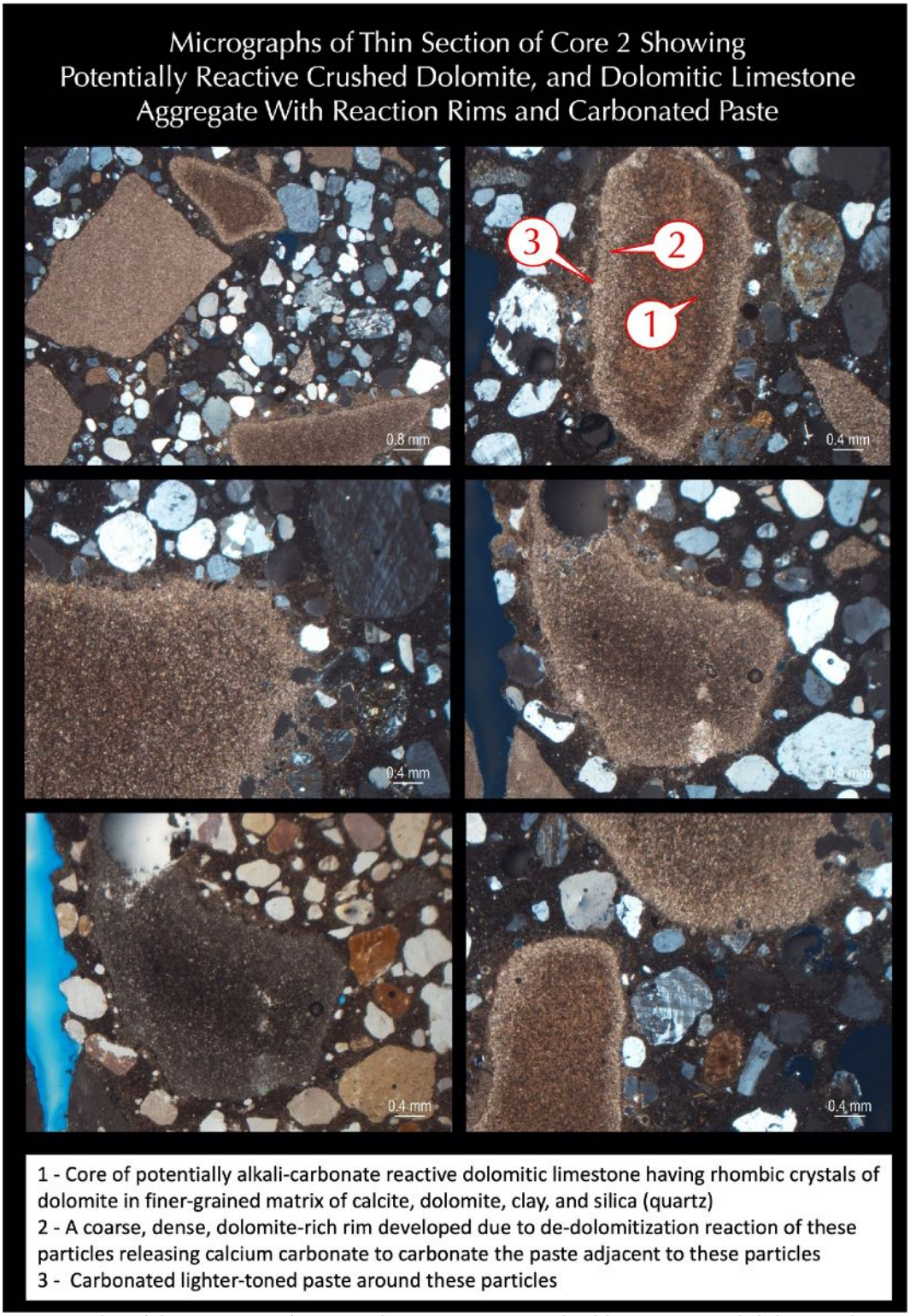

Figure 61: Micrographs of thin section of Core 2 showing many crushed limestone and dolomitic limestone coarse aggregate particles having a core of rhombic crystals of dolomite in finer grains matrix of calcite, dolomite, clay, and quartz (Callout '1'), within a dense rim of coarse dolomite rhombs (Callout '2') and an outer lighter-toned carbonated paste rim (Calklout '3'), which are potentially unsound alkali-carbonate reactive dolomitic limestone particles in aggregate. Images were taken in plane (PPL) or cross (XPL) polarized light modes in a stereozoom microscope.

Figure 62: Micrographs of thin section of Core 2 showing characteristic texture of alkali-carbonate reactive (ACR) rocks in shotcrete in having dolomite rhombs floating in finer-grained matrix of calcite, quartz, and clay.

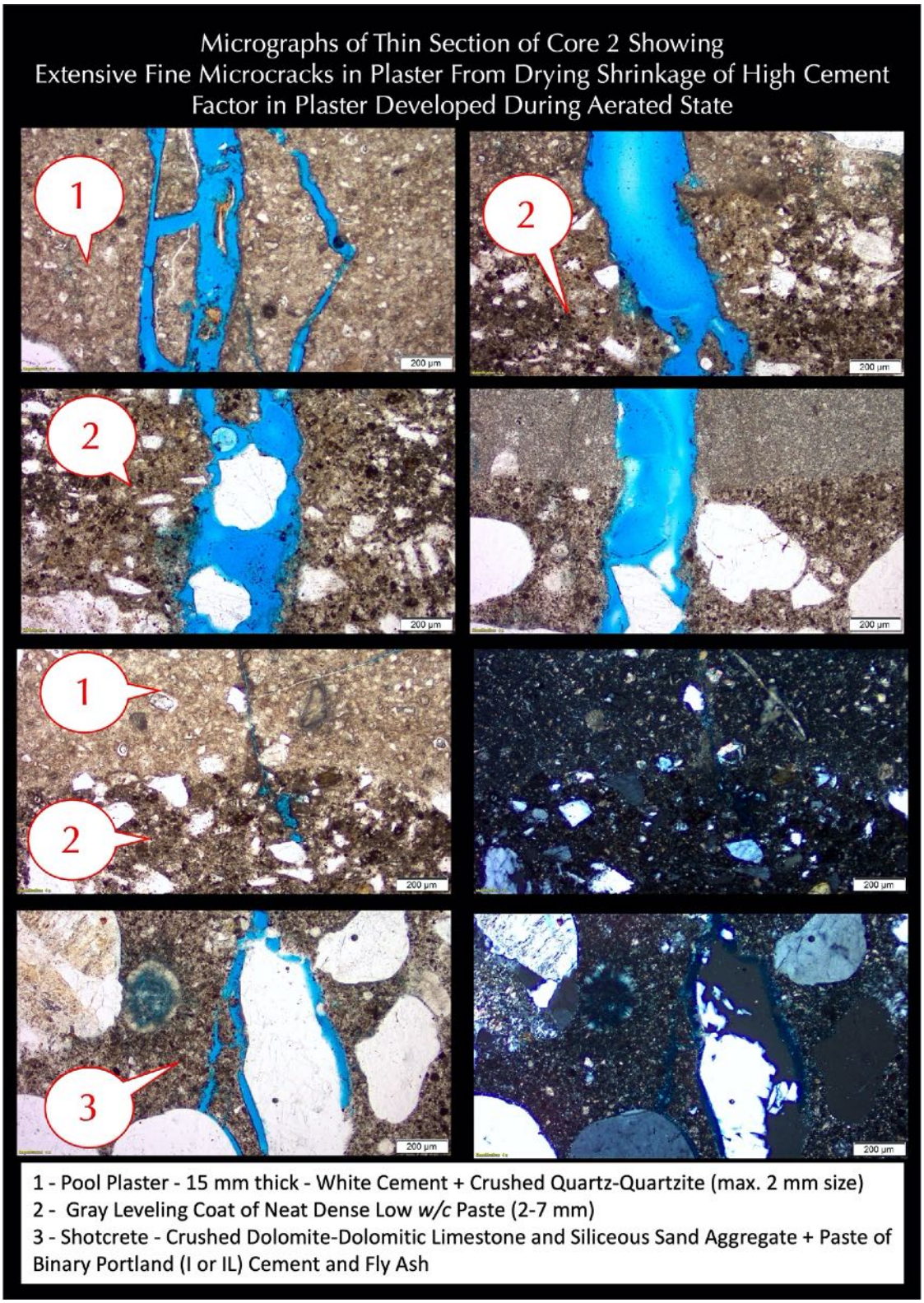

Figure 63: Micrographs of thin section of Core 2 showing microcracks extending from pool plaster through thin dark-toned intermediate leveling coat. Notice very different composition and microstructure of pool plaster and relatively darker brown thin paste of leveling coat where leveling coat have finely ground crushed quartz, quartzite particles and calcium aluminate-based cement (responsible for imparting an overall darker gray color tone). Images were taken in plane (PPL) and cross (XPL) polarized light modes in a petrographic microscope.

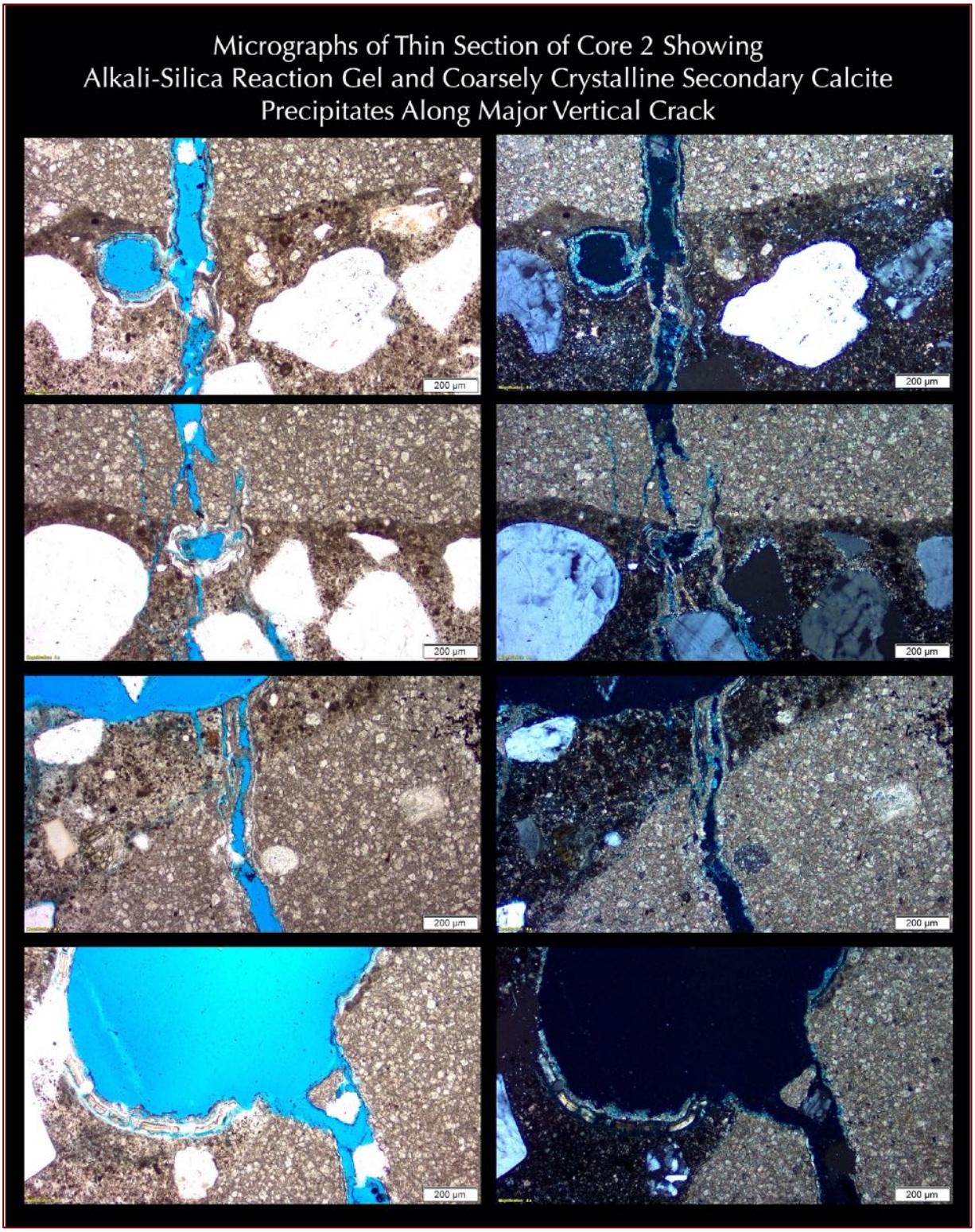

Figure 64: Evidence of alkali-silica reaction gel deposits lining walls of coarse voids where potentially reactive components may have derived from reactive silica particles in dolomitic limestone aggregate and/or reactive silica (chert, microcrystalline silica component in dolomitic limestone, strained quartzite, etc.) in aggregate. Images were taken in plane (PPL, left) and corresponding cross (XPL, right) polarized light modes respectively, in a petrographic microscope.

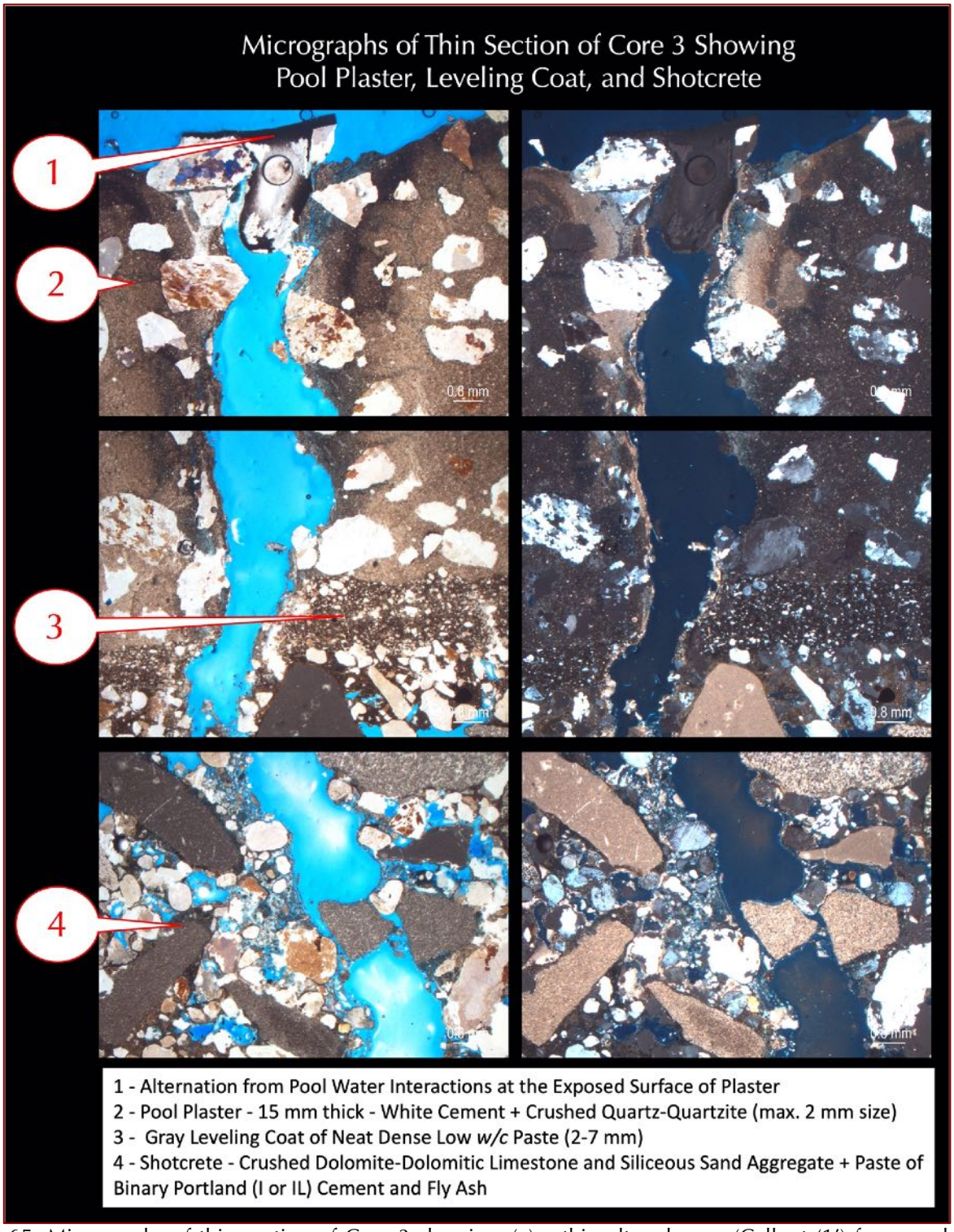

Figure 65: Micrographs of thin section of Core 3 showing: (a) a thin altered zone (Callout '1') from pool water interaction on the dense pool plaster (Callout '2') having many well-graded, well-distributed sub-rounded to angular (crushed) variably strained siliceous sand filler, (b) thin dark brown paste of leveling coat having very finely crushed silica sand and occasional limestone fines (Callout '3'), and (c) the main shotcrete body (Callout '4') having crushed dolomitic limestone aggregate particles, natural siliceous sand aggregate, and interstitial paste with many coarse voids. Images were taken in plane (PPL, left) and corresponding cross (XPL, right) polarized light modes respectively, in a stereozoom microscope.

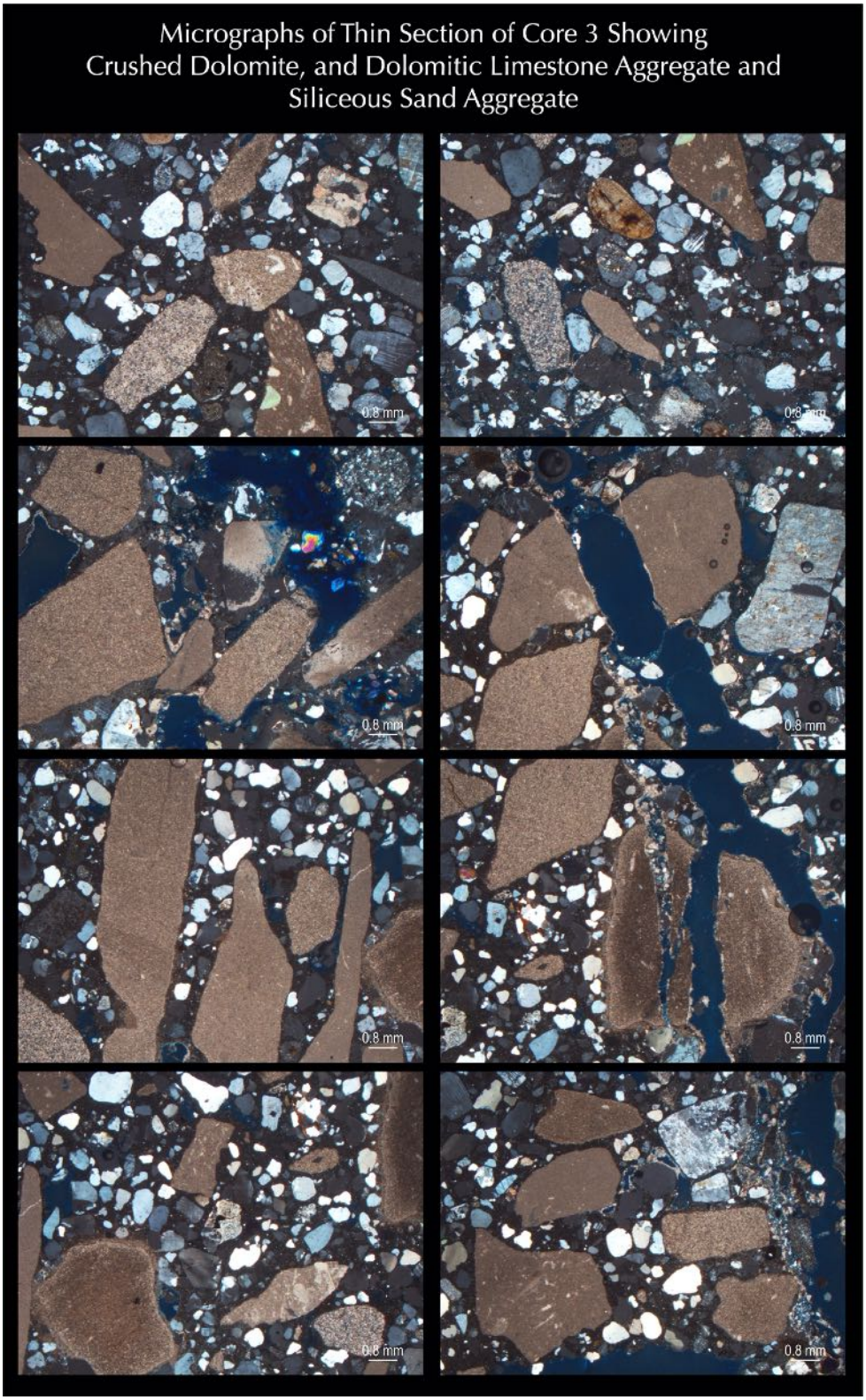

Figure 66: Micrographs of thin section of Core 3 showing: (a) the main shotcrete body having crushed limestone and dolomitic limestone aggregate particles, natural siliceous sand fine aggregate, and interstitial paste with many coarse entrapped air voids. Images were taken in cross (XPL) polarized light mode, in a stereozoom microscope.

Figure 67: Micrographs of thin section of Core 3 showing characteristic texture of alkali-carbonate reactive (ACR) rocks in shotcrete in having dolomite rhombs floating in finer-grained matrix of calcite, quartz, and clay.

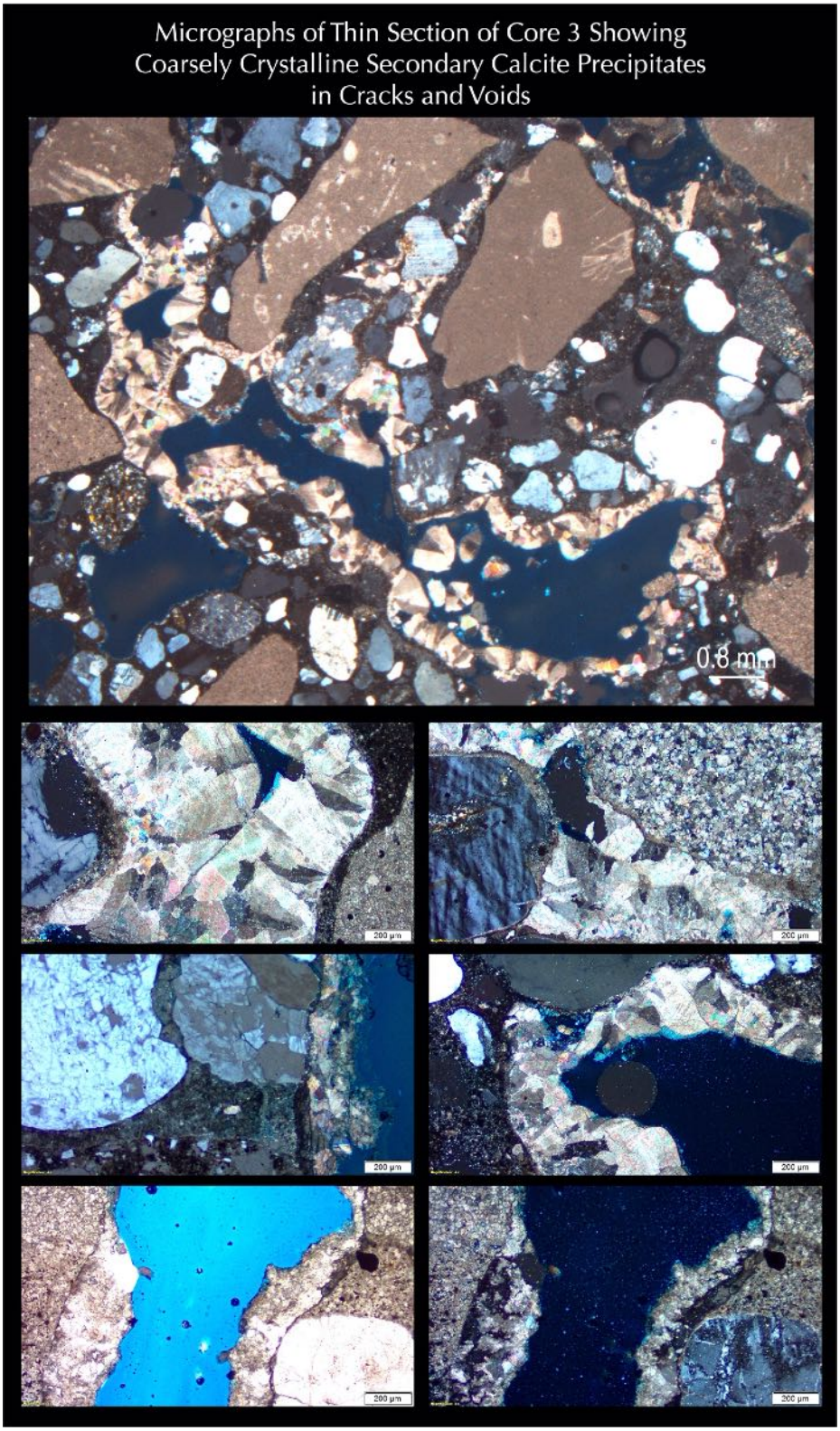

Figure 68: Micrographs of thin section of Core 3 showing coarsely crystalline secondary calcite precipitates lining the walls of coarse entrapped air voids. Images were taken in plane (PPL) or cross (XPL) polarized light modes, in a stereozoom and petrographic microscope

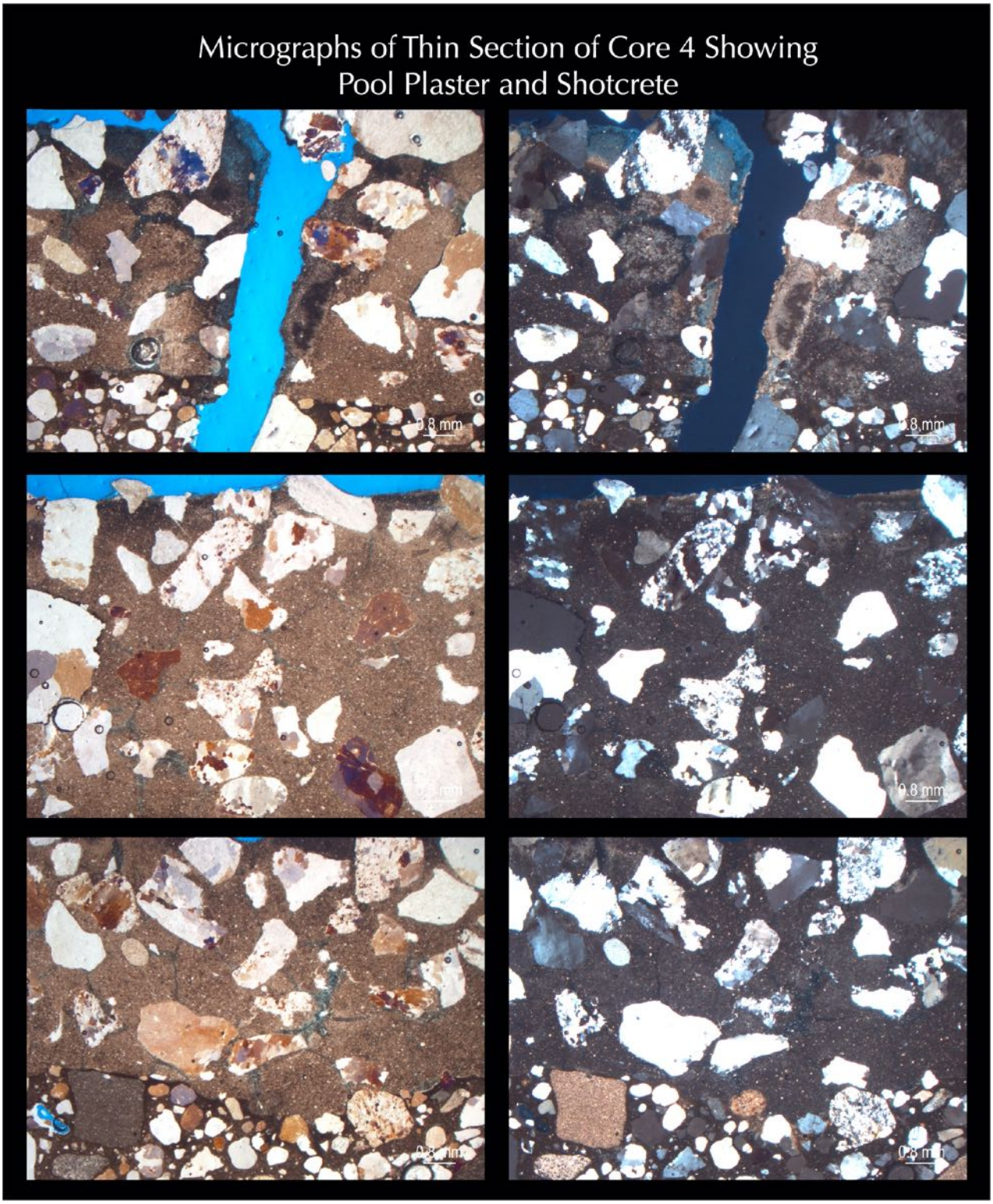

Figure 69: Micrographs of thin section of Core 4 showing: (a) a thin altered zone from pool water interaction on the dense pool plaster having many well-graded, well-distributed sub-rounded to angular (crushed) variably strained siliceous sand filler (2-3 mm size) in dense white cement paste, (b) absence of thin dark brown paste of leveling coat found in three other cores, and (c) the main shotcrete body having crushed limestone and dolomitic limestone aggregate particles, natural siliceous sand aggregate, and interstitial paste with many coarse entrapped air voids. Images were taken in plane (PPL, left) and corresponding cross (XPL, right) polarized light modes respectively, in a stereozoom microscope.

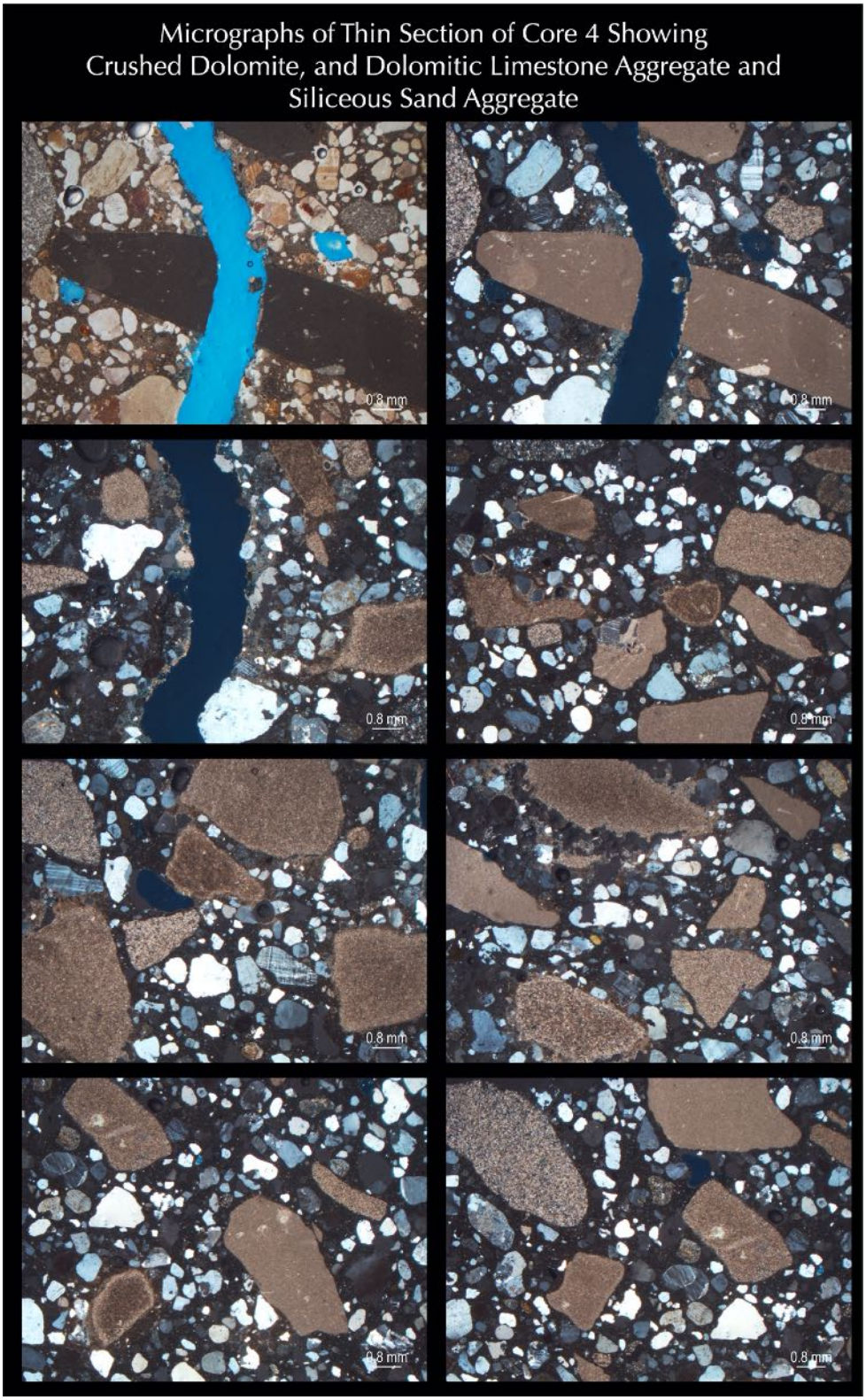

Figure 70: Micrographs of thin section of Core 4 showing: (a) the main shotcrete body having crushed limestone and dolomitic limestone aggregate particles, natural siliceous sand aggregate, and interstitial paste with many coarse entrapped air voids. Images were taken in plane (PPL) and cross (XPL) polarized light modes, in a stereozoom microscope.

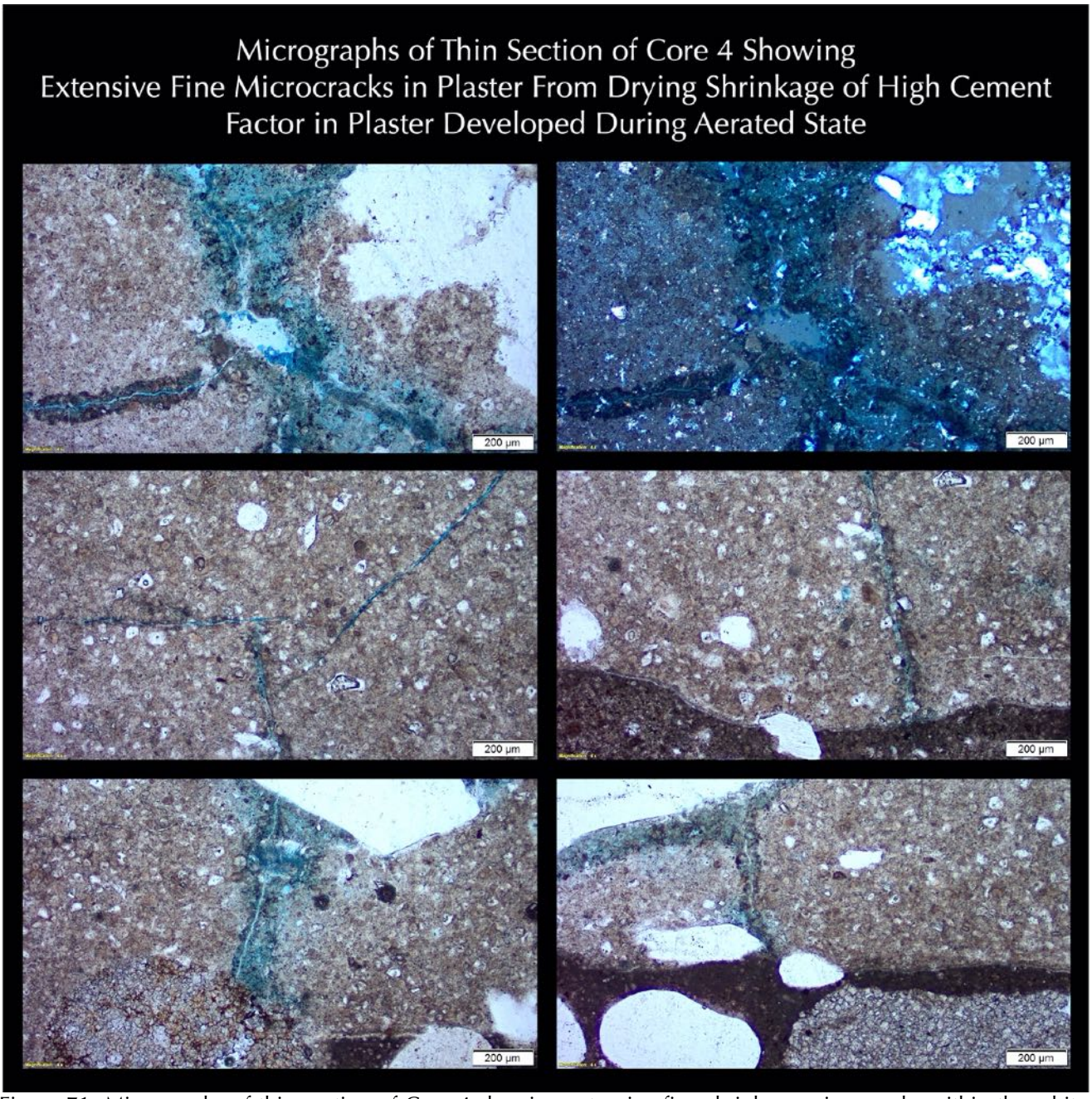

Figure 71: Micrographs of thin section of Core 4 showing extensive fine shrinkage microcracks within the white pool plaster and porous, higher *w/c* paste along the microcracks). Images were taken in plane (PPL) and cross (XPL) polarized light modes in a petrographic microscope.

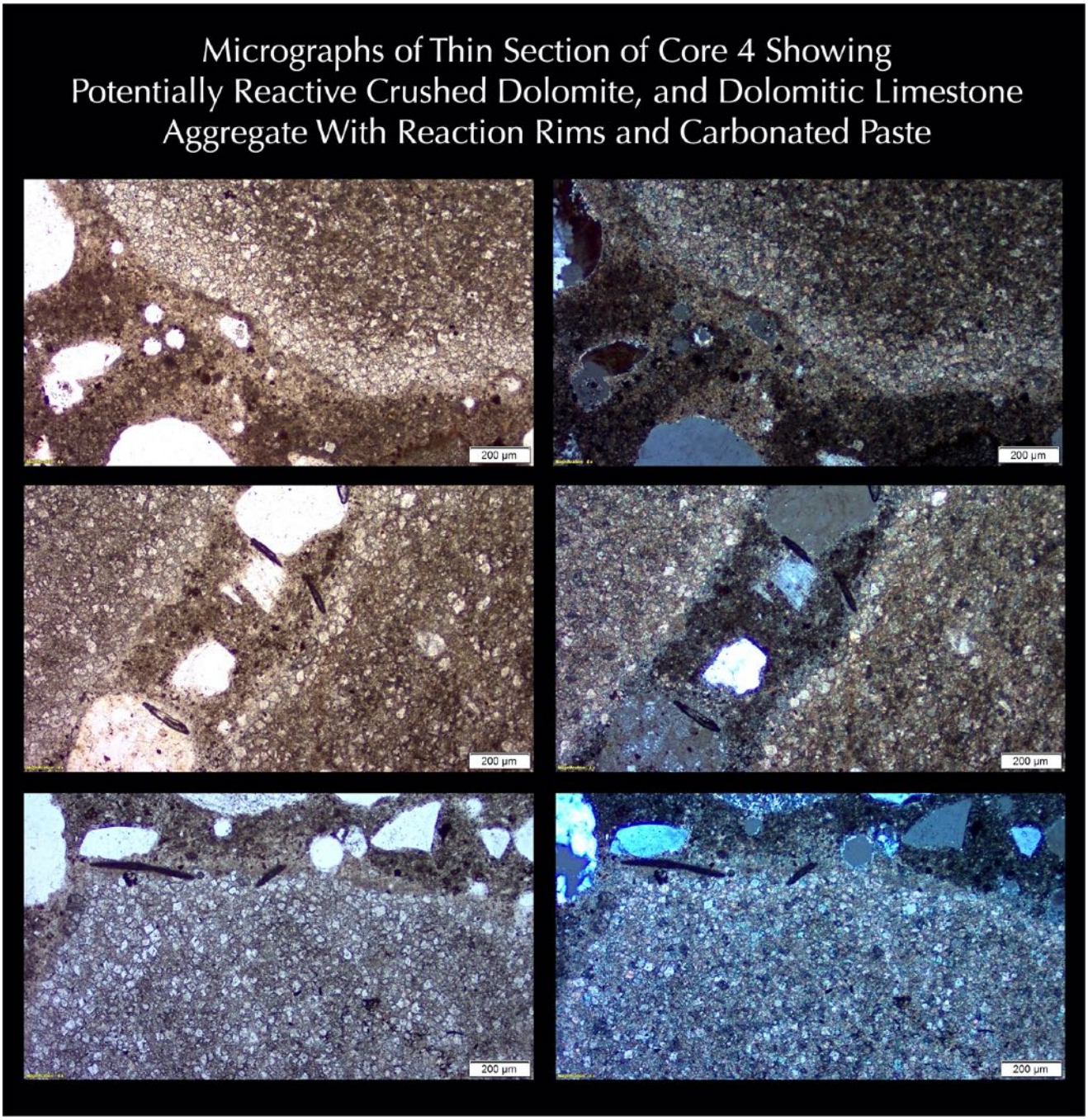

Figure 72: Micrographs of thin section of Core 4 showing many crushed dolomitic limestone aggregate particles having a core of rhombic crystals of dolomite in finer grains matrix of calcite, dolomite, clay, and quartz within a dense rim of coarse dolomite rhombs and an outer lighter-toned carbonated paste rim, which are potentially unsound alkali-carbonate reactive dolomitic limestone particles in aggregate. Images were taken in plane (PPL) or cross (XPL) polarized light modes in a petrographic microscope.

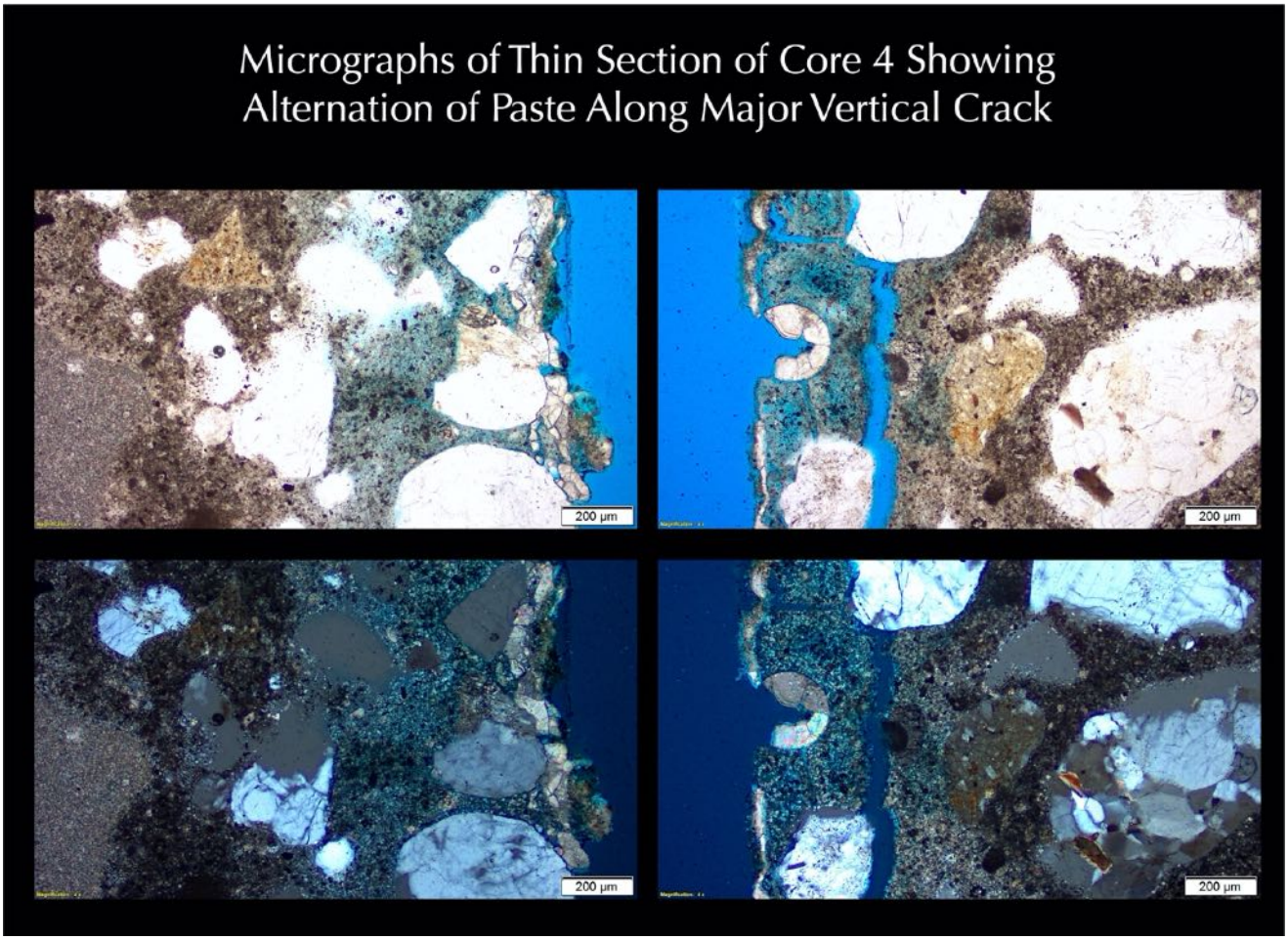

Figure 73: Micrographs of thin section of Core 4 showing alteration of paste along the walls of major vertical crack due to pool water penetration along the cracks. Images were taken in plane (top, PPL) and corresponding cross (bottom, XPL) polarized light modes respectively, in a petrographic microscope.

SEM-EDS STUDIES

Secondary Electron Image and X-Ray Microanalyses of White Pool Plaster in Core 1

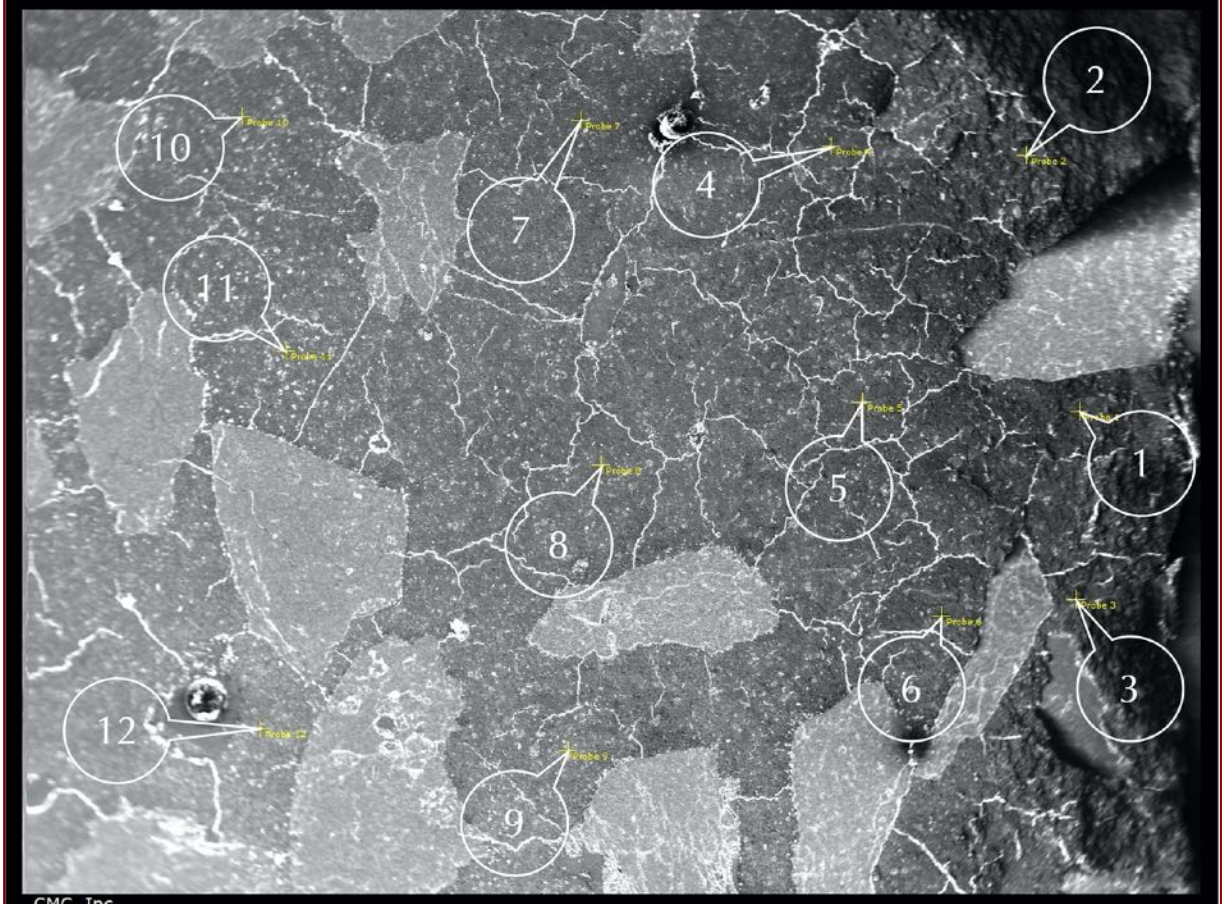

Probe	Si	Al	Na	Mg	S	K	Ca	Ti	Fe	Total	Phase
1	**48.19**	6.10	1.93	4.03	0.00	0.30	**39.22**	0.00	0.22	99.99	Paste
2	**48.38**	8.96	1.03	3.32	9.85	0.24	**27.87**	0.00	0.34	99.99	Paste
3	**45.51**	10.71	2.23	4.21	0.18	0.38	**36.65**	0.13	0.01	100.01	Paste
4	**53.95**	6.77	0.66	1.97	1.68	0.37	**33.88**	0.36	0.35	99.99	Paste
5	**46.43**	4.94	1.16	2.85	2.75	0.34	**41.08**	0.12	0.34	100.01	Paste
6	**39.04**	9.63	1.37	3.55	12.39	0.30	**33.46**	0.08	0.17	99.99	Paste
7	**38.34**	4.17	1.24	1.58	0.00	0.26	**54.22**	0.18	0.00	99.99	Paste
8	**64.18**	6.15	1.13	2.24	0.00	0.23	**25.27**	0.00	0.80	100.00	Paste
9	**53.12**	6.03	0.78	4.78	4.14	0.28	**30.26**	0.31	0.30	100.00	Paste
10	**56.63**	8.93	0.72	1.76	0.79	0.25	**30.49**	0.08	0.35	100.00	Paste
11	**43.89**	8.37	1.38	4.57	6.33	0.20	**34.89**	0.00	0.37	100.00	Paste
12	**61.61**	5.39	1.21	2.49	0.10	0.18	**28.58**	0.00	0.44	100.00	Paste

Figure 74: Backscatter electron image (top) and X-ray microanalyses at the tips of callouts of paste in the pool plaster in Core 1. Image shows extensive shrinkage cracking of plaster due to use of a high volume of white Portland cement paste relative to silica sand filler.

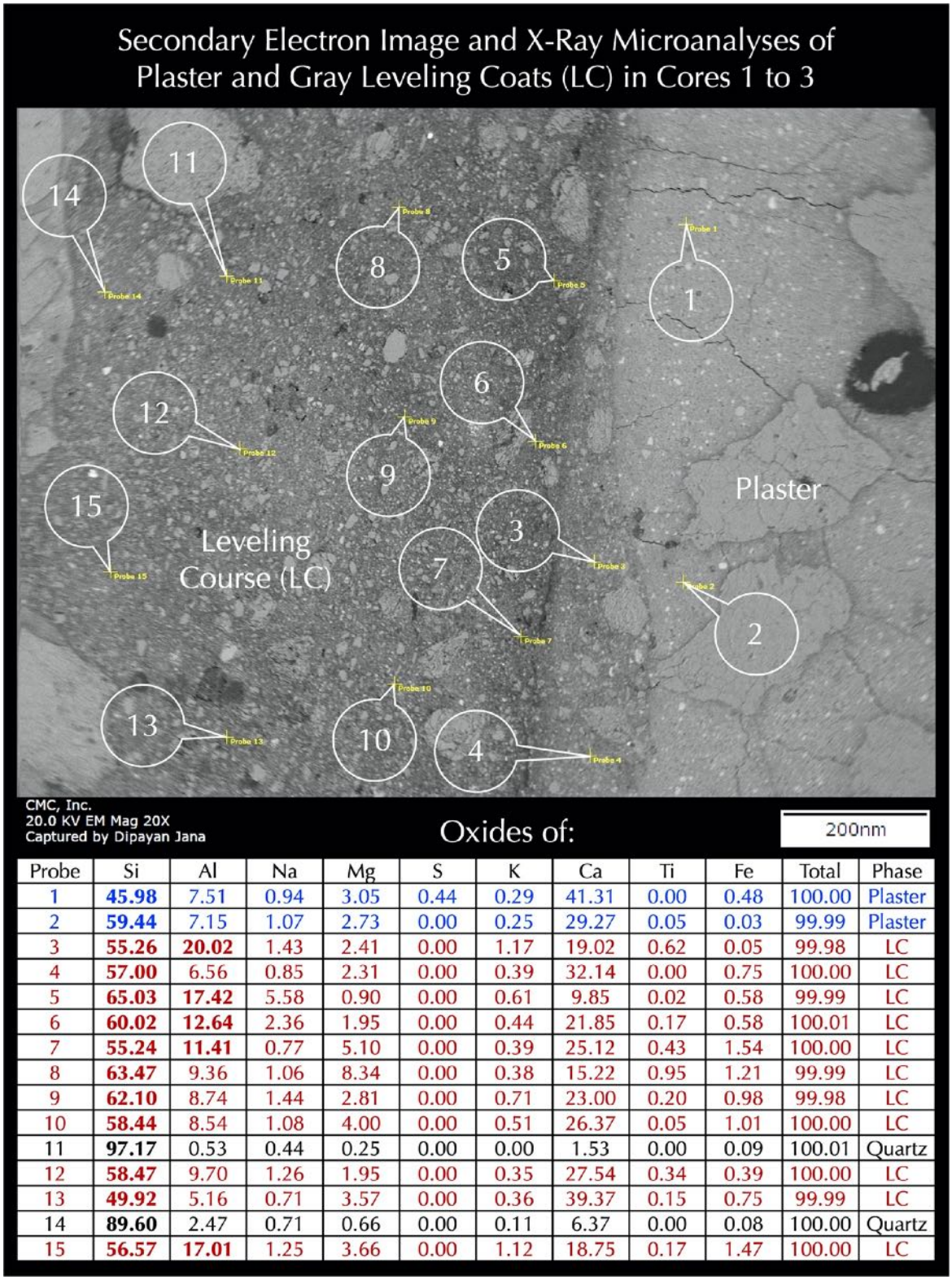

Probe	Si	Al	Na	Mg	S	K	Ca	Ti	Fe	Total	Phase
1	**45.98**	7.51	0.94	3.05	0.44	0.29	41.31	0.00	0.48	100.00	Plaster
2	**59.44**	7.15	1.07	2.73	0.00	0.25	29.27	0.05	0.03	99.99	Plaster
3	**55.26**	**20.02**	1.43	2.41	0.00	1.17	19.02	0.62	0.05	99.98	LC
4	**57.00**	6.56	0.85	2.31	0.00	0.39	32.14	0.00	0.75	100.00	LC
5	**65.03**	**17.42**	5.58	0.90	0.00	0.61	9.85	0.02	0.58	99.99	LC
6	**60.02**	**12.64**	2.36	1.95	0.00	0.44	21.85	0.17	0.58	100.01	LC
7	**55.24**	**11.41**	0.77	5.10	0.00	0.39	25.12	0.43	1.54	100.00	LC
8	**63.47**	9.36	1.06	8.34	0.00	0.38	15.22	0.95	1.21	99.99	LC
9	**62.10**	8.74	1.44	2.81	0.00	0.71	23.00	0.20	0.98	99.98	LC
10	**58.44**	8.54	1.08	4.00	0.00	0.51	26.37	0.05	1.01	100.00	LC
11	**97.17**	0.53	0.44	0.25	0.00	0.00	1.53	0.00	0.09	100.01	Quartz
12	**58.47**	9.70	1.26	1.95	0.00	0.35	27.54	0.34	0.39	100.00	LC
13	**49.92**	5.16	0.71	3.57	0.00	0.36	39.37	0.15	0.75	99.99	LC
14	**89.60**	2.47	0.71	0.66	0.00	0.11	6.37	0.00	0.08	100.00	Quartz
15	**56.57**	**17.01**	1.25	3.66	0.00	1.12	18.75	0.17	1.47	100.00	LC

Figure 75: Backscatter electron image (top) and X-ray microanalyses at the tips of callouts of paste in the pool plaster at right and underlying calcium aluminate based leveling course at left. Notice extensive shrinkage cracking in pool plaster from the use of a high-volume white Portland cement relative to sand compared to no such cracking in the gray calcium aluminate cement based leveling course.

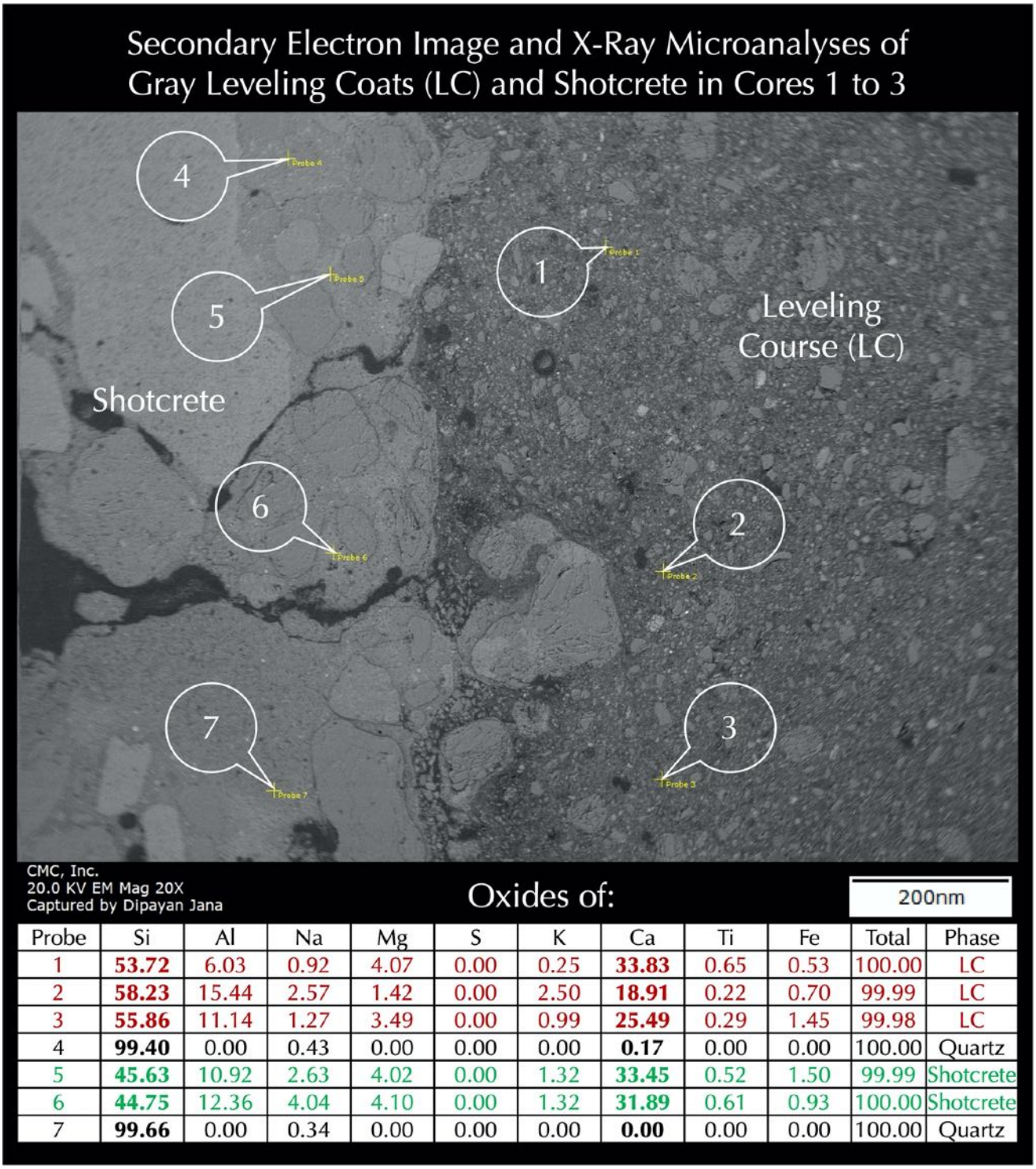

Probe	Si	Al	Na	Mg	S	K	Ca	Ti	Fe	Total	Phase
1	**53.72**	6.03	0.92	4.07	0.00	0.25	**33.83**	0.65	0.53	100.00	LC
2	**58.23**	15.44	2.57	1.42	0.00	2.50	**18.91**	0.22	0.70	99.99	LC
3	**55.86**	11.14	1.27	3.49	0.00	0.99	**25.49**	0.29	1.45	99.98	LC
4	**99.40**	0.00	0.43	0.00	0.00	0.00	**0.17**	0.00	0.00	100.00	Quartz
5	**45.63**	10.92	2.63	4.02	0.00	1.32	**33.45**	0.52	1.50	99.99	Shotcrete
6	**44.75**	12.36	4.04	4.10	0.00	1.32	**31.89**	0.61	0.93	100.00	Shotcrete
7	**99.66**	0.00	0.34	0.00	0.00	0.00	**0.00**	0.00	0.00	100.00	Quartz

Figure 76: Backscatter electron image (top) and X-ray microanalyses at the tips of callouts of calcium aluminate based leveling course at right and main shotcrete body at left.

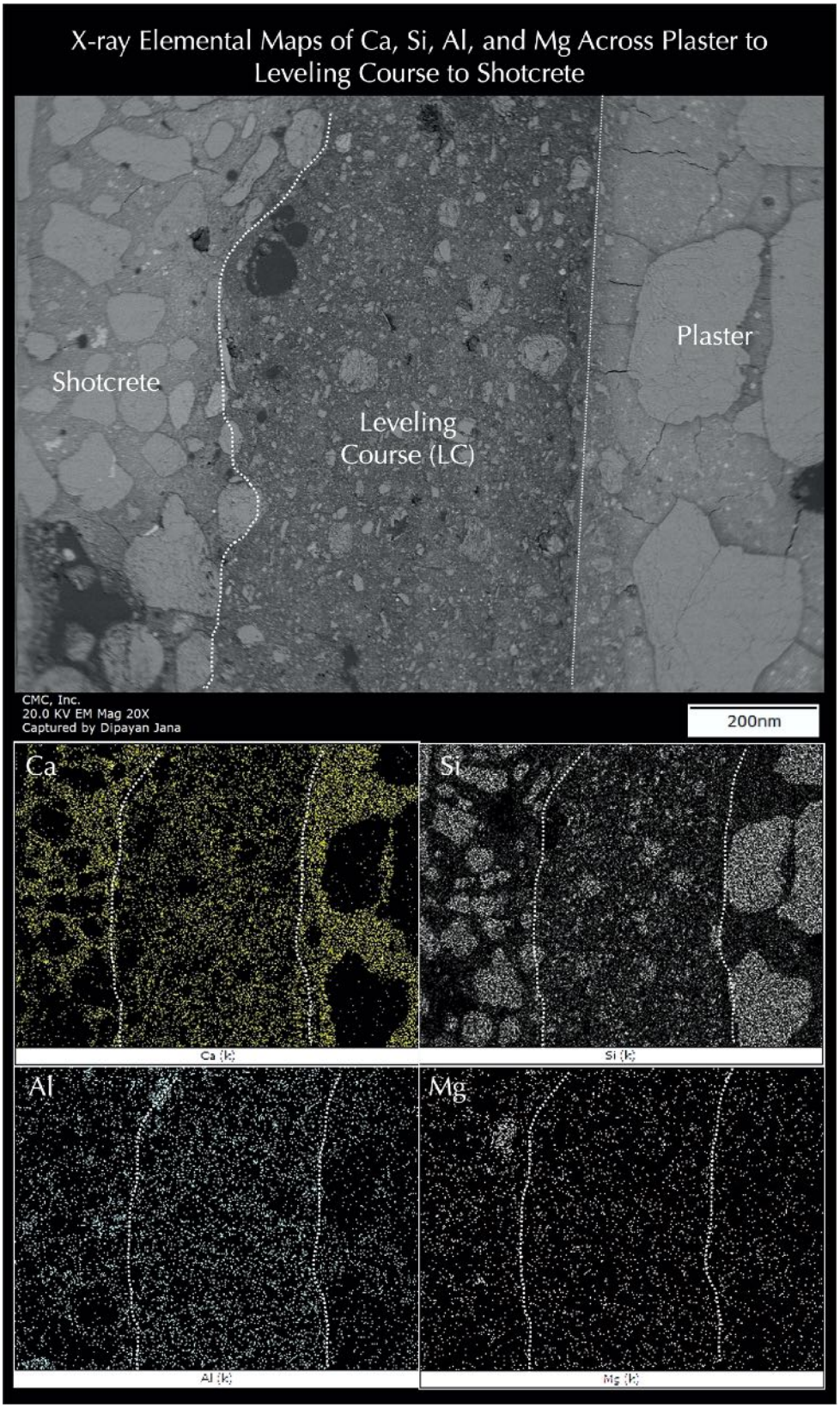

Figure 77: Backscatter electron image (top) and X-ray elemental maps of Ca, Si, Al, and Mg showing the pool plaster with extensive cracking at right, calcium aluminate based leveling course in the middle, and the main shotcrete body at left.

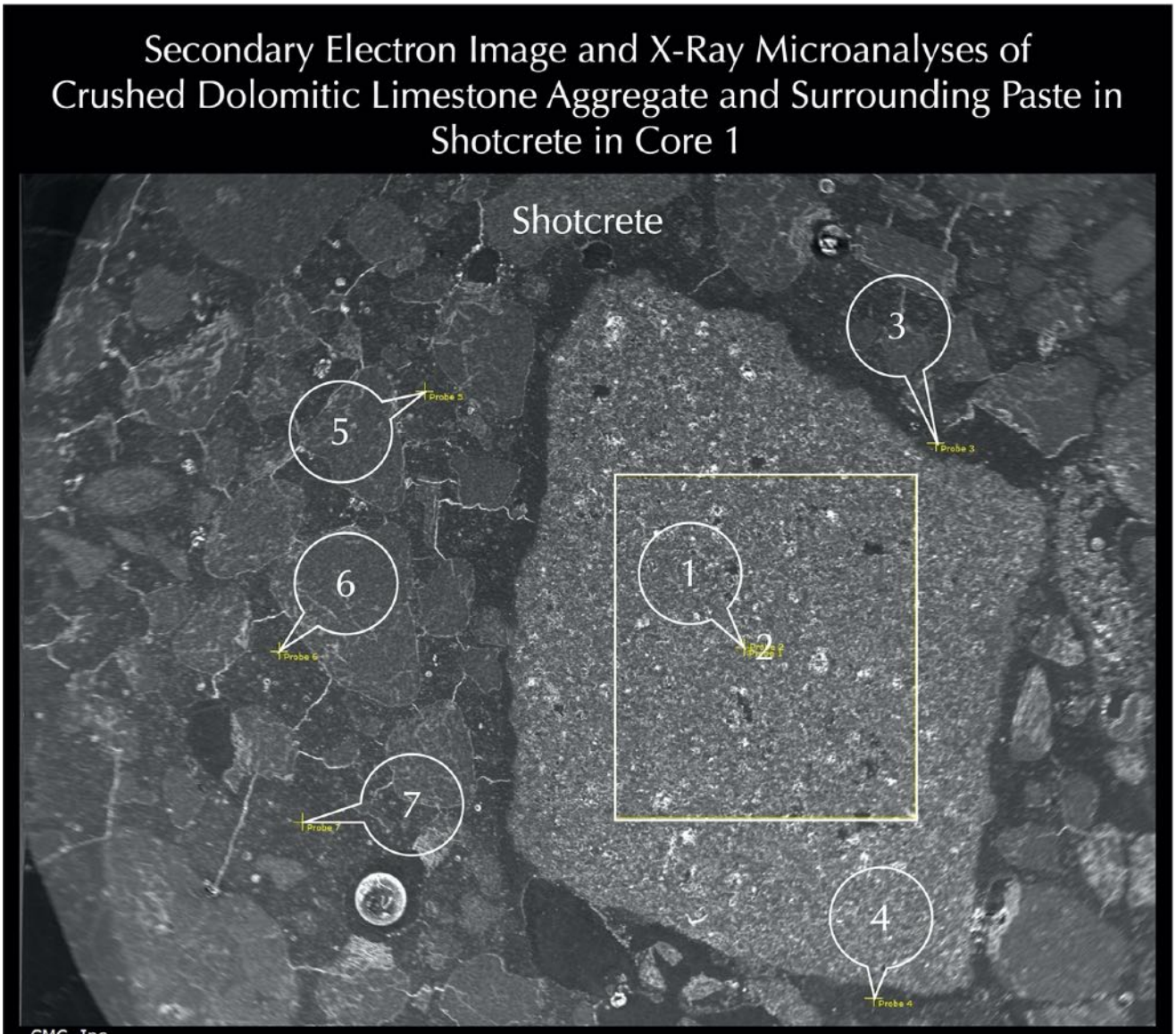

Probe	Si	Mg	Al	Na	S	K	Ca	Ti	Fe	Total	Phase
1	**51.24**	**30.78**	8.60	0.27	0.00	1.29	**6.83**	0.00	0.99	100.00	Agg.
2	**59.84**	**19.15**	6.64	0.50	0.00	1.18	**12.31**	0.18	0.20	100.00	Agg.
3	**39.24**	**10.62**	5.33	2.37	0.00	0.52	**40.04**	0.76	1.12	100.00	Paste
4	**43.89**	**33.26**	8.25	0.22	0.00	1.63	**12.40**	0.04	0.30	99.99	Paste
5	98.67	0.04	0.06	0.45	0.00	0.00	0.00	0.78	0.00	100.00	Quartz
6	**77.15**	3.03	5.81	0.41	0.00	0.15	**12.21**	0.46	0.77	99.99	Paste
7	**54.22**	3.43	8.98	0.99	0.00	0.54	**30.57**	0.50	0.78	100.01	Paste

Figure 78: Secondary electron image (top) and X-ray microanalyses at the tips of callouts and within a boxed area of the main shotcrete body showing rhombic crystal of dolomite in a dolomitic limestone aggregate and surrounding paste.

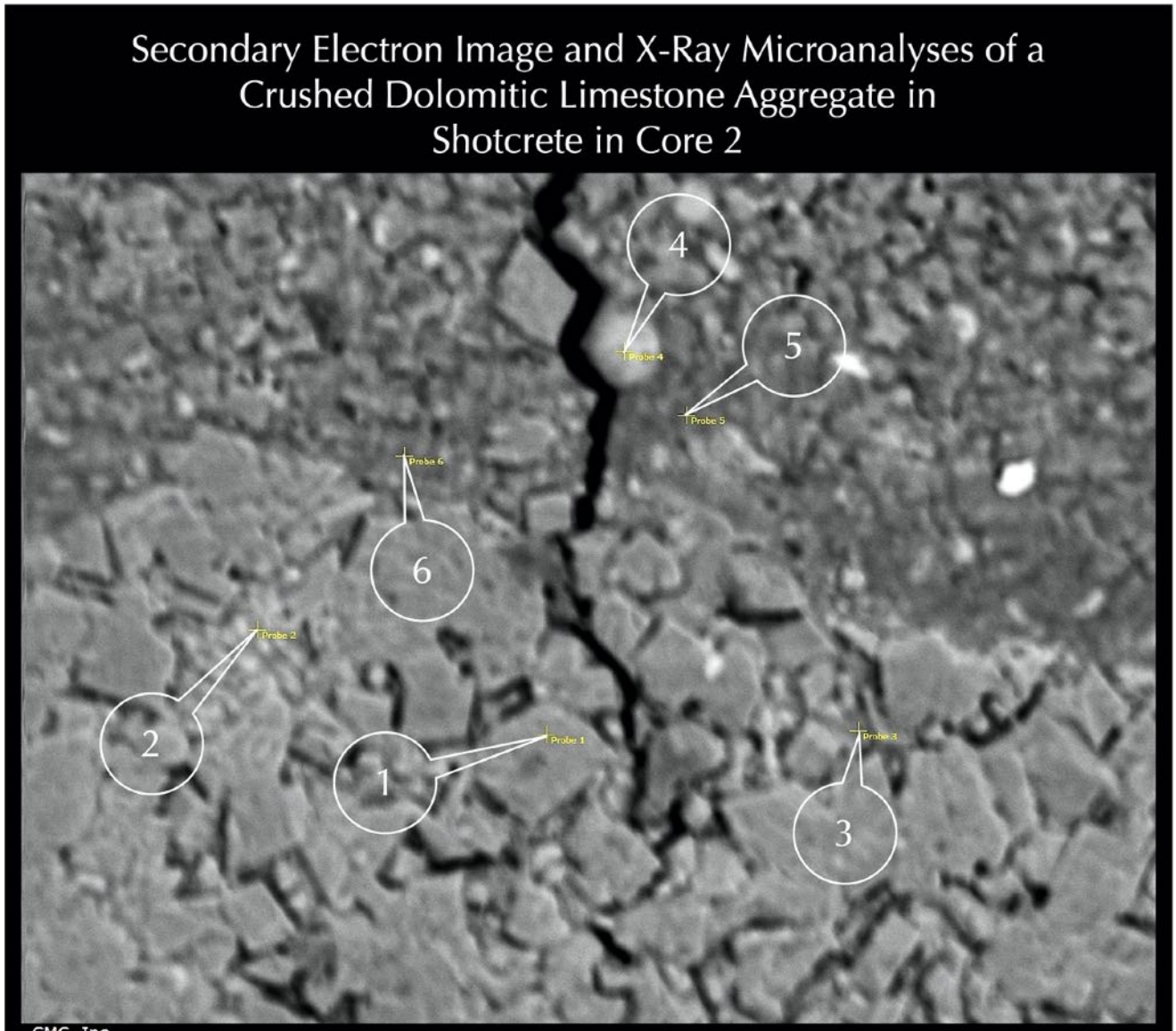

Probe	Mg	Si	Na	Al	S	K	Ca	Ti	Fe	Total	Phase
1	**51.23**	20.11	0.64	3.17	0.00	0.71	**23.94**	0.00	0.20	100.0	Dolomite
2	4.34	**61.49**	0.84	10.05	0.00	2.12	**21.07**	0.10	0.00	100.0	Matrix
3	6.00	**36.42**	0.77	2.52	0.00	10.12	**40.90**	0.07	3.18	99.98	Matrix
4	**30.37**	16.80	0.29	29.17	0.00	0.29	**17.68**	2.04	3.36	100.0	Dolomite
5	3.69	**68.28**	3.08	6.76	0.00	0.54	**16.67**	0.14	0.86	100.0	Matrix
6	3.45	**63.19**	2.84	6.45	0.00	0.36	**22.68**	0.14	0.89	100.0	Matrix

Figure 79: Secondary electron image (top) and X-ray microanalyses at the tips of callouts of main shotcrete body showing rhombic crystal of dolomite in a dolomitic limestone aggregate in shotcrete.

Secondary Electron Image and X-Ray Microanalyses of a Coarsely Crystalline Calcite Precipitates along a Crack in a Crushed Dolomitic Limestone Aggregate in Shotcrete in Core 4

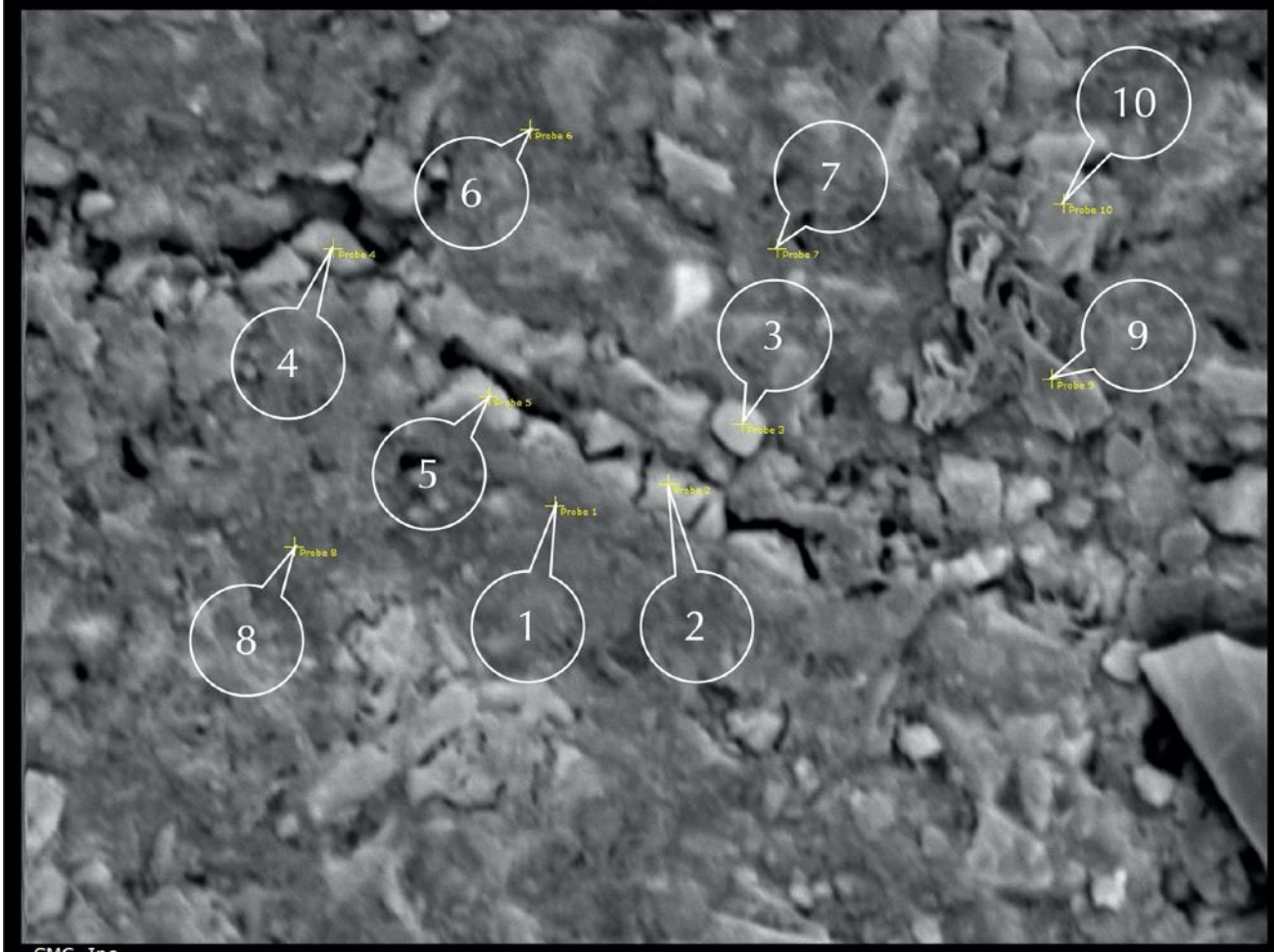

CMC, Inc.
20.0 KV EM Mag 1170X
Captured by Dipayan Jana

Oxides of:

200nm

Probe	Mg	Si	Al	Na	S	K	Ca	Ti	Fe	Total	Phase
1	**44.14**	**37.96**	11.73	0.18	0.00	0.22	5.28	0.00	0.48	99.99	Matrix
2	6.17	9.77	1.65	0.55	0.00	0.78	**81.07**	0.01	0.00	100.00	Calcite
3	**18.76**	**47.95**	10.09	0.28	0.00	0.20	**18.72**	2.98	1.02	100.00	Ca-Mg-Si
4	2.64	8.71	1.56	0.10	0.00	0.88	**84.26**	1.19	0.65	99.99	Calcite
5	16.27	10.52	1.40	0.33	0.00	0.60	**70.22**	0.15	0.51	100.00	Calcite
6	38.44	49.20	9.65	0.01	0.00	0.35	2.06	0.00	0.29	100.00	Dolomite
7	**23.38**	**47.02**	**14.55**	0.29	0.00	2.14	**12.10**	0.10	0.42	100.00	Matrix
8	42.93	40.21	9.59	0.32	0.00	0.69	5.91	0.11	0.24	100.00	Dolomite
9	**22.13**	**53.36**	**14.85**	0.54	0.00	1.67	**6.70**	0.23	0.52	100.00	Matrix
10	**61.34**	4.90	0.00	0.00	0.00	0.18	**32.36**	0.50	0.72	100.00	Dolomite

Figure 80: Secondary electron image (top) and X-ray microanalyses at the tips of callouts of main shotcrete body showing rhombic crystal of dolomite in a dolomitic limestone aggregate in shotcrete.

POOL PLASTER

Pool plaster is compositionally similar cementitious plaster coat across all four cores and consist of: (a) white Portland cement, minor limestone fines, and 2 to 3 mm nominal size well-sorted, well-distributed lightly crushed siliceous (quartz, quartzite) filler (Figures 30, 32, 34, 36, 38 to 45). In all four cores, plaster showed extensive shrinkage cracking in the paste fractions (Figures 46, 54, 55, 63, 65, 761, 74, 75, and 77) due to high paste volume relative to silica fillers where cracks are confined within the plaster and did not extend into the underlying leveling coat or shotcrete. These extensive fine, hairline shrinkage cracks in plaster paste are invisible on the exposed surface of plaster relative to the major visible cracks that have transected through plaster into the shotcrete body and formed entirely due to shrinkage of a high paste-volume cementitious plaster.

LEVELING COURSE

Three cores (Nos. 1 to 3) from the steps but not the fourth one (No. 4) from the floor showed the presence of a thin medium gray (compared to darker gray shotcrete body) leveling course applied on the shotcrete body prior to the placement of pool plaster, which is determined to be a calcium aluminate cement and minor limestone fine based course (Figures 46, 56, 57, 59, 63, 65, and 71) as opposed to white Portland cement and limestone fine at the top plaster or Portland cement and fly ash based binder used in the underlying main shotcrete body. This thin leveling course is well bonded to the shotcrete body beneath, and to the pool plaster above.

SHOTCRETE

Crushed Dolomitic Limestone and Natural Siliceous Sand Aggregates

Shotcrete is compositionally similar in terms of ingredients across all four cores consist of: (a) ¼ in. (6.25 mm) nominal maximum size crushed limestone and argillaceous dolomitic limestone aggregate (Figures 22, 24, 26, and 28), and (b) noticeably finer nominal 2-3 mm size crushed siliceous (quartz, quartzite) sand aggregates (Figures 39, 41, 43, and 45).

Many argillaceous dolomitic limestone particles in aggregate showed dark reaction rims along the periphery of the aggregates (Figures 31, 33, 35, 37, 47-51, 59-62, 66, 67, 70, and 72) and many of those particles additionally showed lighter cream-colored carbonation rims in paste immediately adjacent to those particles. These particles show characteristic texture of many known alkali-carbonate reactive (ACR) rocks of Missouri in having rhombic crystals of dolomite floating in finer-grained matrix of calcite, quartz, and clay.

No cracking, however, was found in the interstitial paste fractions between those reactive particles or within the particles or in dark reaction rims (e.g., see Figures 31, 33, 35, and 37) to indicate distress from ACR.

Along with ACR, also detected are isotropic to birefringent alkali-silica reaction gel in the walls of main vertical cracks and in some coarse voids, which are judged to be the result of alkali-silica reaction of reactive silica inclusions in some of crushed argillaceous dolomitic limestone particles and alkaline pore solutions in shotcrete.

Despite its detection in rather meager amounts, similar to ACR, however no cracking was detected from ASR of reactive silica components in crushed dolomitic limestone aggregate.

Paste

Paste is Portland cement based with evidence of addition of fly ash only at minor amounts (probably as accidental contaminant from mixing truck). Paste is variably dense and medium to darker gray consisting of major amount of Portland cement and minor amount of fly ash having water-cementitious materials ratios estimated to be 0.40 to 0.42 in the denser and darker gray areas to 0.42 to 0.46 in the medium gray areas. Freshly fractured surfaces of paste have subvitreous to dull lusters and subconchoidal textures. Residual and relic Portland cement particles are rare and scattered throughout the paste. There is no evidence of any chemical or physical deterioration of paste found in the shotcrete bodies of cores. Carbonation is detected only along major vertical cracks due to penetration of atmospheric CO_2 through the cracks.

Air

The shotcrete body is non-air-entrained having air contents estimated to be from 3 to 4 percent in the denser areas to as high as 8 to 10 percent in areas having many coarse (honeycombed) visible voids.

CRACKING IN POOL PLASTER AND SHOTCRETE

Core ID	1 (Step Edge, No Crack)	2 (Step, On a crack)	3 (Step, On Corner Cracks)	4 (Floor, On a crack)
Main Vertical Crack length and Surface Width (mm)	None	10.5"(260 mm) 1.5 mm	5.25"(130 mm) 1.5 mm	11" (270 mm) 1.5 mm
Additional Visible Crack	None	Diagonal crack at a depth of 6 in.	Surface-parallel crack at a depth of 6 in.	None other than main through-depth crack
Effects of Visible Cracks on Integrity of Cores	None	Broke the core into two portions by the crack at 6 in. depth	Broke the core into two portions by the crack at 6 in. depth	Broke the core longitudinally into two halves by the through-depth crack
Invisible (Micro) Cracks	Extensive only in plaster but not in shotcrete	Extensive only in plaster but not in shotcrete	Extensive only in plaster but not in shotcrete	Extensive only in plaster but not in shotcrete

PHOTOGRAPHS AND PHOTOMICROGRAPHS

Features/Core ID	1	2	3	4
Side Cylindrical Surfaces Showing Visible Cracking and Coarse Voids	10	13	16	18
Exposed Surfaces of Pool Plaster/Cores with or without visible cracks	9	11, 12	14, 15	17
Plaster-Leveling Course-Shotcrete on Lapped X-Sections of 8-in. depths of Cores	22	24	26	28
Plaster-Leveling Course and Shotcrete on Micrographs of Lapped X-Sections	30	32	34	36
Dark Reaction Rims around Argillaceous Dolomitic Limestone in Micrographs of Lapped X-Sections	31	33	35	37
Plaster-Leveling Course-Shotcrete on Thin Sections of 3-in. depths of Cores	38, 39	40, 41	42, 43	44, 45
Plaster-Leveling Course-Shotcrete on Micrographs of Thin Sections of Cores	46, 56, 57	59, 63	65	71
Extensive Shrinkage Microcracking in Pool Plaster	46, 54, 55, 74	63, 75	65, 77	71
Thin section Micrographs Depicting Characteristic Texture of Alkali-Carbonate Argillaceous Dolomitic Limestone	47 to 51	59 to 62	66, 67	70, 72
Alkali-Silica Reaction Gel in Cracks and Voids	52, 53	64	-	-
Thin Section Micrograph Showing Difference in Paste Compositions Between Plaster, Leveling Course, and Shotcrete	58	-	-	-

DISCUSSIONS

POTENTIAL UNSOUNDNESS AND WRONG CHOICE OF ARGILLACEOUS DOLOMITIC LIMESTONE AGGREGATE

Despite the lack of direct evidence of distress (i.e., cracking) by either ACR or ASR of crushed argillaceous dolomitic limestone aggregates, their presence clearly showed the potential danger of bulk expansion of shotcrete by either or both reactions to cause cracking, which hasn't developed to advanced stage to show cracking of interstitial paste fractions of shotcrete. Missouri is well-known for many alkali-carbonate reactive rocks, which should have checked by petrographic examinations according to the procedures of ASTM C 295 prior to the incorporation in this aggregate in the shotcrete mix.

Another more serious deleterious side effect of using ¼ in. (6.25 mm) crushed limestone-dolomite aggregate, beside its ACR potential, which is judged to have provided more direct role in promoting unaccomodative drying shrinkage of shotcrete is the increased paste volume of shotcrete from such crushed stone of high specific surface with the increased potential for drying shrinkage of high cement content shotcrete mix. Since the water-cement ratio was

low (0.40 to 0.44), cement content must be higher than usual at a given water content to increase the paste volume to adequately coat these aggregates during wet mixing process.

SHRINKAGE CRACKING OF SHOTCRETE

Based on detailed petrographic examinations, e.g., from (a) use of ¼ in. size crushed limestone-dolomite aggregate to increase the paste volume, to (b) configuration of paths of main vertical cracks through depth, from (c) evidence such as trapped paste and aggregate in between crack walls to (d) cracking of some crushed stone particles situated along the crack paths most of the visible cracks in the pool, at least at the locations of examined cores are judged to be due to unaccommodative shrinkage of shotcrete, where a portion of cracks may have formed at an early stage of shotcrete placement (i.e., plastic shrinkage) whereas other portions may have developed at a later hardening stage (i.e., as drying shrinkage) during the aerated stage prior to the filling of pool with water.

THREE POTENTIAL STRESSES FOR DEVELOPMENT AND ADVANCEMENT OF CRACKS

Based on present study, there are at least three different stresses detected at aerated and immersed states, which have the potential to cause cracking –

- Drying shrinkage of pool plaster at aerated states to develop extensive fine hairline microcracking in the cement paste fraction of plaster that are well-documented from optical microscopy and SEM studies here,
- Overall shrinkage of shotcrete body at aerated states from use of high paste volume at low water-cement ratio wet mix, which is also well-documented here, and
- Potential expansion of shotcrete body at immersed states by deleterious expansions from ACR and ASR where only evidence of such reactions are well documented here (e.g., from dark reaction rims, carbonation rims in paste, and ASR products in cracks and voids) but not the resultant cracking due to rather early stages of such reactions.

Therefore, there might be two opposing forces acted –

- One from overall bulk shrinkage of shotcrete body, which has developed the main vertical cracks where pool plaster simply reflected the cracks from shotcrete body (along with a potential contribution from shrinkage cracking of plaster itself, which might have opened additional pathways for pool water penetration through plaster), and
- Another from overall bulk expansion of shotcrete from ACR and/or ASR.

Amongst these two opposing forces, shrinkage clearly won over expansion here for development of visible cracks since expansion mechanisms are found to be at early stages.

REFERENCES

ACI Committee 506, "Guide to Shotcrete (ACI 506R-05)," American Concrete Institute, Farmington Hills, MI, 2005, 40 pp.

Alkali Reactivity of Carbonate Rocks in Missouri, Missouri State Highway Department, Division of Materials and Research, August 1967.

American Shotcrete Association, Position Statement #1 Compressive (Strength) Values of Pool Shotcrete.

ASTM C 856 "Standard Practice for Petrographic Examination of Hardened Concrete," Vol. 4.02, ASTM International, West Conshohocken, PA, 2016.

ASTM C 1723, "Standard Guide for Examination of Hardened Concrete Using Scanning Electron Microscopy," Vol. 4.02, ASTM International, West Conshohocken, PA, 2016.

Axon, E.O., and Lind, J., Alkali-Carbonate Reactivity - An Academic or a Practical Problem

Gillott, J.E. and Swenson, E.G. 1969. "Mechanism of the Alkali-Carbonate Rock reaction." Journal of Engineering Geology, 2: 7-23.

Grattan-Bellew, P.E., Mitchell, L.D., Margeson, J. and Deng, M. 2010. "Is alkali–carbonate reaction just a variant of alkali–silica reaction ACR=ASR?" Cement and Concrete Research, 40: 556–562.

Hadley, D.W. 1961. "Alkali reactivity of carbonate rocks; expansion and dedolomitization." Proceedings of the Highway Research Board, 40: 462-474.

Jana, D., "Sample Preparation Techniques in Petrographic Examinations of Construction Materials: A State-of-the-art Review," *Proceedings of the 28th Conference on Cement Microscopy*, International Cement Microcopy Association, Denver, Colorado, pp. 23-70, 2006.

Katayama, T. 2010. "The so-called alkali-carbonate reaction (ACR) — Its mineralogical and geochemical details, with special reference to ASR." Cement and Concrete Research, 40: 643-675.

Lo, W., Deng, M., Mo, L., Panesar, D., and Mao, Z., Alkali carbonate reaction (ACR): Investigations on mechanism of dedolomitization of dolomite in dolostones, Construction and Building Materials, Volume 351, 10 October 2022.

Mather, K., Buck, A.D., and Luke, W.I., Alkali-Silica and Alkali-Carbonate Reactivity of Some Aggregates from South Dakota, Kansas, and Missouri.

Ozol, M.A. 2006. "Alkali-carbonate rock reaction." Significance of Tests and Properties of Concrete and Concrete Making Materials (Ed. J.F. Lamond and J.H. Pielert), ASTM STP 169D, Chapter 35, American Society for Testing and Materials, West Conshohocken, PA, 410-424.

Swenson, E.G. and Gillott, J.E. 1964. "Alkali-carbonate rock reaction." Highway Research Record, 45: 21-40.

Tang, M., Liu, Z. and Han, S. 1987. "Mechanism of alkali-carbonate reaction." Proceedings of the 7th International Conference on Concrete Alkali-Aggregate Reactions (Ed. P.E. GrattanBellew), Noyes Publications, New Jersey, 275-279.

Walker, H.N. 1978. "Chemical Reactions of Carbonate Aggregates in Cement Paste." Special Technical Publication 169-B, ASTM, Philadelphia, PA, 722-743.

✪ ✪ ✪ END OF TEXT ✪ ✪ ✪

END OF REPORT[2]

[2] The CMC logo is made using a lapped polished section of a 1930's concrete from an underground tunnel in the U.S. Capitol.